Dear Dr. Pantoja,

Thank you for taking the time to handle our manuscript and your assessment. We have carefully addressed each comment from you and two referees and tried our best to improve the manuscript according to the suggestions. Our responses to all comments are listed below. We welcome any further comments. Thank you again for your time and kind efforts.

Best wishes,

Yao Zhang

Manuscript Number: bg-2019-132
Manuscript title: Major role of ammonia-oxidizing bacteria in N_2O production in the Pearl River Estuary

Response to Editor

Comments to the Author:
Review of bg-2019-132 Major role of ammonia-oxidizing bacteria in N_2O production in the Pearl River Estuary
August 7, 2019
Dear Dr. Zhang
Thanks for submitting responses to reviewers of bg-2019-132 "Major role of ammonia oxidizing bacteria in N_2O production in the Pearl River Estuary". Based on those and my own reading I think the article is promising due to sound data and interpretation but it is not publishable in the present form in Biogeosciences since it lacks some structure as pointed out by Reviewer 1. This aspect precludes full understanding of your work in mainly two aspects:
1) Mixing of results and discussion such as in Figure 2 that shows field data combined with panels i and j that, according to text, ΔN_2O is calculated for incubations so, they are probably results from incubations. Since there is no explanation of experimental treatments with variable O_2 concentration, I would assume that those are derived from field sampling, right? If that were the case, results are mixed with discussion in this figure and text in page 8, paragraph starting in L24. Alternatively, oxygenation conditions of incubations are missing in the method section.

Response:

ΔN_2O in Figure 2 is not calculated for incubations; it is calculated from the filed data as the difference between the measured concentrations of N_2O in the waters and the estimated equilibrium values of N_2O (based on the global mean atmospheric N_2O from http://www.esrl.noaa.gov/gmd). We described the calculation in the Methods section 2.2 (Page 6, Lines 1−11). O_2 concentration in Figure 2 is also from filed sampling. So, Figure 2 and text in the original page 8, L24 (Page 10, Lines 10−19 in the revised version) all are the results from field, not mixed with discussion.

ΔN_2O in Table 2 (original Table 1) is calculated for incubations as the variation of N_2O concentration along incubation time. This was described in the Methods section 2.4 (Page 8, Lines 22−24). To distinguish ΔN_2O from field data (the excess N_2O) and incubations, we revised ΔN_2O in field as "ΔN_2O_{excess}" throughout the manuscript (Page 1, Line 16; Page 6, Lines 1, 2; Page 10, Lines 12, 13, 17; Page 13, Line 19; Page 15, Line 15; Page 17, Lines 21, 24; Page 31, Lines 2, 3; Page 41, Table 1). O_2 concentration was not measured during incubations; we listed the in situ O_2 concentration of incubation sites in Table S1.

2) Better explanation is needed regarding "concentration-based "rate" measurements …" (Reviewer 2) that not only refers to "… changing of the nutrients can be sensitively detected during incubations" as you pointed out, but also to multiple and simultaneous sources and sinks, therefore at the most you obtain a net rate since it is likely that these nutrients are simultaneously removed.
In any case, this aspect is not clear in the text. Please clearly show how you interpret each of rates (net production or decay/ incubation time) of Table 1:
ΔN_2O (nmol $L^{-1}h^{-1}$)
ΔNO_3^- (μmol $L^{-1}h^{-1}$)
ΔNO_2^- (μmol $L^{-1}h^{-1}$)
$\Delta(NH_3 + NH_4^+)$ (μmol $L^{-1}h^{-1}$). You mean $NH_3 + NH_4^+$ instead of NH_3/NH_4^+ (a ratio), don't you?

Response:

Many thanks for your comment. We agree that concentration-based "rate" measurements essentially give a net rate. We clarified these rates as net rates in Table

2 (original Table 1) and the text. Please see below.

Table 2: "[a]*These rates are net rates since Δ(NH_3+NH_4^+) is the net consumption and ΔNO_2^-, ΔNO_3^-, and ΔN_2O is the net production during incubation.*" (Page 42)

Methods 2.4 subsection: "*All of the concentration-based rates described from the incubations represent net rates.*" (Page 8, Lines 26–27).

We also revised $\Delta NH_3/NH_4^+$ as $\Delta(NH_3 + NH_4^+)$ in Table 2 as well as Figures 2, 5 (original Figure 4), and 6.

A cartoon similar to the one below may help to explain your rationale for interpreting these rates and better sustain conclusions such as "… results clearly indicate that nitrification occurred during the entire P01 incubations, and suggest that denitrification may be present in the ending phase… "(Page 10, L11-12).

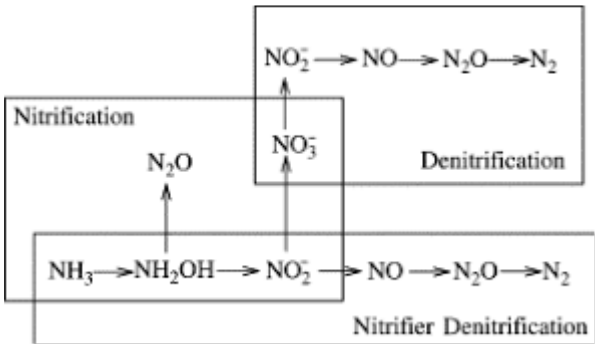

Response:

Thanks for your suggestion. We added a diagram in Figure 5 (original Figure 4) for a better understanding of our results. Please see below:

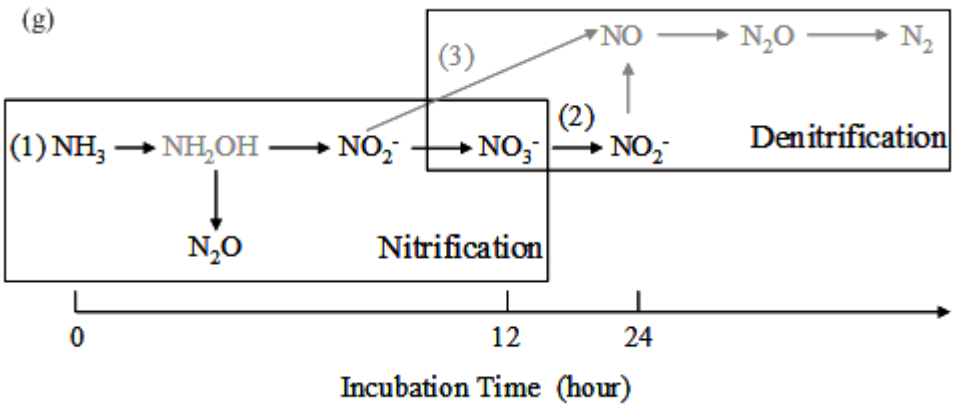

Figure R1 (Figure 5 in the revised MS): A diagram showing the transformations of nitrogen compounds and N_2O productions during incubation experiments. Nitrification (1) occurred during the entire P01 and P05 incubations and denitrification (2 and/or 3) may be present in the end phase of the P01 incubation. The gray arrows indicate the pathways of nitrogen loss unanalyzed here, and the gray compounds indicate the unmeasured nitrogen compound.

In addition, please consider the following:

1. Pag. 1. Line 19. All "N_2O parameters". Do you mean N_2O-related parameters?

Response:

Yes, we mean N_2O-related parameters. Revised as suggested (Page 1, Line 19; Page 15, Lines 5, 10 and 15).

2. P. 1, Line 22-25 "Taken together, the in situ incubation experiments, N_2O isotopic composition and concentrations, and gene datasets suggested that the high concentration of N_2O (oversaturated) is mainly produced from strong nitrification by the relatively high abundance of AOB in the upper reaches as the major source of N_2O emitted to the atmosphere in the whole estuary. "

What is the evidence for the whole estuary? What about seasonal variability?

Response:

Sorry, "the whole estuary" could be confusing. We mean that the upper reaches acts as the major source of N_2O emitted to the atmosphere in the Pearl River Estuary. We revised this sentence as "*Taken together, the in situ incubation experiments, N_2O isotopic composition and concentrations, and gene datasets suggested that the high concentration of N_2O (oversaturated) is mainly produced from strong nitrification by the relatively high abundance of AOB in the upper reaches and is the major source of N_2O emitted to the atmosphere in the Pearl River Estuary*." (Page 1, Lines 22−26)

While this study was performed in summer, the Pearl River Estuary acts as a net source of N_2O all year according to Lin et al. (2016). Lin et al. reported the seasonal variability of N_2O distributions in the Pearl River Estuary based on six cruises covering Spring, Summer, Autumn, and Winter. The results indicate that the

saturations of N_2O in the water column varied from 101–3800% along the Pearl River Estuary, acting as a net source of atmospheric N_2O, and N_2O production was predominantly modulated by nitrification in the upper estuary. There are significantly higher N_2O concentrations and elevated N_2O fluxes during winter and spring compared with summer and autumn.

Reference:

Lin, H., Dai, M., Kao, S. J., Wang, L., Roberts, E., Yang, J., Huang, T., and He, B.: Spatiotemporal variability of nitrous oxide in a large eutrophic estuarine system: The Pearl River Estuary, China, Mar. Chem., 182, 14–24, 2016.

3. Pag. 3, L.12. “anaerobic particle interiors ” . Do you mean anoxic particle interiors?

Response:

Sorry for this mistake. Revised (Page 4, Line 2).

4. Page 3, L 20 (de)nitrification. Why using ()?

Response:

We revised “which support (de)nitrification and N_2O production” as “*which may support strong nitrification, denitrification, and N_2O production*” (Page 4, Lines 9−10).

5. Page 4, L25. “Temperature and salinity were continuously measured with the CTD system. ” Define continuously and in detail depths

Response:

Sorry for this misleading. We deleted “continuously”. The sampling depths were described in Methods section 2.1 (Page 4, Lines 23−25) — “*water samples were taken from the surface (2 m) and bottom (4–15 m) of each site by using a conductivity, temperature, and depth (CTD) rosette sampling system (SBE 25; Sea-Bird Scientific, USA) fitted with 12 L Niskin bottles (General Oceanics).*”

6. Page 4. L24. “2.2 Biogeochemical parameters, N_2O emissions, and isotopic analysis” Detail whether this is in the water column in your 11 sites or in experiments,

or both

Response:

Section 2.2 is for the water column in 22 sites in the PRE (11 sites in the upper reaches and 11 sites in the lower reaches). We revised the 2.2 title as "*Biogeochemical parameters, N_2O emissions and isotopic analysis of environmental samples*" for clarification. All measurements for incubation experiments were described in Methods section 2.4 Incubation experiments.

Figure 1. Enlarge symbols + and * (or change colors). There is an extra red dot, isn't?

Response:

We enlarged symbols + and * in Figure 1 according to the editor's suggestion and revised the legend as "*Map of the PRE showing the sampling sites. Biogeochemical analyses were performed on samples from all sites (green and red circles). The green circles indicate sites where genes were analyzed. The black crosses indicate in situ incubation experiment sites (P01 and P05). The black asterisks indicate sites where the isotopic composition of N_2O was analyzed.*" (Page 29, Lines 2−5).

Table 1. a) Fix typos such as "Liner Equation". Use either regression or equation b) Since this is regression, R2 is the coefficient of determination!

Response:

We revised "Liner Equation/Regression" as "Equation" and "*R*" as "R^2" in Table 2 (original Table 2) as suggested.

Figure 6. Since there is an equation (y = f(x)) with a line, it is a regression analysis (one independent and one dependent variable) whereas in correlation there are not dependent or independent variable. Coefficient must be R2 for regression.

Response:

Thanks for your comment. We deleted the regression lines and revised "R" as "ρ" in Figure 6 since the Mantel statistic was calculated as the Spearman rank correlation coefficient.

Page 7, L 19. Explain this please

Response:

Sorry for the confusion. We deleted Eq. (9) (N_2O_{yield} (%) = ΔN_2O-N / $\Delta(NO_2^-$ + $NO_3^-)$-N) in the revised MS (Page 9, Line 1), which is not suitable to estimate N_2O yield from nitrification in this study since denitrification could occur and nitrate and nitrite concentrations decreased in the ending phase of the incubation at site P01.

When the only nitrification occurs during incubation, the decrease of ammonia-N ($\Delta(NH_3 + NH_4^+)$-N is theoretically equal to the increase of nitrite/nitrate-N ($\Delta(NO_2^-$ + $NO_3^-)$-N (part of nitrite may have been oxidized to nitrate). In this case, we can estimate the N_2O yield based on either Eq (8) (N_2O_{yield} (%) = ΔN_2O-N / $\Delta(NH_3$ + $NH_4^+)$-N) or Eq (9).

Page 10, L10. Why is there a "… but… " here? This sentence is not clear.

Response:

We deleted "but". This sentence was revised as "*The ammonia and nitrite concentrations consistently decreased and increased, respectively, during the incubation experiments; the nitrate concentrations decreased in the end phase after a slight increase (Fig. 5b).*" (Page 12, Lines 11−13)

Response to Reviewer #1

Anonymous Referee #1

Received and published: 5 June 2019

Ma et al. investigated the relationship between N_2O production and spatial distribution of AOA and AOB along a salinity gradient in the Pearl River Estuary, China by using qPCR, chemical analysis and in situ incubation experiment. Data are well analyzed and presented. However, the manuscript's structure should be modified because the some results were presented in the discussion section, and some conclusions needs to be rephrased because the main findings in this study were mainly based on the correlation analysis OR statistical analysis (e.g., between N_2O production and the abundance of functional genes), which can't provide a solid

support for a causal relationship between microbial contributors and N_2O production.

Response:

Many thanks for the reviewer's comments. We moved the results pointed out by the reviewer into the Results section. We also revised some conclusion sentences with the appropriate tone according to the reviewer's suggestions. Please see below for detail.

More specific comments and suggestions are given below:

1. As mentioned by authors, both nirK and nirS genes are the key functional genes in the denitrification pathway, so why did not determine the abundance of nirK gene here?

Response:

The *nir*S and *nir*K genes encode cytochrome cd1 and copper-containing nitrite reductase, respectively. They were functionally and physiologically equivalent, but structurally different and could not be detected in the same strains in the previous research (Coyne et al., 1989), while the recent genomic analyses found a few bacteria contain both *nir*S and *nir*K (Graf et al., 2014). A recent genomic analysis revealed that a great many *nir*K-encoding bacteria have both denitrification and DNRA (Dissimilatory Nitrate Reduction to Ammonium) pathways (Helen et al., 2016). Furthermore, it was reported that *nir*S genes were more widely distributed than the *nir*K genes (Zumft, 1997; Bothe et al., 2000), and *nir*S genes were both more abundant and more diverse than *nir*K in the estuarine water columns (Zhu et al., 2018; Wang et al., 2019) and various estuarine sediments (Nogales et al, 2002; Santoro et al, 2006; Abell et al., 2010; Mosier and Francis, 2010; Beman, 2014; Smith et al., 2015; Lee and Francis, 2017). The previous study on the Pearl River sediment also showed that *nir*K abundance was much lower than *nir*S abundance (Huang et al., 2011). Therefore, we used the *nir*S gene to identify the distribution of denitrifiers in the PRE and reflect the denitrification potential.

References

Abell, G. C. J., Revill, A. T., Smith, C., Bissett, A. P., Volkman, J. K., and Robert, S. S.: Archaeal ammonia oxidizers and *nirS*-type denitrifiers dominate sediment nitrifying and denitrifying populations in a subtropical macrotidal estuary, ISME J., 4, 286–300, 2010.

Beman, J. M.: Activity, abundance, and diversity of nitrifying archaea and denitrifying bacteria in sediments of a subtropical estuary: Bahía del Tóbari, Mexico. Estuar. Coast, 37, 1343–1352, 2014.

Bothe, H., Jost, G., Schloter, M., Ward, B. B., and Witzel, K. P.: Molecular analysis of ammonia oxidation and denitrification in natural environments, FEMS Microbiol. Rev., 24, 673–690, 2000.

Coyne, M. S., Arunakumari, A., Averill, B. A., and Tiedje, J. M.: Immunological identification and distribution of dissimilatory heme cd1 and non-heme copper nitrite reductases in denitrifying bacteria, Appl. Environ. Microbiol., 55, 2924–2931, 1989.

Graf, D. R. H., Jones, C. M., and Hallin,. S.: Intergenomic comparisons highlight modularity of the denitrification pathway and underpin the importance of community structure for N_2O emissions. PloS One 9: e114118. https://doi.org/10.1371/journal.pone.0114118. s008. 2014.

Helen, D., Kim, H., Tytgat, B., and Anne, W.: Highly diverse nirK genes comprise two major clades that harbour ammoniumproducing denitrifiers, BMC Genomics 17, 155, 2016. https://doi.org/10.1186/s12864-016-2465-0

Huang, S., Chen, C., Yang, X., Wu, Q., and Zhang, R.: Distribution of typical denitrifying functional genes and diversity of the nirS-encoding bacterial community related to environmental characteristics of river sediments, Biogeosciences, 8, 3041–3051, 2011.

Lee, J. A., and Francis, C.A.: Spatiotemporal characterization of San Francisco Bay denitrifying communities: A comparison of *nir*K and *nir*S diversity and abundance. Microbial Ecology 73, 271–284, 2017.

Mosier, A. C., and Francis, C. A.: Denitrifier abundance and activity across the San Francisco Bay Estuary, Env. Microbiol. Rep., 2, 667–676, 2010.

Nogales, B., Timmis, K. N., Nedwell, D. B., and Osborn, A. M.: Detection and diversity of expressed denitrification genes in estuarine sediments after reverse transcription-PCR amplification from mRNA, Appl. Environ. Microbiol., 68, 5017–5025, 2002.

Santoro, A. E., Boehm, A. B., and Francis, C.A.: Denitrifier community composition along a nitrate and salinity gradient in a coastal aquifer. Appl. Environ.

Microbiol., 72, 2102–2109, 2006.

Smith, J. M., Mosier, A. C., and Francis, C. A.: Spatiotemporal relationships between the abundance, distribution, and potential activities of ammonia-oxidizing and denitrifyingmicroorganisms in intertidal sediments. Microb. Ecol., 69, 13–24, 2015.

Wang, J., Kan, J., Qian, G., Chen, J., Xia, Z., Zhang, X., Liu, H., and Sun, J.: Denitrification and anammox: Understanding nitrogen loss from Yangtze Estuary to the east China sea (ECS), Environ. Pollut., 2019. https://doi.org/10.1016/j.envpol.2019.06.025.

Zhu, W., Wang, C., Hill, J., He, Y., Tao, B., Mao, Z., and Wu, W.: A missing link in the estuarine nitrogen cycle?: Coupled nitrification-denitrification mediated by suspended particulate matter, Sci. Rep., 8, 2282, 2018. DOI:10.1038/s41598-018-20688-4

Zumft, W. G.: Cell biology and molecular basis of denitrification, Microbiol. Mol. Biol. R., 61, 533–616, 1997.

2. Page 7, line 18-19, make subscript for some chemistry formulas (N_2O, NH_3 etc.);

Response:

Revised as suggested (Page 6, Line 12−17).

3. Page 7, line 24, please correct the P value using the Bonferroni correction or other multiple-comparison methods;

Response:

Thanks for the reviewer's suggestion. As normal distribution of the individual data sets was not always met, we could not use Bonferroni correction to correct *P* value. So, we used the False Discovery Rate (FDR)-based procedures to identify truly significant comparisons, which has been considered as the best choice available in many studies of ecology and evolution (Pike, 2011). In the revised manuscript, we corrected the *P* value using the False Discovery Rate (FDR)-based multiple comparison procedures, and added the statement in the "2.5 Statistical analyses" (Page 9, Lines 6−8): "*False discovery rate (FDR)-based multiple comparison procedures were applied to evaluate the significance of multiple hypotheses and identify truly significant comparisons (FDR-adjusted P value) (Pike, 2011).*" We also revised Table 1 (original Table 2) according to the FDR-adjusted *P* values (Page 41).

Reference

Pike, N.: Using false discovery rates for multiple comparisons in ecology and evolution, Methods in Ecology and Evolution, 2, 278–282, 2011.

4. Page 7, line 25, and Fig. 5. Please check the multicollinearity problems before perform the RDA analysis. Some environmental parameters are highly correlated with each other, some of them should be removed from the RDA analysis;

Response:

Thanks for the reviewer's suggestion. We used the value of Variance Inflation Factor (VIF) to check the multicollinearity (Ter Braak et al., 1998; Ricart et al., 2010). The variables Temperature, Silicate, NH_3, NO_3^-, and pH had a high VIF (> 20), so we removed these factors from the RDA analysis. We added a statement in Method 2.5 subsection —"*Significant environmental parameters (P < 0.05) without multicollinearity (variance inflation factor <20) (Ter Braak, 1986) were obtained.*" We also revised the RDA description in the Results 3.3 subsection of the revised manuscript (Page 11, Lines 25−27; Page 12, Lines 1−3). —"*The RDA was used to further analyze variations in the AOA and AOB distributions under the environmental constraints. The results confirmed that the relatively high AOB abundances in the upper estuary were constrained by low salinity water, high nitrite and TSM concentrations, low DO conditions, and high N_2O concentrations whereas high salinity water and opposite environmental conditions constrained the relatively high AOA abundances in the Lingdingyang area (Fig. 4). These constraints explained 89.3% of the variation in the ammonia oxidizers distribution along the PRE.*" Please see the revised Figure 4 (original Figure 5) below.

References

Ricart, M., Guasch, H., Barceló, D., Brix, R., Conceicao, M. H., Geiszinger, A., de Alda, M. J. L., López-Doval, J. C., Munoz, I., Postigo, C., Romaní, A. M., Villagrasa, M., Sabater, S.: Primary and complex stressors in polluted mediterranean rivers: Pesticide effects on biological communities, J. Hydrol., 383, 52–61, 2010.

Ter Braak, C .J. F., Smilauer, P.: CANOCO Reference Manual and User's Guide to

Canoco for Windows: Software for Canonical Community Ordination (Version 4). Microcomputer Power, Ithaca, New York, 352, 1998.

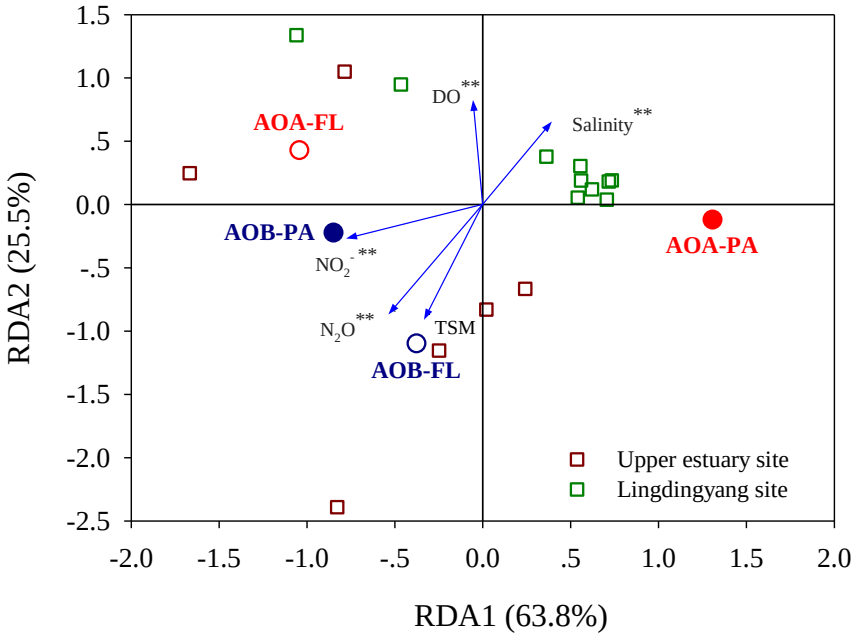

Figure R2 (Figure 4 in the revised MS): RDA of the relative abundance of AOA *amo*A and AOB *amo*A under biogeochemical constraints. Each square represents an individual sample. Vectors represent environmental variables. $^{*}P < 0.05$, $^{**}P < 0.01$ (Monte Carlo permutation test).

5. Page 8, line 5-8 and Fig. 6. I am not convinced with the usage of Mantel and partial Mantel tests here due to two following reasons: 1) for ammonia oxidizer community, actually there were only four variables based on qPCR analysis (PA AOA, FL AOA, PA AOB and FL AOB) but not community data based on sequencing, so I don't think the results of qPCR reflected the truly community composition of ammonia oxidizers; and 2) the authors divided the environmental into four groups, but the classification seems a bit confusing. For example, why classify silicate into water mass but not substrate parameters? And TSM, DO and pH were classify as water mass parameters by numerous previous studies;

Response:

1) Sequencing-based community structure has higher resolutions than qPCR-based community structure. For community composition based on sequencing, the

dissimilarity matrices were calculated with the relative abundance of OTUs (Operational Taxonomic Units). Similarly, for community composition based on qPCR, the relative abundance of PA AOA, FL AOA, PA AOB, and FL AOB were used to calculate the dissimilarity matrices, just like merging some OTUs into one OTU. Despite lower resolutions of community composition, the dissimilarity matrices can be calculated and the Mantel and partial Mantel tests can be performed. Similarly, Castellano-Hinojosa et al. (2018) and Huang et al. (2011) also used qPCR data in NDMS analysis and CCA analysis of community structure.

2) Silicate has long been recognized as one of the most common indicators to trace river water in the ocean, and the low salinity and high silicate contents were the best indicators for river source (Moore, 1986). We added a three-dimensional scatter plot in the revised MS (Figure S1; see below) to show the relationships between potential temperature (θ) (^{o}C), salinity, and silicate (SiO_3^{2-}) concentration. The waters from the upper estuary, where the salinity of most sites was close to zero, had high potential temperature and silicate concentration. The mixing behaviors of waters occurred at the Humen outlet (sites P07 and A01), and the waters from the off-shore sites (A10 and A11) had high salinity and low potential temperature and silicate concentration. Therefore, we chose temperature, salinity, and silicate as the indicators to trace estuarine water masses and mixing. The related statements and explanations were added in the Discussion 4.2 subsection (Page 15, Lines 15−19).

We defined the substrate parameters as nitrogen substrates (ammonium, nitrite, and nitrate), which are related to the N_2O producing processes nitrification and denitrification. TSM, DO, and pH are not conservative parameters and thus cannot trace water masses. These factors represent the biogeochemical characteristics of waters and could influence the availability of electron donors (or substrates) during nitrification and denitrification. For example, the suspended particles could be beneficial to microbial activity because of nutrients or substrates supply (Belser, 1979; Crump et al., 1998; Ouverney and Fuhrman, 2000; Teira et al., 2006; Zhang et al., 2014); DO concentration and pH also could influence the availability of ammonia, etc. (Geets et al., 2006; Ward, 2008; Martens-Habbena et al., 2009; Zhu et al., 2013; Huesemann et al., 2002; Hutchins et al., 2009; Fulweiler et al., 2010; Beman et al., 2011).

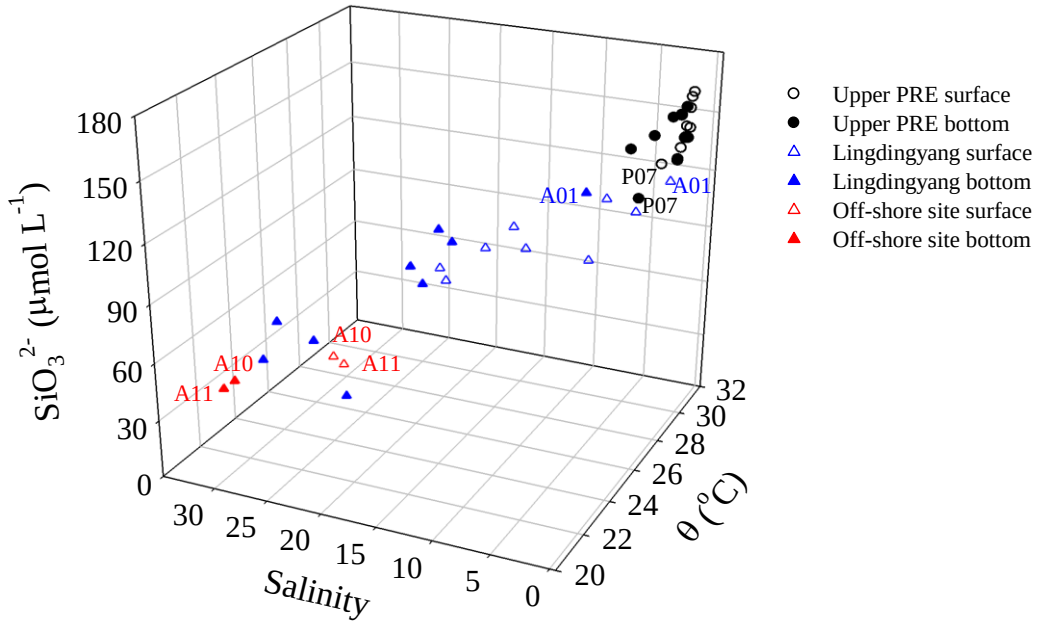

Figure R3 (Figure S1 in the revised MS): Three-dimensional scatter plot of potential temperature (θ) (°C), salinity, and silicate (SiO_3^{2-}) concentration.

References

Belser, L. W.: Population ecology of nitrifying bacteria, Annu. Rev. Microbiol., 33, 309–333, 1979.

Beman, J. M., Chow, C. E., King, A. L., Feng, Y., Fuhrman, J. A., Andersson, A., Bates, N. R., Poppa, B. N., and Hutchins, D. A.: Global declines in oceanic nitrification rates as a consequence of ocean acidification, PNAS, 108, 208–213, 2011.

Castellano-Hinojosa, A., González-López, J., and Bedmar, E. J.: Distinct effect of nitrogen fertilisation and soil depth on nitrous oxide emissions and nitrifiers and denitrifiers abundance, Biol. Fert. Soils., 54, 829–840, 2018.

Crump, B. C., Baross, J. A., and Simenstad, C. A.: Dominance of particle-attached bacteria in the Columbia River estuary, USA, Aquat. Microb. Ecol., 14, 7–18, 1998.

Fulweiler, R. W., Emery, H. E., Heiss, E. M., and Berounsky, V. M.: Assessing the Role of pH in Determining Water Column Nitrification Rates in a Coastal System, Estuaries and Coasts, 34, 1095–1102, 2010.

Geets, J., Boon, N., and Verstraete, W.: Strategies of aerobic ammonia-oxidizing

bacteria for coping with nutrient and oxygen fuctuations, FEMS Microbiol Ecol., 58, 1–13, 2006.

Huang, S., Chen, C., Yang, X., Wu, Q., and Zhang, R.: Distribution of typical denitrifying functional genes and diversity of the nirS-encoding bacterial community related to environmental characteristics of river sediments, Biogeosciences, 8, 3041–3051, 2011.

Huesemann, M. H., Skillman, A. D., and Crecelius, E. A.: The inhibition of marine nitrification by ocean disposal of carbon dioxide, Mar. Pollut. Bull., 44, 142–148, 2002.

Hutchins, D. A., Mulholland, M. R., and Fu, F.: Nutrient cycles and marine microbes in a CO_2-enriched ocean, Oceanogr., 22, 128–145, 2009.

Martens-Habbena, W., Berube, P. M., Urakawa, H., de la Torre, J. R., and Stahl, D. A.: Ammonia oxidation kinetics determine niche separation of nitrifying Archaea and Bacteria, Nature, 461, 976–979, 2009.

Moore, W. S., Sarmiento, J. L., and Key, R. M.: Tracing the Amazon component of surface Atlantic water using 228Ra, salinity and silica, J. Geophys. Res., 91, 2574–2580, 1986.

Ouverney, C. C., and Fuhrman, J. A.: Marine planktonic archaea take up amino acids, App. Environ. Microbiol., 66, 4829–4833, 2000.

Ward, B. B. Nitrification in marine systems, In. Capone, D. G., Bronk, D. A., Mulholl, M. R., and Carpenter, E. J. (ed), Nitrogen in the Marine Environment (2nd Edition) [M]. Burlington: Academic Press, 199–261, 2008.

Teira, E., van Aken, H., Veth, C., and Herndl, G. J.: Archaeal uptake of enantiomeric amino acids in the meso-and bathypelagic waters of the North Atlantic, Limnol. Oceanogr., 51, 60–69, 2006.

Zhang, Y., Xie, X., Jiao, N., Hsiao, S. S. Y., and Kao, S. J.: Diversity and distribution of amoA-type nitrifying and nirS-type denitrifying microbial communities in the Yangtze River estuary, Biogeosciences, 11, 2131–2145, 2014.

Zhu, X., Burger, M., Doane, T. A., and Horwath, W. R.: Ammonia oxidation pathways and nitrifier denitrification are significant sources of N_2O and NO under low oxygen availability, PNAS, 110, 6328–6333, 2013.

6. Page 8, line 20, is the 63.0 μmol/L the hypoxic threshold?

Response:

Yes, the DO concentration of 63.0 μmol L^{-1} (equaling to 2 mg L^{-1}) is the hypoxic threshold, which was cited from Rabalais et al. (2010).

Reference

Rabalais, N. N., Díaz, R. J., Levin, L. A., Turner, R. E., Gilbert, D., and Zhang, J.: Dynamics and distribution of natural and human-caused hypoxia, Biogeosciences, 7, 585–619, 2010.

7. Page 9, line 11, please re-phrase this subtitle because only the transcripts of *amo*A and *nir*S genes from two freshwater stations were quantified here;

Response:

We re-phrased this subtitle as "*Distributions of amoA and nirS genes along the salinity transect*" in the revised manuscript (Page 10, Line 23).

8. Page 12, line 12-13, too much speculation;

Response:

This sentence was revised as "*This suggests that AOB might be active in the ammonium and particle-enriched PRE despite their low abundance (Füssel, 2014; Hou et al., 2018).*" (Page 14, Lines 24−25).

9. Page 12, line 15-26, please move this part into Results section, and again, I don't think the classification for environmental parameters is on the right way;

Response:

This part was moved into the Results section as suggested (Page 11, Lines 15−24) and we revised "*the water mass parameters temperature (negatively), salinity (positively), and silicate concentration (negatively)*" as "*the hydrographic parameters temperature (negatively) and salinity (positively), as well as silicate concentration (negatively)*". As for the water mass parameters and the parameters influencing substrate availability, please refer to our response above.

10. Page 12, line 23, "positive correlations between AOB *amo*A abundances and all N_2O parameters", should be except for FL AOB;

Response:

This sentence was revised as "*Notably, there were positive correlations between AOB amoA abundances and all N_2O parameters as well as ammonia concentrations (Table 1; $P < 0.05-0.01$) except for the extremely low-abundance of FL AOB*" (Page 11, Lines 21−23).

11. Page 12, line 27, the results of RDA analysis also should be presented in Results section;

Response:

We moved this part into the Results 3.3 subsection (Page 11, Lines 25−27, and Page 12, Lines 1−5).

12. The most part of first paragraph of 4.3 subsection should be moved into Results section;

Response:

We added a supplementary Table S3 showing the data in Figure 7 according to Reviewer #2's suggestion. The results descriptions on Table S3 and Figure 7 in the original 4.3 subsection were moved into the Results 3.4 subsection (Page 13, Lines 5−10).

13. How about the potential role of comammox and *nir*K-type denitrifier for N_2O production in PRE, please discuss it in the 4.3 subsection.

Response:

Thanks for the reviewer's suggestion. We added this discussion in the 4.3 subsection (Page 17, Lines 3−16). —"*In addition, it is possible that comammox (COMplete AMMonia OXidiser) species, newly discovered in terrestrial systems (Daims et al., 2015; Santoro, 2016; Kits et al., 2017), are also involved in N_2O production (Hu and He, 2017) given the similar ammonia oxidation pathway to AOB. It has been further reported that the comammox Nitrospira inopinata has a lower N_2O yield than AOB due to a lack of NO reductases and the formation of N_2O from the abiotic conversion of hydroxylamine (Kits et al., 2019). However, comammox has not been widely observed in estuarine waters. Also, nirK-type denitrifiers may contribute to N_2O*

production despite being much less abundant than nirS-type denitrifiers (Huang et al., 2011; Maeda et al., 2017). Furthermore, nirS-type denitrifiers are more likely to be capable of complete denitrification because of a higher co-occurrence of the N_2O reductase gene (nosZ) with nirS than nirK (Graf et al., 2014). However, there is currently no direct evidence that denitrification or nitrifier-denitrification is responsible for N_2O production in the PRE water column. A release of N_2O into the overlying waters through denitrification was reported in the PRE sediments (Tan et al., 2019). Further study is needed to clarify the potential of both nirK and nirS-type denitrifiers in N_2O production from the interface between sediment and water in the PRE."

References

Daims, H., Lebedeva, E. V., Pjevac, P., Han, P., Herbold, C., Albertsen, M., Jehmlich, N., Palatinszky, M., Vierheilig, J., and Bulaev, A.: Complete nitrification by Nitrospira bacteria, Nature, 528, 504–509, 2015.

Graf, D. R. H., Jones, C. M., and Hallin,. S.: Intergenomic comparisons highlight modularity of the denitrification pathway and underpin the importance of community structure for N_2O emissions. PloS One 9: e114118. https://doi.org/10.1371/journal.pone.0114118. s008. 2014

Huang, S., Chen, C., Yang, X., Wu, Q., and Zhang, R.: Distribution of typical denitrifying functional genes and diversity of the nirS-encoding bacterial community related to environmental characteristics of river sediments, Biogeosciences, 8, 3041–3051, 2011.

Hu, H. W., and He, J. Z.: Comammox–a newly discovered nitrification process in the terrestrial nitrogen cycle, J. Soils Sediments, 17, 2709–2717, 2017.

Kits, K. D., Sedlacek, C. J., Lebedeva, E. V., Han, P., Bulaev, A., Pjevac, P., Daebeler, A., Romano, S., Albertsen, M., Stein, L. Y., Daims, H., and Wagner, M.: Kinetic analysis of a complete nitrifier reveals an oligotrophic lifestyle, Nature, 549, 269–272, 2017.

Kits, K. D., Jung, M.Y., Vierheilig, J., Pjevac, P., Sedlacek, C. J., Liu, S., Herbold, C., Stein, L. Y., Richter, A., Wisse, H., Brüggemann, N., Wagner, M., and Daims, H.: Low yield and abiotic origin of N_2O formed by the complete nitrifier

Nitrospira inopinata, Nat. Commun., 2019. https://doi.org/10.1038/s41467-019-09790-x

Maeda, K., Toyoda, S., Philippot, L., Hattori, S., Nakajima, K., Ito, Y., and Yoshida, N.: Relative Contribution of nirK- and nirS- Bacterial Denitrifiers as Well as Fungal Denitrifiers to Nitrous Oxide Production from Dairy Manure Compost, Environ. Sci. Technol., 51, 14083–14091, 2017.

Santoro, A. E: The do-it-all nitrifier, Science, 351, 342–343, 2016.

Tan, E., Zou, W., Jiang, X., Wan, X., Hsu, T. C., Zheng, Z., Chen, L., Xu, M., Dai, M., Kao, S.: Organic matter decomposition sustains sedimentary nitrogen loss in the Pearl River Estuary, China, Sci. Total. Environ., 648, 508–517, 2019.

14. Fig. 7. It is a little difficult to understand this figure. It seems like the AOA contributed more for N_2O production and yield in site P01, right?

Response:

We attempted to assess the relative contributions of AOA and AOB to N_2O production in the PRE by plotting the N_2O production rates (Fig. 7a) and yields (Fig. 7b) normalized to total (sum of AOA and AOB) *amo*A gene copies or transcripts at sites P01 and P05 along the x-y axes that represent the relative contributions of AOA and AOB to the total *amo*A gene or transcript pools. The results indicate that compared to AOA, higher AOB abundance in the *amo*A gene-based DNA or cDNA pool resulted in distinctly higher (disproportionately higher relative to enhanced abundance) average *amo*A gene copy or transcript-specific N_2O production rates (Fig. 7a) and yields (Fig. 7b), suggesting that AOB may have higher cell-specific activities in the upper estuary and thus be more active in producing N_2O than AOA. For clarification, we added a supplementary Table S3 showing the data in Figure 7 according to Reviewer #2's suggestion.

15. Table 2, Spearman rank correlation analysis generate a rho () value rather than a R value.

Response:

Sorry for this mistake. We revised "R" as "Rho (ρ) " in Table 1 of the revised version (original Table 2) (Page 41, Line 1).

Response to Reviewer #2

Anonymous Referee #2

Received and published: 12 June 2019

Major comments:

More caution is needed on these concentration-based "rate" measurements. Without isotope tracers, very little can be said about actual rates. Evidence for this is in the N_2O yields. The yields reported here are about 100X lower than ever reported from cultures or the field (see Ji et al. 2018 GBC).

Response:

(1) We admit that concentration-based "rate" measurements essentially give a net rate. We clarified these rates as net rates in Table 2 (original Table 1) and the text of the revised MS. Please see below.

Table 2: "[a]*These rates are net rates since* $\Delta(NH_3+NH_4^+)$ *is the net consumption and* ΔNO_2^-, ΔNO_3^-, *and* ΔN_2O *is the net production during incubation.*" (Page 42)

Methods 2.4 subsection: "*All of the concentration-based rates described from the incubations represent net rates.*" (Page 8, Lines 26–27).

(2) We also agree that the ^{15}N-labeled methods are of high sensitivity, which is more reliable for low nitrification activity in natural environments (Damashek et al., 2016; Damashek and Francis 2018). However, in the nutrient-rich estuary waters, changes in nutrient concentrations (ammonium, nitrite, and nitrate) during incubations can be used to calculate nitrification rates when dissolved inorganic nitrogen is in balance (i.e. no nitrogen loss). In the upper-PRE, where high nitrification activity has been reported in the hypoxic zone (Dai et al., 2008; Hou et al., 2018), the in-situ concentrations of ammonium (33.3−167.2 μM), nitrite (11.6−24.5 μM), and nitrate (82.0−126.1 μM) at the incubation sites were high, so the changing of the nutrients can be sensitively detected during incubations.

(3) We compared our ammonium oxidation rates with the ^{15}N-labeled-based rates in the PRE from Hou et al. (2018) (see Table R1 below). Hou et al. reported that during the PRE cruises in July to August 2012 and September 2014, the nitrification rates in the bottom waters of the PRE were 40.25 to 40.70 μmol L^{-1} d^{-1} in the hypoxic sites. Actually, during our cruise, the nitrification rates in the upstream of Humen were also

measured using the ^{15}N-labeled method by simulating in-situ condition incubations, which ranged from 1.23-28.32 μmol L^{-1} d^{-1} (Zhang, 2016, Thesis). These ^{15}N-labeled-based nitrification rates are comparable to our estimated rates (11.28–26.88 μmol L^{-1} d^{-1}) in the upper reach of PRE.

(4) We also compared our N_2O yields with reported by Ji et al. (2018, GBC) (see Table R1 below). The N_2O yields were 0.003−0.06% at >50 μM O_2 and >2% at <0.5 μM O_2 in the Eastern Tropical Pacific (Ji et al., 2018), which are 2−10-fold lower than those from the AOB strain cultures under the 10−100 μM O_2 concentration (Goreau et al., 1980; Table R1). Our N_2O yield ranged from 0.21 to 0.32% during nitrification (the initial in-situ O_2 concentration: 30−61.3 μM; the terminal O_2 concentration: 0.7−2.5 μM). The estimated range of N_2O yield is 0.16±0.09 to 0.37±0.23% when fitting our measured O_2 concentrations into the empirical equation of the relationship between N_2O yield (%) from nitrification and O_2 concentration (μM) given by Ji et al. (2018), which was comparable with our measured N_2O yield.

Table R1 Nitrification rates/ammonia oxidation rates and N_2O yield from literatures and our study.

Study area/Microorganisms	Method	Nitrification rates ($\mu M\ day^{-1}$)	NH_3 concentrations (μM)	N_2O yield	Reference
Rhône River plume	Nutrients + N-serve	0.23 – 2.20	0 – 10	–	Bianchi et al., 1994
Mississippi River	Nutrients	0 – 13.44	0.3 – 2.4	–	Pakulski et al., 1995
Mississippi & Atchafalaya River plume	Nutrients	0 – 14.16	0.5 – 2.5	–	Pakulski et al., 2000
Scheldt	^{14}C+ methylfluoride Nutrients	Up to 19.2 Up to 153.6	0 – 400	0.10–0.40%	De Wilde & De Bie, 2000
Saanich Inlet	Nutrients + allyithiourea	0 – 7.66	0 – 4.9	–	Grundle & Juniper, 2011
Pearl River	Nutrients + allyithiourea	12.47 – 33.10[a]	1.2 – 341.9	–	Dai et al., 2008
Pearl River	^{15}N, denitrifier method	40.25 – 40.70[b]	–	–	Hou et al., 2018
Pearl River	^{15}N, denitrifier method	1.23–28.32	–	–	Zhang, 2016
Eastern Tropical Pacific	^{15}N tracer	–	0 – 0.5	0.003−0.06%[c] >2%[d]	Ji et al., 2018

Nitrosomonas europaea	Nutrients, N_2O concentrations	–	–	2.6–26%[e] 2.6–18%[h]	Yoshida & Alexander, 1970
Nitrosomonas sp. (Marine)	Nutrients, N_2O concentrations	–	–	0.26–0.99%[i] 2.5–9.9%[j]	Goreau et al., 1980
Nitrosomonas marina C-113a	Nutrients, N_2O isotopic analyses	–	50[g]	0.04–2.2%	Frame & Casciotti, 2010
Pearl River	Nutrients	11.28–26.88[a]	33.3 – 167.2	0.21–0.32%	This study

[a] The ammonia oxidation rates observed at the upper reach of PRE in summer.

[b] The nitrification rates observed at the upper estuary where the O_2 concentration from 0.67 to 1.41 mg L^{-1}, which were little lower than that ranging from 0.9 to 2.0 mg L^{-1} in our study.

[c] N_2O yield from ammonia oxidation under the O_2 >50 μM.

[d] N_2O yield from ammonia oxidation under the O_2 <0.5 μM.

[e] This experiment was designed to study the influence of different levels of ammonium concentration on N_2O formation by *Nitrosomonas europaea*.

[f] The ammonia oxidation rates were estimated based on the difference of ammonium concentrations between initial- and terminal- incubation time using the data from Yoshida and Alexander, 1970.

[g] Ammonium concentrations in the medium.

[h] This experiment was designed to study the influence of cells in different growth stages on N_2O formation by *Nitrosomonas europaea*.

[i] N_2O yield from ammonia oxidation under the O_2 ranging from 5–20% (56.3 –218.8 μM).

[j] N_2O yield from ammonia oxidation under the O_2 ranging from 0.5–1% (5.6 –10.9 μM).

References

Bianchi, M., Bonin, P., and Feliatra.: Bacterial nitrification and denitrification rates in the Rhône River plume (northwestern Mediterranean Sea), Mar. Ecol-Prog. Ser., 103, 197–202, 1994.

Damashek, J., Casciotti, K. L., and Francis, C. A.: Variable Nitrification Rates Across Environmental Gradients in Turbid, Nutrient-Rich Estuary Waters of San Francisco Bay, Estuaries and Coasts, 39, 1050–1071, 2016.

Damashek, J., and Francis, C. A.: Microbial Nitrogen Cycling in Estuaries: From Genes to Ecosystem Processes, Estuaries and Coasts, 41, 626–660, 2018.

Dai, M., Wang, L., Guo, X., Zhai, W., Li, Q., He, B., and Kao, S. J.: Nitrification and inorganic nitrogen distribution in a large perturbed river/estuarine system: the Pearl River Estuary, China, Biogeosciences, 5, 1545–1585, 2008.

De Wilde, H. P. J., and De Bie, M. J. M.: Nitrous oxide in the Schelde Estuary: production by nitrification and emission to the atmosphere, Mar. Chem., 69, 203–216, 2000.

Frame, C. H., and Casciotti, K. L.: Biogeochemical controls and isotopic signatures of nitrous oxide production by a marine ammonia-oxidizing bacterium, Biogeosciences, 7, 2695–2709, 2010.

Goreau, T. J., Kaplan, W. A., Wofsy, S. C., McElroy, M. B., Valois, F. W., and Watson, S. W.: Production of NO_2^- and N_2O by Nitrifying Bacteria at Reduced Concentrations of Oxygen, Appl. Environ. Microbiol., 40, 526–532, 1980.

Grundle, D. S., and Juniper, S. K.: Nitrification from the lower euphotic zone to the sub-oxic waters of a highly productive British Columbia fjord, Mar. Chem., 126, 173–181, 2011.

Hou, L., Xie, X., Wan, X., Kao, S. J., Jiao, N., and Zhang, Y.: Niche differentiation of ammonia and nitrite oxidizers along a salinity gradientnfrom the Pearl River estuary to the South China Sea, Biogeosciences, 15, 5169–5187, 2018.

Ji, Q., Buitenhuis, E., Suntharalingam, P., Sarmiento, J. L., and Ward, B. B.: Global Nitrous Oxide Production Determined by Oxygen Sensitivity of Nitrification and Denitrification, Global Biogeochem. Cy., 32, 1790–1802, 2018.

Pakulski, J. D., Amon, R., Eadie, B., and Whitledge, T.: Community metabolism and nutrient cycling in the Mississippi River: evidence for intense nitrification at intermediate salinities. Mar. Ecol-Prog. Ser., 117, 207–218, 1995.

Pakulski, J. D., Benner, R., Whitledge, T., Amon, R., Eadie, B., Cifuentes, L., Ammerman, J., and Stockwell, D.: Microbial metabolism and nutrient cycling in the Mississippi and Atchafalaya River plumes. Estuar. Coast. Shelf S., 50, 173–184, 2000.

Yoshida, T., and Alexander, M.: Nitrous Oxide Formation by Nitrosomonas europaea and Heterotrophic Microorganisms, Soil Sci. Soc. Amer. Proc., 34, 880–882,1970.

Zhang, X: Rates and Influence Factor of Water Nitrification and Inorganic Nitrogen Uptake in Pearl River Estuary, MA.Sc thesis, Xiamen University, Xiamen, China, 22 pp., 2016.

The strength of the correlation between genes and rates absolutely cannot be used to apportion a relative importance of one group of ammonia oxidizers or the other to the total rates. Nothing can be concluded from the data presented about who the important nitrifiers are. One possibility would be to obtain to a range of cell-specific ammonia oxidation rates from the literature and then use those in combination with the qPCR data to calculation the relative contribution of each group to the observed "rates."

Response:

The cell-specific ammonia oxidation rates, nitrite production rates, and N_2O production rates from the literature on AOA and AOB strains varied in a very large range, due to the different species cultures, cell densities, cell stages, and incubation conditions such as O_2 or substrates concentrations (see Table R2 below). It is fairly uncertain to use these greatly varying cell-specific rates from cultures to estimate the contribution of AOA and AOB to the N_2O production in natural environments. Notably, although the cell-specific N_2O production rates from AOB and AOA strains varied greatly, the N_2O yields from the AOB strains, ranging from 0.09 to 26 % (Table R2), were generally higher than the N_2O yield from the AOA strains (0.002−0.09%; Table R2). In addition, the higher N_2O yield from AOB has been observed in soils although the abundance of AOB was lower than AOA (Hink et al., 2017, 2018). We modified the discussion based on more literature on AOA and AOB cultures for better support. (Page 16, Lines 10−14).

We admit that the conclusions of this study mainly based on the correlation analysis and statistical analysis between multi-parameters. But there are two analyses providing more strong evidence supporting these statistical analyses:

(1) We attempted to accurately assess the relative contributions of AOA and AOB to N_2O production in the PRE by plotting the N_2O production rates (Fig. 7a) and yields (Fig. 7b) normalized to total (sum of AOA and AOB) *amo*A gene copies or transcripts at sites P01 and P05 along the x-y axes that represent the relative contributions of AOA and AOB to the total *amo*A gene or transcript pools.

Notably, compared to AOA, higher AOB abundance in the *amo*A gene-based DNA or cDNA pool resulted in distinctly higher (disproportionately higher relative to enhanced abundance) average *amo*A gene copy or transcript-specific N_2O production rates (Fig. 7a) and yields (Fig. 7b), suggesting that AOB may have higher cell-specific activities in the upper estuary and thus be more active in producing N_2O than AOA.

(2) The values of N stable isotopes in N_2O ($\delta^{15}N$) were analyzed. The much lower $\delta^{15}N$-N_2O (−27.9 to −12.6‰) upstream of the Humen outlet is consistent with AOB nitrification or denitrification processes, whereas enriched $^{15}N_2O$ (5.2−7.1‰) in the lower reaches approaches AOA nitrification and air ^{15}N-N_2O (Santoro et al., 2011). Taken together, the isotopic compositions of N_2O (Fig. 2h in the MS) and N_2O concentration distribution (Fig. 2e−g) suggest that the high concentrations of N_2O (oversaturation) were produced from strong nitrification by AOB and probably concurrent minor denitrification in the upper estuary, however in the lower reaches, low concentrations of N_2O could be explained by AOA nitrification or water atmospheric exchange of N_2O.

Table R2 Cell-specific ammonia oxidation rates, cell-specific N_2O production rates, and N_2O yield from archaeal and bacterial strains.

Microorganisms	Species (source of isolate)	Ammonia oxidation rates (fmol cell^{-1} h^{-1})[a]	N_2O production rates (fmol cell^{-1} h^{-1})[b]	N_2O yield[c]	Reference
AOA	*Nitrosopumilus maritimus* (Marine)	19.0	–	–	Martens-Habbena et al., 2009
		–	0.02–1.01	0.002–0.026%	Löscher et al., 2012
		–	–	0.03–0.05%	Stieglmeier et al., 2014
	Nitrososphaera viennensis (Soil)	2.6–2.8	0.004–0.005	0.03–0.09%	Stieglmeier et al., 2014
AOB	*Nitrosomonas sp.* (Marine)	2.0–15.4	0.04–0.21	0.26–9.9%	Goreau et al., 1980
	Nitrosomonas marina (Marine)	0.9–4.9	–	–	Glover, 1985
		13.7–31.3	–	–	Glover, 1985
	Nitrosococcus oceanus (Ocean)	83.3	–	–	Waston, 1965
	Nitrosomonas europaea (Soil)	–	–	0.26±0.1%	Goreau et al., 1980
		12.4–18.3	–	2.6–26%	Yoshida & Alexander, 1970
		–	–	0.47±0.1%	Goreau et al., 1980
	Nitrosospira tenuis NV12 (Soil)	–	0.002	–	Shaw et al., 2006
	Nitrosomonas europaea ATCC 19718	–	0.06	–	Shaw et al., 2006
	Nitrosospira multiformis (Soil)	–	–	0.09–0.27%	Stieglmeier et al., 2014

Nitrosolobus multiformis (Soil)	–	–	0.09 ±0.02%	Goreau et al., 1980
Nitrosospira briensis (Soil)	–	–	0.11 ±0.04%	Goreau et al., 1980

[a] The units for cell-specific ammonia oxidation rates in the citied references were unified as fmol $cell^{-1}$ h^{-1}.

[b] The units for cell-specific N_2O production rates in the citied references were unified as fmol $cell^{-1}$ h^{-1}.

[c] The range of N_2O yield of different cell densities under different O_2 conditions.

References

Glover, H. E.: The relationship between inorganic nitrogen oxidation and organic carbon production in batch and chemostat culture of marine nitrifying bacteria. Arch. Microbio., 142, 45–50, 1985.

Goreau, T. J., Kaplan, W. A., Wofsy, S. C., McElroy, M. B., Valois, F. W., and Watson, S. W.: Production of NO_2^- and N_2O by Nitrifying Bacteria at Reduced Concentrations of Oxygen, Appl. Environ. Microbiol., 40, 526–532, 1980.

Hink, L., Nicol, G. W., and Prosser, J. I.: Archaea produce lower yields of N_2O than bacteria during aerobic ammonia oxidation in soil, Environ. Microbiol., 19, 4829–4837, 2017.

Hink, L., Gubry-Rangin, C., Nicol, G. W., and Prosser, J. I.: The consequences of niche and physiological differentiation of archaeal and bacterial ammonia oxidisers for nitrous oxide emissions, ISME J., 12,1084–1093, 2018.

Löscher, C. R., Kock, A., Könneke, M., LaRoche, J., Bange, H. W., and Schmitz, R. A.: Production of oceanic nitrous oxide by ammonia-oxidizing archaea, Biogeosciences, 9, 2419–2429, 2012.

Martens-Habbena, W., Berube, P. M., Urakawa, H., de la Torre, J. R., and Stahl, D. A.: Ammonia oxidation kinetics determine niche separation of nitrifying Archaea and Bacteria, Nature, 461, 976–979, 2009.

Shaw, L. J., Nicol, G. W., Smith, Z., Fear, J., Prosser, J. I., Baggs, E. M.: *Nitrosospira* spp. can produce nitrous oxide via a nitrifier denitrification pathway, Environ. Microbiol., 8, 214–222, 2006.

Stieglmeier, M., Mooshammer, M., Kitzler, B., Wanek, W., Zechmeister-Boltenstern, S., Richter, A., and Schleper, C.: Aerobic nitrous oxide production through N-nitrosating hybrid formation in ammonia-oxidizing archaea, ISME J., 8, 1135–1146, 2014.

Waston, S. W: Characteristics of a marine nitrifying bacterium, Nitrosocystis oceanus sp. N., Limnol Oceanogr., 10, R274–R289, 1965.

Yoshida, T., and Alexander, M.: Nitrous Oxide Formation by Nitrosomonas europaea and Heterotrophic Microorganisms, Soil Sci. Soc. Amer. Proc., 34, 880–882,1970.

The literature review, both in the Introduction and Discussion, is severely lacking. There is a substantial literature about nitrification and N_2O production in estuaries, almost none of which are referenced here. Normally I would provide some specific suggestions, but the omissions are too

vast to list. One place to start would be a review by Damashek and Francis 2018 Estuaries and Coasts, or a nice earlier paper with a summary of nitrification rates in estuaries, Damashek et al. 2016 Estuaries and Coasts.

Response:

Very sorry for this problem. We added the estuarine studies literature review on nitrification and N_2O production in the Introduction and Discussion of the revised version.

Introduction (Page 3, Lines 9−24): "*Estuaries are highly impacted by coastal nutrient pollution and eutrophication because of anthropogenic activity; they play a significant role in nitrogen cycling at the land−sea interface (Bricker et al., 2008; Damashek et al., 2016; Damashek and Francis 2018). Estuarine and coastal regimes have long been recognized as major zones of N_2O production in the marine system (Seitzinger and Kroeze, 1998; Mortazavi et al., 2000; Usui et al., 2001; Kroeze et al., 2010; Allen et al., 2011). In particular, eutrophic estuaries with extensive oxygen-deficient zones have been considered hotspot regions for N_2O production (Abril et al., 2000; De Wilde and De Bie, 2000; Garnier et al., 2006; Lin et al., 2016), with oversaturated N_2O and high N_2O concentrations and flux (De Wilde and De Bie 2000; De Bie et al. 2002; Garnier et al., 2006; Rajkumar et al., 2008; Barnes and Upstill-Goddard 2011; Lin et al., 2016). The dynamics of N_2O emissions in these ecosystems are regulated by complex physical and biogeochemical processes; for example, mixing between freshwater and oceanic waters influences the biogeochemistry of estuarine waters as well as microbial activity (Huertas et al., 2018; Laperriere et al., 2019).*"

"*Nitrification is often credited as the dominant N_2O production pathway in estuaries (De Bie et al. 2002; Barnes and Upstill-Goddard 2011; Kim et al. 2013; Lin et al. 2016; Huertas et al., 2018; Laperriere et al., 2019).*"

Discussion 4.1 subsection (Page 13, Lines 26−27, and Page 14, Lines 1−5): "*Previous studies also proposed that nitrification may be the major source of N_2O production in the water column in estuarine systems, such as the Guadalquivir (Huertas et al., 2018), Schelde (De Wilde and De Bie, 2000), and Chesapeake Bay (Laperriere et al., 2019). However, in the estuarine sediments, N_2O production was attributed to both nitrification and denitrification, such as in the Tama (Japan) (Usui et al., 2001) and Yangtze (China) estuaries (Liu et al., 2019; Wang et al., 2019), where denitrification is the major nitrogen removal pathway with N_2O production and consumption"*

References

Abril, G., Riou, S. A., Etcheber, H., Frankignoulle, M., de Wit, R., Middelburg, J. J.: Transient tidal time-scale, nitrogen transformations in an estuarine turbidity maximumfluid mud system (the

Gironde, south-west France), Estuar. Coast. Shelf S. 50, 703–715, 2000.

Allen, D., Dalal, R. C., Rennenberg, H., and Schmidt, S.: Seasonal variation in nitrous oxide and methane emissions from subtropical estuary and coastal mangrove ediments, Australia, Plant Biol., 13, 126-133, 2011.

Barnes, J., and Upstill-Goddard, R. C.: N_2O seasonal distributions and air–sea exchange in UK estuaries: Implications for the tropospheric N_2O source from European coastal waters, J. Geophys. Res., 116, G01006, 2011. http://dx.doi.org/10.1029/2009JG001156.

Bricker, S. B., Longstaff, B., Dennison, W., Jones, A., Boicourt, K.,Wicks, C., and Woerner, J.: Effects of nutrient enrichment in the nation's estuaries: a decade of change, Harmful Algae, 8, 21–32, 2008.

Damashek, J., Casciotti, K. L., and Francis, C. A.: Variable Nitrification Rates Across Environmental Gradients in Turbid, Nutrient-Rich Estuary Waters of San Francisco Bay, Estuaries and Coasts, 39, 1050–1071, 2016.

Damashek, J., and Francis, C. A.: Microbial Nitrogen Cycling in Estuaries: From Genes to Ecosystem Processes, Estuaries and Coasts, 41, 626–660, 2018.

De Wilde, H. P. J., and De Bie, M. J. M.: Nitrous oxide in the Schelde Estuary: production by nitrification and emission to the atmosphere, Mar. Chem., 69, 203–216, 2000.

De Bie, M. J. M., Middelburg, J .J., Starink, M., and Laanbroek, H. J.: Factors controlling nitrous oxide at the microbial community and estuarine scale, Mar. Ecol- Prog. Ser., 240, 1–9, 2002.

Garnier, J., Cébron, A., Tallec, G., Billen, G., Sebilo, M., and Martinez, A.: Nitrogen behaviour and nitrous oxide emission in the tidal Seine River estuary (France) as influenced by human activities in the upstream watershed. Biogeochemistry, 77, 305–326, 2006.

Huertas, I. E., Flecha, S., Navarro, G., andPerez, F. F., de la Paz, M.: Spatio-temporal variability and controls on methane and nitrous oxide in the Guadalquivir Estuary, Southwestern Europe, Aquat Sci., 80, 29, 2018.

Kim, I. N., Lee, K., Bange, H.W., Macdonald, A. M.: Interannual variation in summer N_2O concentration in the hypoxic region of the northern gulf of Mexico, 1985–2007, Biogeosciences, 10, 6783–6792, 2013.

Kroeze, C., Dumont, E., and Seitzinger, S.: Future trends in emissions of N_2O from rivers and estuaries, J. Integr. Environ. Sci., 7, 71–78, 2010.

Laperriere, S. M., Nidzieko, N. J., Fox, R. J., Fisher, A. W., Santoro, A. E.: Observations of variable ammonia oxidation and nitrous oxide flux in a eutrophic estuary, Estuar Coast, 42, 33–44, 2019.

Lin, H., Dai, M., Kao, S. J., Wang, L., Roberts, E., Yang, J., Huang, T., and He, B.: Spatiotemporal

variability of nitrous oxide in a large eutrophic estuarine system: The Pearl River Estuary, China, Mar. Chem., 182, 14–24, 2016.

Liu, C., Hou, L., Liu, M., Zheng, Y., Yin, G., Han, P., Dong, H., Gao, J., Gao, D., Chang, Y., Zhang, Z.: Coupling of denitrification and anaerobic ammonium oxidation with nitrification in sediments of the Yangtze Estuary: Importance and controlling factors, Estura. Coast. Shelf. S., 220, 64–72, 2019.

Mortazavi, B., Iverson, R. L., Huang, W., Graham Lewis, F., Caffrey, J. M.: Nitrogen budget of Apalachicola Bay, a bar-built estuary in the northeastern Gulf of Mexico, Mar. Ecol.-Prog. Ser., 195, 1–14, 2000.

Rajkumar, A. N., Barnes, J., Ramesh, R., Purvaja, R., and Upstill-Goddard, R. C.: Methane and nitrous oxide fluxes in the polluted Adyar River and estuary, SE India., Mar. Pollut. Bull., 56, 2043–2051, 2008.

Seitzinger, S. P., and Kroeze, C.: Global distribution of nitrous oxide production and N inputs in freshwater and coastal marine ecosystems, Glob. Biogeochem. Cycle, 12, 93-113, 1998.

Usui, T., Koike, I., and Ogura, N.: N_2O production, nitrification and denitrification in an estuarine sediment, Estuar. Coast. Shelf S., 52, 769-781, 2001.

Wang, J., Kan, J., Qian, G., Chen, J., Xia, Z., Zhang, X., Liu, H., and Sun, J.: Denitrification and anammox: Understanding nitrogen loss from Yangtze Estuary to the east China sea (ECS), Environ. Pollut., 2019. https://doi.org/10.1016/j.envpol.2019.06.025.

The nirS data are not very useful to this manuscript in that there is essentially no relationship between nirS abundance and N_2O production from denitrification. nirS presence could just as easily be a marker for N_2O consumption.

Response:

The *nir*S and *nir*K genes encode cytochrome cd1 and copper-containing nitrite reductase, respectively. They were functionally and physiologically equivalent, but structurally different and could not be detected in the same strains in the previous research (Coyne et al., 1989), while the recent genomic analyses found a few bacteria contain both *nir*S and *nir*K (Graf et al., 2014).

Indeed, *nir*S-type denitrifiers are more likely to be capable of complete denitrification due to a higher frequency of co-occurrence of the N_2O reductase gene (*nos*Z) with *nir*S than *nir*K gene (Graf et al., 2014).

However, it was reported that *nir*S genes were more widely distributed than the *nir*K genes (Zumft, 1997; Bothe et al., 2000), and *nir*S genes were both more abundant and more diverse than *nir*K in

the estuarine water columns (Zhu et al., 2018; Wang et al., 2019) and various estuarine sediments (Nogales et al, 2002; Santoro et al, 2006; Abell et al., 2010; Mosier and Francis, 2010; Beman, 2014; Smith et al., 2015; Lee and Francis, 2017). The previous study on the Pearl River sediment also showed that *nir*K abundance was much lower than *nir*S abundance (Huang et al., 2011). Therefore, we used the *nir*S gene to identify the distribution of denitrifiers in the PRE and reflect the denitrification potential.

Our incubation experiments indicated that denitrification was not the main process contributing to N_2O production in the water column of the Pearl River Estuary. So far, there is no direct evidence showing that denitrification or nitrifier-denitrification are responsible for N_2O production in the PRE water column, but a release of N_2O into the overlying waters through denitrification was reported in the PRE sediments (Tan et al., 2019). Further study is needed to clarify the potentials of both *nir*K- and *nir*S-type denitrifiers in N_2O production from the interface between sediment and water in the PRE.

We added the discussion of the potential role of *nir*K-type denitrifier for N_2O production in PRE in the 4.3 subsection (Page 17, Lines 10−16).

References

Abell, G. C. J., Revill, A. T., Smith, C., Bissett, A. P., Volkman, J. K., and Robert, S. S.: Archaeal ammonia oxidizers and *nirS*-type denitrifiers dominate sediment nitrifying and denitrifying populations in a subtropical macrotidal estuary, ISME J., 4, 286–300, 2010.

Beman, J. M.: Activity, abundance, and diversity of nitrifying archaea and denitrifying bacteria in sediments of a subtropical estuary: Bah á del T óbari, Mexico. Estuar. Coast, 37, 1343–1352, 2014.

Bothe, H., Jost, G., Schloter, M., Ward, B. B., and Witzel, K. P.: Molecular analysis of ammonia oxidation and denitrification in natural environments, FEMS Microbiol. Rev., 24, 673–690, 2000.

Coyne, M. S., Arunakumari, A., Averill, B. A., and Tiedje, J. M.: Immunological identification and distribution of dissimilatory heme cd1 and non-heme copper nitrite reductases in denitrifying bacteria, Appl. Environ. Microbiol., 55, 2924–2931, 1989.

Graf, D. R. H., Jones, C. M., and Hallin,. S.: Intergenomic comparisons highlight modularity of the denitrification pathway and underpin the importance of community structure for N_2O emissions. PloS One 9: e114118. https://doi.org/10.1371/journal.pone.0114118. s008. 2014

Huang, S., Chen, C., Yang, X., Wu, Q., and Zhang, R.: Distribution of typical denitrifying

functional genes and diversity of the nirS-encoding bacterial community related to environmental characteristics of river sediments, Biogeosciences, 8, 3041–3051, 2011.

Lee, J. A., and Francis, C.A.: Spatiotemporal characterization of San Francisco Bay denitrifying communities: A comparison of *nir*K and *nir*S diversity and abundance. Microbial Ecology 73, 271–284, 2017.

Mosier, A. C., and Francis, C. A.: Denitrifier abundance and activity across the San Francisco Bay Estuary, Env. Microbiol. Rep., 2, 667–676, 2010.

Nogales, B., Timmis, K. N., Nedwell, D. B., and Osborn, A. M.: Detection and diversity of expressed denitrification genes in estuarine sediments after reverse transcription-PCR amplification from mRNA, Appl. Environ. Microbiol., 68, 5017–5025, 2002.

Santoro, A. E., Boehm, A. B., and Francis, C.A.: Denitrifier community composition along a nitrate and salinity gradient in a coastal aquifer. Appl. Environ. Microbiol., 72, 2102–2109, 2006.

Smith, J. M., Mosier, A. C., and Francis, C. A.: Spatiotemporal relationships between the abundance, distribution, and potential activities of ammonia-oxidizing and denitrifyingmicroorganisms in intertidal sediments. Microb. Ecol., 69, 13–24, 2015.

Tan, E., Zou, W., Jiang, X., Wan, X., Hsu, T. C., Zheng, Z., Chen, L., Xu, M., Dai, M., Kao, S.: Organic matter decomposition sustains sedimentary nitrogen loss in the Pearl River Estuary, China, Sci. Total. Environ., 648, 508–517, 2019.

Wang, J., Kan, J., Qian, G., Chen, J., Xia, Z., Zhang, X., Liu, H., and Sun, J.: Denitrification and anammox: Understanding nitrogen loss from Yangtze Estuary to the east China sea (ECS), Environ. Pollut., 2019. https://doi.org/10.1016/j.envpol.2019.06.025.

Zhu, W., Wang, C., Hill, J., He, Y., Tao, B., Mao, Z., and Wu, W.: A missing link in the estuarine nitrogen cycle?: Coupled nitrification-denitrification mediated by suspended particulate matter, Sci. Rep., 8, 2282, 2018. DOI:10.1038/s41598-018-20688-4

Zumft, W. G.: Cell biology and molecular basis of denitrification, Microbiol. Mol. Biol. R., 61, 533–616, 1997.

All the physical dynamics in the system have been reduced to a very naive "water mass" identification. Basic concepts in estuarine biogeochemistry are absent–for example, using salinity as a conservative tracer in a two-end member mixing model to determine production and loss of the various biogeochemical parameters.

Response:

According to the reviewer’s suggestion, we performed the end-member mixing analysis. We

conclude that the two end-member model is not appropriate for the upper estuary where however, the major N_2O produced and which acts as a strong N_2O source of the PRE and is the highlight of this study. The two-end member mixing analysis in Lingdingyang (the mid-estuary and lower-estuary) reveal the removal of N_2O and this removal is attributed to the water-air exchange. However, a significant positive correlation between the removal portion of N_2O (ΔN_2O) and ammonia consumption ($\Delta(NH_3+NH_4^+)$) suggests that the removal portion of N_2O maybe mostly related to ammonia oxidation in the Lingdingyang surface water. Please see below for detail.

We plotted a three-dimensional scatter (Figure R3; see below) to show the relationships between potential temperature (θ) (^oC), salinity, and silicate (SiO_3^{2-}) concentration. Silicate has long been recognized as one of the most common indicators to trace river water in the ocean, and the low salinity and high silicate contents were the best indicators for river source (Moore, 1986). The results indicate that the waters from the upper estuary, where the salinity of most sites was close to zero, had high potential temperature and silicate concentration. The mixing behaviors of waters occurred at the Humen outlet (sites P07 and A01), and the waters from the off-shore sites (A10 and A11) had high salinity and low potential temperature and silicate concentration.

Therefore, we divide the transect into the northern (upstream of the Humen outlet) and southern (Lingdingyang) areas to analyze the end-member mixing. Obviously, the two end-member model with salinity is not appropriate for the upper estuary since the salinity of the upper-estuary sites (upstream of Humen) all is close to zero and the upper estuary is highly impacted by the wastewater inputs, sewage discharged from Guangzhou, and different tributaries (Dai et al., 2006). We only discuss the estuarine mixing in Lingdinngyang using the end-member mixing model (Lin et al., 2016). The water from the Humen-outlet site (A01) with the lowest salinity was defined as the freshwater end-member and the water from the most off-shore site (A11) with the highest salinity was defined as the seawater end member. The mixing model is based on mass balance equations for salinity and the water fractions originating from the two end-members (Lin et al., 2016).

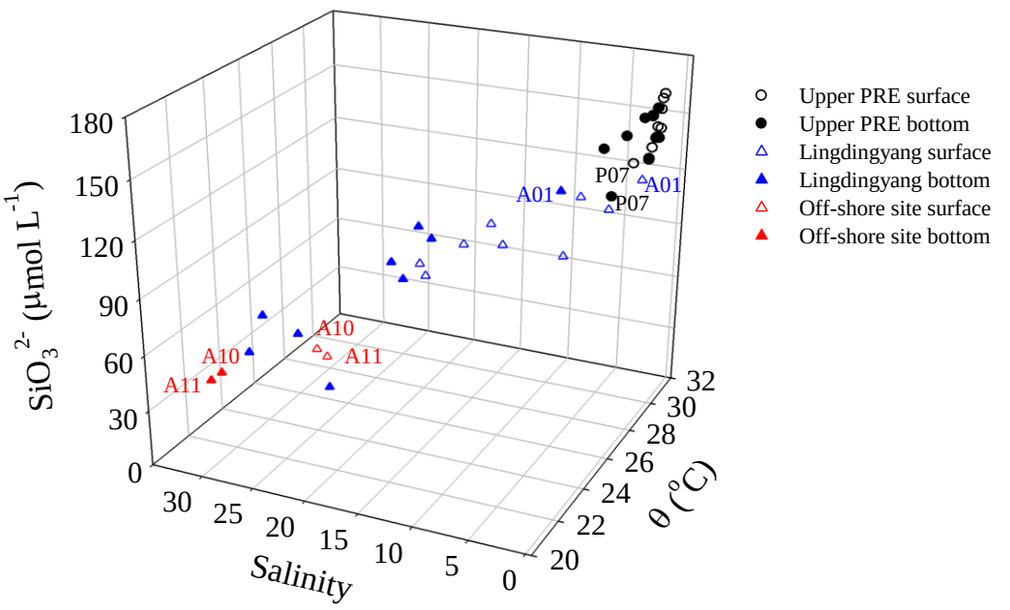

Figure R3 (Figure S1 in the revised MS): Three-dimensional scatter plot of potential temperature (θ) (°C), salinity, and silicate (SiO_3^{2-}) concentration.

The conservative mixing behavior of silicate along salinity was observed in Figure R4a. Based on the theoretical dilution line, NO_2^- and NO_3^- (weak) accumulations were observed in the Lingdingyang transect (Figure R4c and d); in contrast, N_2O removal was observed in Figure R4e.

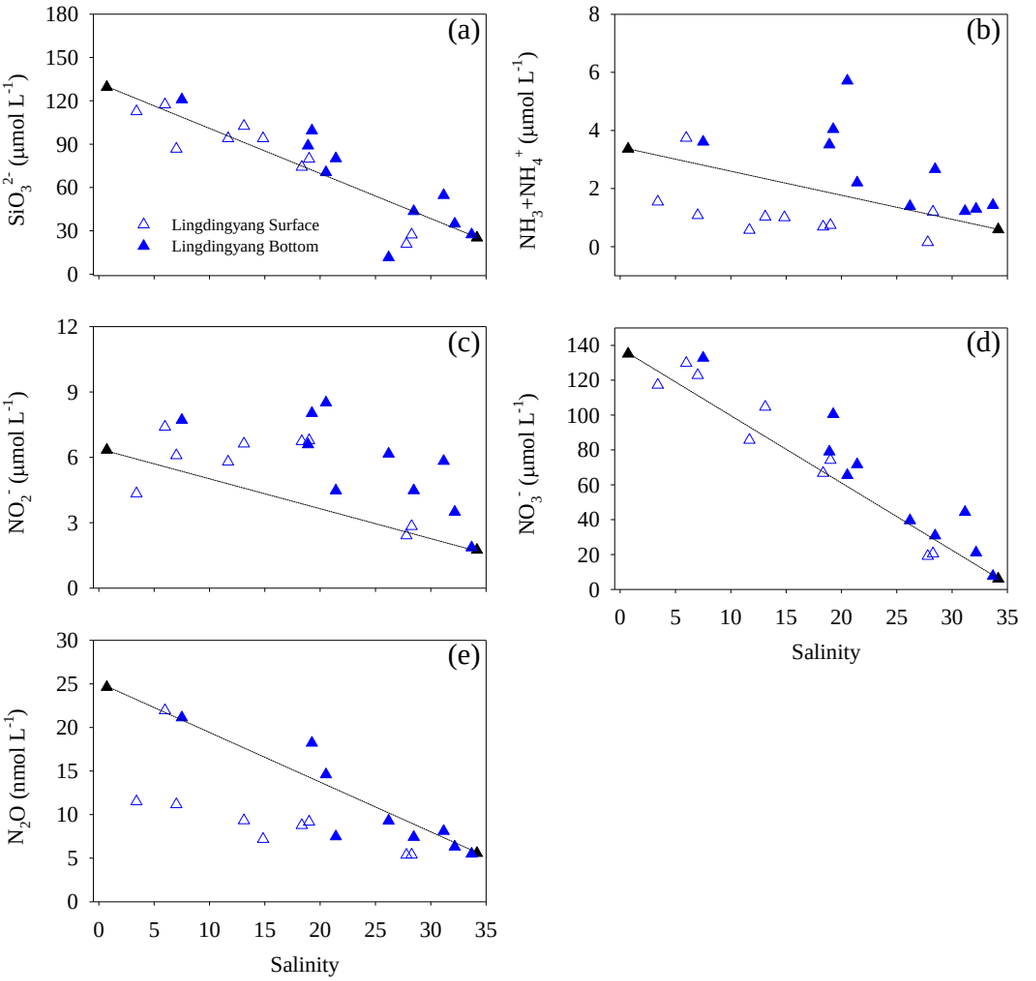

Figure R4: Mixing processes of (a) SiO_3^{2-}, (b) NH_3+NH_4^+, (c) NO_2^-, (d) NO_3^-, and (e) N_2O in Lingdingyang area of the PRE. End-members applied in the mixing model are presented as black solid triangles and the dashed lines represent the theoretical dilution line.

We calculated the fractions of the two end-members based on mass balance and salinity and estimated the conservative concentrations of ammonia ($(NH_3+NH_4^+)_{con}$), nitrite ($NO_2^-{}_{con}$), nitrate ($NO_3^-{}_{con}$), and N_2O (N_2O_{con}) from conservative mixing by model prediction. The relationships between the field-observed concentrations of ammonium ($(NH_3+NH_4^+{}_{obs})$), nitrite ($NO_2^-{}_{obs}$), nitrate ($NO_3^-{}_{obs}$), and N_2O (N_2O_{obs}) and the model-predicted conservative concentrations were shown in Figure R5. The results show that the points of $(NH_3+NH_4^+)_{obs}$ versus $(NH_3+NH_4^+)_{con}$ are mostly below the 1:1 line (Figure R5a), suggesting the consumption of ammonia, and the points of $NO_2^-{}_{obs}$ versus $NO_2^-{}_{con}$ are mostly above the 1:1 line, suggesting the nitrite addition (Figure R5b). The points of $NO_3^-{}_{obs}$ versus $NO_3^-{}_{con}$ are mostly near the 1:1 line (Figure R5c). The points of N_2O_{obs} versus N_2O_{con} in the surface water are mostly below the 1:1 line (Figure R5d), suggesting the

removal of N_2O. This removal is attributed to the water-air exchange (Lin et al., 2016). Notably, there is a significant positive correlation between the removal portion of N_2O (ΔN_2O) and ammonia consumption ($\Delta(NH_3+NH_4^+)$) in the Lingdingyang surface water (Figure R5f), suggesting that the removal portion of N_2O maybe mostly related to ammonia oxidation in the surface water.

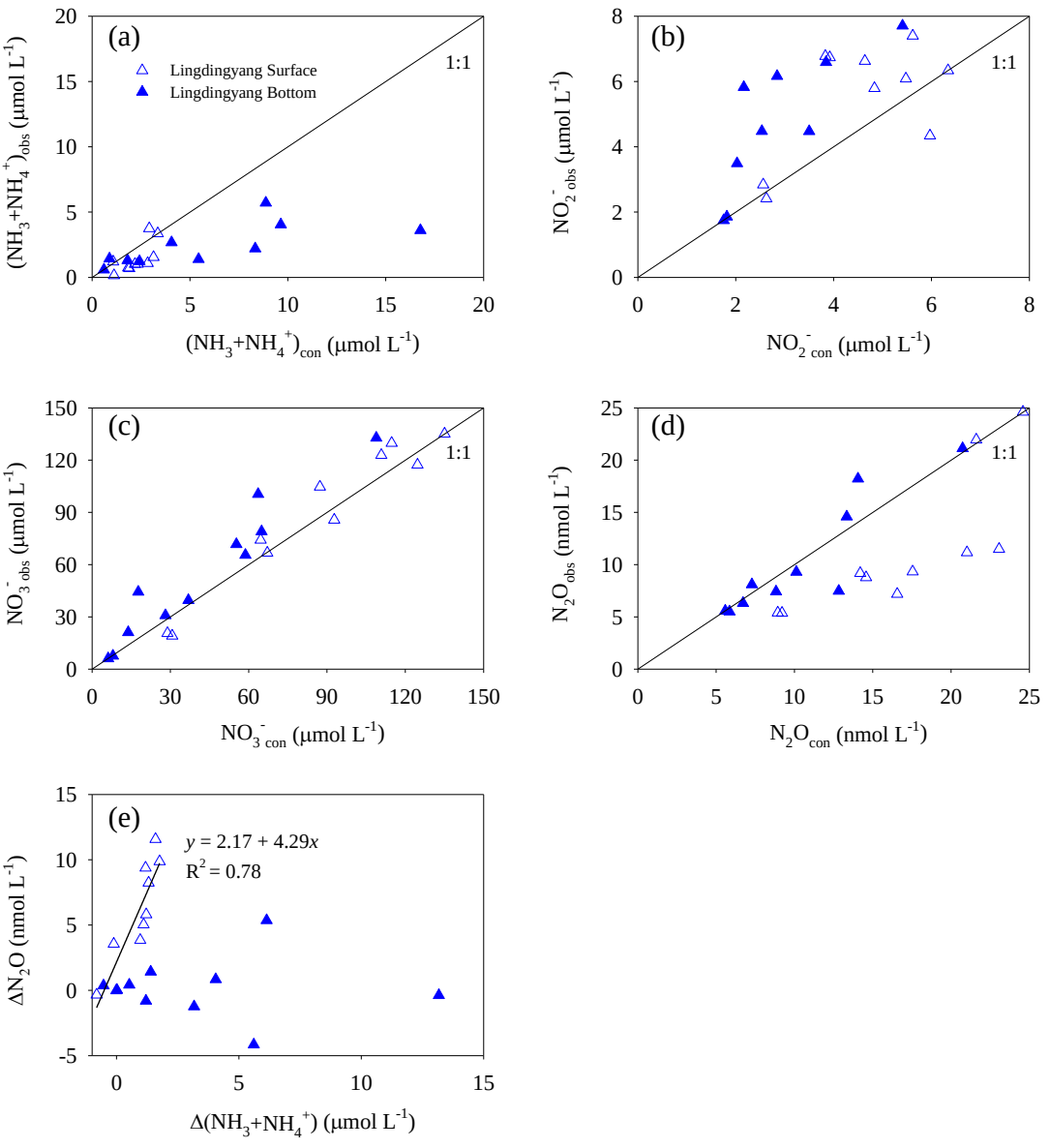

Figure R5: The field-observed versus the model-predicted conservative concentrations of (a) ammonia, (b) nitrite, (c) nitrate, and (d) N_2O. (e) The relationship between the removal portion of N_2O (ΔN_2O) and ammonia consumption ($\Delta(NH_3+NH_4^+)$).

References

Dai, M., Guo, X., Zhai, W., Yuan, L., Wang, B., Wang, L., Cai, P., Tang, T., and Cai, W. J.: Oxygen

depletion in the upper reach of the Pearl River estuary during a winter drought, Mar. Chem., 102, 159–169, 2006.

Lin, H., Dai, M., Kao, S. J., Wang, L., Roberts, E., Yang, J., Huang, T., and He, B.: Spatiotemporal variability of nitrous oxide in a large eutrophic estuarine system: The Pearl River Estuary, China, Mar. Chem., 182, 14–24, 2016.

Moore, W. S., Sarmiento, J. L., and Key, R. M.: Tracing the Amazon component of surface Atlantic water using 228Ra, salinity and silica, J. Geophys. Res., 91, 2574–2580, 1986.

Specific comments:

p. 3 lines 15-16 Unclear to me what is meant by "runoff ranked 17th".

Response:

Sorry for the unclear sentence. We modified this sentence as "*The Pearl River Estuary (PRE) is one of the world's most complex estuarine systems with a total discharge of 285.2×10^9 m^3 yr^{-1}*" (Page 4, Lines 5−6).

p. 5 lines 2-4 What N_2O standards were used? How was the GC calibrated?

Response:

We added this information and revised this sentence as "*N_2O concentrations were analyzed by gas chromatography (GC, Agilent 6890 μECD) coupled with a purge-trap system (Tekmar Velocity XPT) at 25 ℃ (Lin et al., 2016). N_2O standard gases of 1.02 and 2.94 ppmv N_2O/N_2 (National Center of Reference Material, China, Beijing) were used. The relative standard deviation of the slope of the standard working curve was 1.77% (n=8). The detection limit was calculated to be about ~0.1 nmol L^{-1}, and the precision was better than ±5%. When water samples were analyzed, every 5−10 samples were spiked with N_2O standards to calibrate the GC.*" (Page 5, Lines 21−27).

Reference

Lin, H., Dai, M., Kao, S. J., Wang, L., Roberts, E., Yang, J., Huang, T., and He, B.: Spatiotemporal variability of nitrous oxide in a large eutrophic estuarine system: The Pearl River Estuary, China, Mar. Chem., 182, 14–24, 2016.

p. 5 line 6 How was $N_2O_{aquatic}$ calculated?

Response:

We stated "*$N_2O_{aquatic}$ represents the measured concentrations of N_2O in the water*" below the equation (Page 6, Line 4), which were measured using gas chromatography (Agilent 6890 μECD) coupled with a purge-trap system (Tekmar Velocity XPT) according to Lin et al. (2016). We described detailedly the method above the equations (Page 5, Lines 21−27; please also see our previous response).

For clarification, we revised $N_2O_{aquatic}$ as $N_2O_{observed}$.

p.7 lines 3 How much did DO concentration change over the course of the 24 h incubations? What effect would this have on the measured N2O production?

Response:

DO in the incubation system was fast consumed and below the detection limit of the Winkler method during 24-hour incubation at site P01 (in-situ DO below 1.0 mg kg^{-1}). Obvious reduction of both NH_3 and NO_3^- and accumulation of NO_2^- were observed (Fig. 5 a-c) in the late phase (18−24 hours) of the incubation, suggesting that nitrification and denitrification might be coupled under suboxic/anoxic conditions. The accumulation of N_2O could be reduced along with the incubation time when occurring complete denitrification in the ending phase. When N_2O production and consumption co-occurred, the N_2O yield during nitrification would be underestimated. Thus we only calculated the N_2O production rate and yield during the early-middle phase of the incubation where DIN was in balance, which was stated in Methods 2.4 subsection (Page 8, Lines 20−27, and Page 9, Line 1) and Results 3.4 subsection (Page 12, Lines 17−22).

At site P05, ~55% of DO was consumed during the 12-hour incubation in the bottom water, decreasing from 54.7 to 24.6 μmol L^{-1}; ~34% of DO was consumed in the surface water during 12 hours, decreasing from 61.3 to 40.3 μmol L^{-1}. But there was no N loss and DIN was in balance during the incubations, so there was no effect on the measurement of N_2O production.

p. 7 lines 18-19 Were both N_2O yield equations used? Compared? Were they equal?

Response:

Sorry for the confusion. We only used Eq. (8) (N_2O_{yield} (%) = ΔN_2O-N / $\Delta(NH_3 + NH_4^+)$-N) to estimate N_2O yield. Eq. (9) (N_2O_{yield} (%) = ΔN_2O-N / $\Delta(NO_2^- + NO_3^-)$-N) was deleted in the revised MS (Page 9, Line 1), which is not suitable to estimate N_2O yield from nitrification in this study since denitrification could occur and nitrate and nitrite concentrations decreased in the ending phase

of the incubation at site P01.

In addition, we also compared the N_2O yield estimated by Eq (8) and Eq (9) for site P05, where the only nitrification occurred during 12-hour incubation. The N_2O yield estimated by Eq (8) and Eq (9) was 0.21% and 0.19%, respectively in the surface water and 0.32% and 0.33%, in the bottom water. They are almost equal.

More details are needed about how you arrived at the Schmidt number for N_2O. Is this the Raymond and Cole reference?

Response:

We added more details in Methods 2.2 subsection (Page 6, Lines 15−24). Please also see below.

"k_{N_2O} was estimated using Eq. (6) according to Wanninkhof (1992):

$$k_{N_2O} = 0.31 \times u_{av}^2 \times (Sc_{N_2O}/600)^{-0.5} \quad (6)$$

where u_{av} is the average wind speed at 10 m above the water surface. In this study, a CO_2 Schmidt number (Sc) of 600 at 20 ℃ in fresh water (Wanninkhof, 1992) was used for estuarine systems (Raymond and Cole, 2001). The Sc is defined as the kinematic viscosity of water divided by the diffusion coefficient of the gas and calculated from temperature (Wanninkhof, 1992). For N_2O in waters with salinities <35 and temperatures ranging from 0−30 ℃, Sc_{N_2O} was estimated using Eq. (7) according to Wanninkhof (1992): ..."

Need additional details of the calibration of the isotopic values.

Response:

We added more details of the calibration of the isotopic values in the revised version (2.2 subsection).

Page 7, Lines 1−7: "*The molecular ions of N_2O (N_2O^+, m/z 44, 45, and 46) were quantified by IRMS to calculate isotope ratios for the entire molecule ($^{15}N/^{14}N$ and $^{18}O/^{16}O$). The $\delta^{15}N$ values of N_2O in samples were calculated using the $^{15}N/^{14}N$ of the pure N_2O reference gas and samples (Frame and Casciotti, 2010; Mohn et al., 2014). The reference gas was previously calibrated against N_2O isotopic standard gas ($\delta^{15}N$ (vs Air-N_2) = −0.320‰) produced by Shoko Co. Ltd. (Tokyo, Japan) and the $\delta^{15}N$ value (vs Air-N_2) of the N_2O reference gas is 6.579 ± 0.030‰. The precision of the method for $\delta^{15}N$-N_2O was estimated as 0.3‰.*"

References:

Frame, C. H., and Casciotti, K. L.: Biogeochemical controls and isotopic signatures of nitrous oxide production by a marine ammonia-oxidizing bacterium, Biogeosciences, 7, 2695–2709, 2010.

Mohn, J., Wolf, B., Toyoda, S., Lin, C. T., Liang, M. C., Brüggemann, N., Wissel, H., Dyckmans, A. E. S, J., Szwec, L., Ostrom, N. E., Casciotti, K. L., Forbes, M., Giesemann, A., R., Doucett, R. R., Well, Yarnes, C. T., Ridley, A. R., Kaiser, J., and Yoshida, N.: Interlaboratory assessment of nitrous oxide isotopomer analysis by isotope ratio mass spectrometry and laser spectroscopy: current status and perspectives, Rapid Commun Mass Spectrom. 28, 1995–2007, 2014.

p.7 Why is N_2O yield in units of permil? (line 18-19, and also in the Discussion). Also would be more conventional to list this as N_2O-N not N-N_2O

Response:

We revised the unit as % and replaced N-N_2O with N_2O-N as suggested.

No discussion of particle attached versus free living amoA copies. Data is presented in multiple figures. Previous literature show no association. Did the filters clog?

Response:

We added more details in Methods 2.1 subsection (Page 5, Lines 3−4) —"*For the upper estuary samples, more membrane filters were used to avoid the filters clogging.*"

We also added more discussion of particle attached versus free living amoA copies in Discussion 4.2 subsection (Page 14, Lines 21−27, and Page 15, Lines 1−4) —"*The more abundant AOA amoA genes, relative to AOB, and the more abundant genes in the PA communities than FL communities are consistent with our previous study in the PRE (Hou et al., 2018), …. Lower oxygen availability in particle micro-niches has been reported to be favorable for both nitrification and denitrification potential in oxygenated water (Kester et al., 1997). The Spearman correlations and RDA analyses in this study indicate that high nutrient and TSM concentrations and low DO and pH conditions were favourable for relatively high abundance distribution of AOB in the upper estuary, which is also consistent with our previous PRE study that found high TSM concentrations and low DO and pH influenced substrate availability and thus AOB distribution (Hou et al., 2018).*"

References:

Hou, L., Xie, X., Wan, X., Kao, S. J., Jiao, N., and Zhang, Y.: Niche differentiation of ammonia and

nitrite oxidizers along a salinity gradientnfrom the Pearl River estuary to the South China Sea, Biogeosciences, 15, 5169–5187, 2018.

Kester, R. A., de Boer, W., and Laanbroek, H. J.: Production of NO and N2O by pure cultures of nitrifying and denitrifying bacteria during changes in aeration, Appl. Environ. Microbiol., 63, 3872–3877, 1997.

P. 9 lines 4-6 “the entire PRE acts as a N_2O source” but negative air-sea fluxes are reported in the previous sentence?

Response:

The estimated water–air N_2O fluxes were 100.4 to 344.0 μmol m^{-2} d^{-1} upstream and decreased in Lingdingyang (42.4 to -2.6 μmol m^{-2} d^{-1}). Taken together, the PRE was a strong source. We revised this sentence as “*Together, the PRE acts as a N_2O source*” (Page 10, Line 16).

p.11 lines 19-26: This paragraph confuses some important concepts. Some of these numbers are the isotopic composition of N_2O produced by ammonia oxidizers, but some of these numbers are the isotope effect (epsilon). Also, the isotopic composition of the N_2O being produced by nitrification is dependent on the isotopic composition of the NH_3 being oxidized, for which no measurements or even estimates are provided.

Response:

All data in this paragraph are from literature. We only used the isotopic composition of N_2O from literature in this paragraph and supplementary Table S2. But sorry for the wrong title and footnote of supplementary Table S2. We revised the title as “*Isotopic composition of N_2O during bacterial and archaeal ammonia oxidation, bacterial nitrifier-denitrification, and bacterial denitrification.*” We revised the footnote as “*[b]Although the $\delta^{15}N$-N_2O when using NH_2OH as a substrate are listed here, the isotopic composition of N_2O only when using NH_4^+ as a substrate was discussed in natural environments.*”

p.12 lines 15-17: Doesn’t make sense to refer to ’water masses’ in estuaries. There is a tremendous amount of mixing that leads to variation in these parameters. Just because something is a different salinity doesn’t mean it’s a different ’water mass.’ These parameters are just ’hydrography.’

Response:

Here, we revised “water masses parameters” as “hydrographic parameters” (Page 11, Line 18). We

also revised “water masses” as “water mixing” in other places of the MS (Page 15, Lines 8, 10, 13, 15, and 19, and Page 37, Line 2).

p. 12 lines 15-28 and p. 13 lines 1-18 A lot of results presented that should be moved to the results section.

Response:

Thanks for the reviewer’s suggestion. We moved the Spearman correlations and RDA analyses into the Results 3.3 subsection “Correlations between genes abundances and biogeochemical parameters” (Page 11, Lines 15−27, and Page 12, Lines 1−5).

p. 12 line 27 “ammonia oxidizer community” The use of the word “community” throughout the paper is confusing. More accurate to state the abundances of AOA and AOB?

Response:

We revised “ammonia oxidizer community” as “AOA and AOB distributions”, and moved this part into the Results 3.3 subsection according to the reviewer’s suggestion (Page 11, Line 25). The similar use of “community” in other places was also revised (Page 9, Lines 10 and 17; Page 34, Lines 2; Page 37, Lines 2, 5 and 6).

p. 24 Fig 1 i,j It looks like two different slopes in the data upstream and Lingdingyang. This could be quantified using a break point analysis.

Response:

Thanks for the suggestion. We re-quantified using a breakpoint analysis (see below) and revised the related description —“*notably, a significant negative relationship was observed between ΔN_2O_{excess} or N_2O flux and DO ($P < 0.01$ for each) in the upper estuary (Fig. 2i and j).*” (Page 10, Lines 17−18)

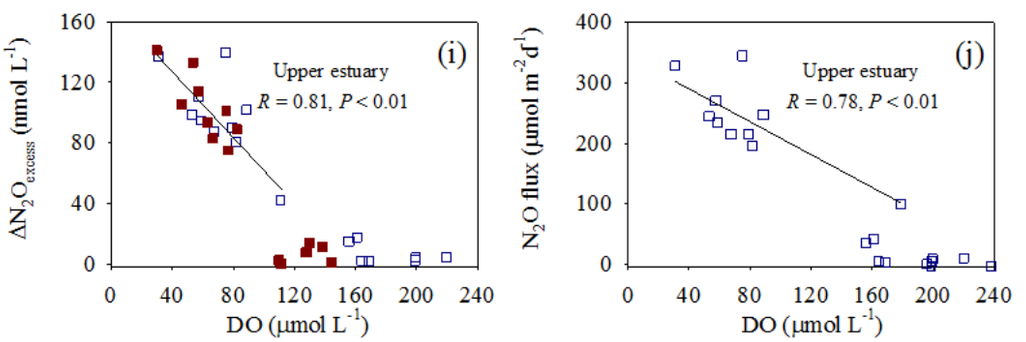

Figure R6: (i) ΔN_2O vs. DO and (j) N_2O flux vs. DO.

p. 32 I found this figure confusing. Perhaps it would be useful to have a table with the data presented in the figure? It is unclear using AOB and AOA% if the normalized N_2O production values are a result of the N_2O yield or low/high amoA abundance.

Response:

We added a supplementary Table S3 (below) showing the data in Figure 7. We plotted the N_2O production rates (Fig. 7a) and yields (Fig. 7b) normalized to total (sum of AOA and AOB) *amo*A gene copies or transcripts at sites P01 and P05 along the x-y axes that represent the relative contributions of AOA and AOB to the total *amo*A gene or transcript pools. The results indicate that compared to AOA, higher AOB abundance in the *amo*A gene-based DNA or cDNA pool resulted in distinctly higher (disproportionately higher relative to enhanced abundance) average *amo*A gene copy or transcript-specific N_2O production rates (Fig. 7a) and yields (Fig. 7b), suggesting that AOB may have higher cell-specific activities in the upper estuary and thus be more active in producing N_2O than AOA. We modified the statements for clarification (Page 16, Lines 2−10).

Table R3 (Table S3 in the MS) The abundances of DNA- and cDNA-based *amo*A gene and the N_2O production net rates and yields normalized to total *amo*A gene copy or transcript numbers of AOA and AOB in a given sample at the incubation experiment sites.

Site_ Layer	DNA-based AOB (All) (copies L^{-1})	DNA-based AOA (All) (copies L^{-1})	N_2O production rates (All) (f mol $cell^{-1}$ h^{-1})	N_2O yields (All) (10^{-6})	DNA-based AOB (PA) (copies L^{-1})	DNA-based AOA (PA) (copies L^{-1})	N_2O production rates (PA) (f mol $cell^{-1}$ h^{-1})	N_2O yields (PA) (10^{-6})	cDNA-based AOB (PA) (copies L^{-1})	cDNA-based AOA (PA) (copies L^{-1})	N_2O production rates (PA) (f mol $cell^{-1}$ h^{-1})	N_2O yields (PA) (10^{-6})
P05_S	14030	34427	23.70	21.30	12125	29082	27.90	25.00	382928	138646	2.20	1.97
P05_B	87915	397740	2.90	3.25	77820	357308	3.24	3.63	89559	12559	13.80	15.50
P01_S	19623	642905	0.91	1.93	9343	578974	1.02	2.18	500	461578	1.30	2.77
P01_B	21334	251163	5.91	5.47	16458	221184	6.77	6.27	362	7436	206.00	191.00

S, surface; B, bottom; All, sum of particle-attached and free-living fractions; PA, particle-attached fraction.

Technical corrections

p. 2 lines 18-22 Needs citation “Denitrification by heterotrophic denitrifiers is another major pathway of N_2O production in marine environments. NO_2^- is reduced by a copper-containing (NirK) or cytochrome cd1-containing nitrite reductase (NirS) to nitric oxide (NO), and then by a heme-copper NO reductase (NOR) to N_2O.”

Response:

We added citations.

Page 2, Lines 19−26: “*Denitrification by heterotrophic denitrifiers is another major pathway of N_2O production in marine environments, occurring under anoxic conditions or at the suboxic-anoxic interface (Naqvi et al., 2010; Yamagishi et al., 2007; Ji et al., 2018). NO_2^- is reduced by a copper-containing (NirK) or cytochrome cd1-containing nitrite reductase (NirS) to nitric oxide (NO), and then by a heme-copper NO reductase (NOR) to N_2O (Coyne et al., 1989; Treusch et a1., 2005; Abell et al., 2010; Bartossek et a1., 2010; Lund et a1., 2012; Graf et al., 2014). As an intermediary product during denitrification, production and further reduction of N_2O are sensitive to different O_2 conditions (Babbin et al., 2015; Ji et al., 2015).*”

References:

Abell, G. C. J., Revill, A. T., Smith, C., Bissett, A. P., Volkman, J. K., and Robert, S. S.: Archaeal ammonia oxidizers and *nirS*-type denitrifiers dominate sediment nitrifying and denitrifying populations in a subtropical macrotidal estuary, ISME J., 4, 286–300, 2010.

Babbin, A. R., Bianchi, D., Jayakumar, A., and Ward, B. B.: Rapid nitrous oxide cycling in the suboxic ocean, Science, 348, 1127–1129, 2015.

Bartossek, R., Nicol, G.W., Lanzen, A., Klenk, H. P., and Schleper, C.: Homologues of nitrite reductases in ammonia-oxidizing archaea: diversity and genomic context, Environ. Microbiol., 12, 1075–1088, 2010.

Coyne, M. S., Arunakumari, A., Averill, B. A., and Tiedje, J. M.: Immunological identification and distribution of dissimilatory heme cd1 and non-heme copper nitrite reductases in denitrifying bacteria, Appl. Environ. Microbiol., 55, 2924–2931, 1989.

Graf, D. R. H., Jones, C. M., and Hallin,. S.: Intergenomic comparisons highlight

modularity of the denitrification pathway and underpin the importance of community structure for N_2O emissions. PloS One 9: e114118. https://doi.org/10.1371/journal.pone.0114118. s008. 2014.

Ji, Q., Babbin, A. R., Jayakumar, A., Oleynik, S., and Ward, B. B.: Nitrous oxide production by nitrication and denitrication in the Eastern Tropical South Pacific oxygen minimum zone, Geophy. Res. Lett., 42, 10, 755–10, 764, 2015.

Ji, Q., Buitenhuis, E., Suntharalingam, P., Sarmiento, J. L., and Ward, B. B.: Global Nitrous Oxide Production Determined by Oxygen Sensitivity of Nitrification and Denitrification, Global Biogeochem. Cy., 32, 1790–1802, 2018.

Lund, M. B., Smith, J. M., and Francis, C. A.: Diversity, abundance and expression of nitrite reductase *(nirK)*-like genes in marine thaumarchaea, ISME J., 6, 1966–1977, 2012.

Naqvi, S. W. A., Bange, H. W., Far ás, L., Monteiro, P. M. S., Scranton, M. I., and Zhang, J.: Marine hypoxia/anoxia as a source of CH_4 and N_2O, Biogeosciences, 7, 2159–2190, 2010.

Yamagishi, H., Westley, M. B., Popp, B. N., Toyoda, S., Yoshida, N., Watanabe, S., Koba, K., and Yamanak, Y.: Role of nitrification and denitrification on the nitrous oxide cycle in the eastern tropical North Pacific and Gulf of California, J Geophy. Res., 112, G02015, doi:10.1029/2006JG000227, 2007.

Treusch, A. H., Leininger, S., Kletzin, A., Schuster, S. C., Klenk, H., and Schleper, C.: Novel genes for nitrite reductase and Amo-related proteins indicate a role of uncultivated mesophilic crenarchaeota in nitrogen cycling, Environ. Microbiol., 7, 1985–1995, 2005.

p.3 lines 3 citation should be after “soil” “and arable (Clark et al., 2012; Jones et al., 2014) soils”

Response:

Revised (Page 3, Line7).

p. 3 lines 10-11 Needs citation

“Moreover, there is a potential niche overlap between nitrifiers and denitrifiers in low oxygen conditions.”

Response:

We added three citations (Page 3, Line 28, and Page 4, Line 1) as follows:

Frame, C. H., and Casciotti, K. L.: Biogeochemical controls and isotopic signatures of nitrous oxide production by a marine ammonia-oxidizing bacterium, Biogeosciences, 7, 2695–2709, 2010.

Penn, J., Weber, T., and Deutsch, C.: Microbial functional diversity alters the structure and sensitivity of oxygen deficient zones, J. Geophys. Res. Lett., 43, 9773–9780, 2016.

Zhang, Y., Xie, X., Jiao, N., Hsiao, S. S. Y., and Kao, S. J.: Diversity and distribution of *amoA*-type nitrifying and *nir*S-type denitrifying microbial communities in the Yangtze River estuary, Biogeosciences, 11, 2131–2145, 2014.

p. 4 lines 15-16 Should be moved to results section 2.2 discussing ammonia analysis "Ammonia/ammonium concentrations were analyzed onboard."

Response:

We moved this sentence to 2.2 subsection.

Page 5, Lines 18−19: "*Ammonia was measured using the indophenol blue spectrophotometric method (Pai et al., 2001) on board*"

p. 4 line 25-26 What salinity, temperature and DO probes were used?

Response:

We revised this sentence.

Page 5, Lines 17−18: "*Temperature and salinity were measured with the SBE 25 CTD system. Dissolved oxygen (DO) concentrations were measured using the Winkler method (Dai et al., 2006).*"

p. 5 lines 5-23 Not all variables in the equations are defined.

Response:

We added more details for the equations and defined all variables in the revised MS (Page 6, Lines 1−24).

p. 31 Fig 6 Should axes be swapped?

Response:

We swapped X and Y axes in Fig. 6 of the revised version (Page 37).

Major role of ammonia-oxidizing bacteria in N_2O production in the Pearl River Estuary

Li Ma[1,2], Hua Lin[1,2,3], Xiabing Xie[1], Minhan Dai[1,2], Yao Zhang[1,2]

[1]State Key Laboratory of Marine Environmental Science, Xiamen University, Xiamen 361101, China

[2]College of Ocean and Earth Sciences, Xiamen University, Xiamen 361101, China

[3]Key Laboratory of Marine Ecosystem and Biogeochemistry, State Oceanic Administration, Second Institute of Oceanography, Ministry of Natural Resources, Hangzhou 310012, China

Correspondence to: Yao Zhang (yaozhang@xmu.edu.cn)

Abstract. Nitrous oxide (N_2O) has significant global warming potential as a greenhouse gas. Estuarine and coastal regimes are the major zones of N_2O production in the marine system. However, biological sources of N_2O in estuarine ecosystems remain controversial, but are of great importance for understanding global N_2O emission patterns. Here, we measured concentrations and isotopic compositions of N_2O as well as distributions of ammonia-oxidizing bacterial and archaeal *amo*A and denitrifier *nir*S genes by quantitative polymerase chain reaction along a salinity gradient in the Pearl River Estuary, and performed in situ incubation experiments to estimate N_2O yields. Our results indicated that nitrification predominantly occurred, with significant N_2O production during ammonia oxidation, in the hypoxic waters of the upper estuary where the maximum N_2O and ΔN_2O_{excess} concentrations were observed, although minor denitrification might be concurrent at the site with the lowest dissolved oxygen. Ammonia-oxidizing *β*-proteobacteria (AOB) were significantly positively correlated with all N_2O-related parameters, although their *amo*A gene abundances were distinctly lower than ammonia-oxidizing Archaea (AOA) throughout the estuary. Furthermore, the N_2O production rate and the N_2O yield normalized to *amo*A gene copies or transcripts estimated a higher relative contribution of AOB to the N_2O production in the upper estuary. Taken together, the in situ incubation experiments, N_2O isotopic composition and concentrations, and gene datasets suggested that the high concentration of N_2O (oversaturated) is mainly produced from strong nitrification by the relatively high abundance of AOB in the upper reaches and is the major source of N_2O emitted to the atmosphere in the Pearl River Estuary.

Deleted: s

Deleted: is

Deleted: the

Deleted: and transcript levels

Deleted: as

Deleted: whole

Deleted: e

1 Introduction

Nitrous oxide (N_2O) is a potent greenhouse gas with global warming potential 298 times that of carbon dioxide (CO_2) on a 100 yr timescale, and contributes to stratospheric ozone depletion as a major precursor of free radicals (Ravishankara et al., 2009). N_2O emissions from soils and marine systems are estimated to account for 56%–70% (6–7 Tg N_2O-N yr^{-1}) (Syakila and Kroeze, 2011; Butterbach-Bahl et al., 2013; Hink et al., 2017) and 30% (4 Tg N_2O-N yr^{-1}) (Nevison et al., 2004; Naqvi et al., 2010; Voss et al., 2013) of the total global N_2O emissions, respectively. The main processes responsible for N_2O emissions are microbial transformation of ammonia, nitrite, and nitrate through nitrification and denitrification (Butterbach-Bahl et al., 2013). It has been estimated that oceanic N_2O production is dominated by nitrification, whereas only 7% is contributed by denitrification (Freing et al., 2012).

N_2O is released as a byproduct during nitrification via incomplete oxidation of hydroxylamine (NH_2OH) to nitrite (NO_2^-) by ammonia-oxidizing bacteria (AOB) (Stein, 2011). This process may be enhanced under suboxic conditions (Naqvi et al., 2010). While no equivalent of the hydroxylamine-oxidoreductase that catalyzes N_2O formation through NH_2OH oxidation has been found in ammonia-oxidizing archaea (AOA) (Hatzenpichler, 2012), recent studies indicated that AOA possibly produces hybrid N_2O via a combination of an ammonia oxidation intermediate (NH_2OH, HNO, or NO) and NO_2^- (Stieglmeier et al., 2014; Frame et al., 2017). In addition, AOB have been shown to produce N_2O from NO_2^- during nitrifier denitrification (Shaw et al., 2006). This process is also promoted under micro-oxic and anoxic conditions (Yu et al., 2010). Denitrification by heterotrophic denitrifiers is another major pathway of N_2O production in marine environments, occurring under anoxic conditions or at the suboxic–anoxic interface (Naqvi et al., 2010; Yamagishi et al., 2007; Ji et al., 2018). NO_2^- is reduced by a copper-containing (NirK) or cytochrome cd1-containing nitrite reductase (NirS) to nitric oxide (NO), and then by a heme-copper NO reductase (NOR) to N_2O (Coyne et al., 1989; Treusch et a1., 2005; Abell et al., 2010; Bartossek et a1., 2010; Lund et a1., 2012; Graf et al., 2014). As an intermediary product during denitrification, production and further reduction of N_2O are sensitive to different O_2 conditions (Babbin et al., 2015; Ji et al., 2015).

Biological nitrogen transformations are catalyzed by various microbial enzymes, of which ammonium monooxygenase (AMO) and nitrite reductases (NIRs) are key enzymes responsible for

Formatted: Superscript
Deleted:
Deleted:
Deleted:
Deleted:
Deleted:
Deleted:
Deleted:

nitrification and denitrification, respectively (Canfield et al., 2010). The genes encoding for AMO subunit A (*amo*A) and NIRs (*nir*S and *nir*K) have been widely applied as functional marker genes to identify the distribution of ammonia oxidizers and denitrifiers. Previous studies have shown significant correlations of *amo*A with spatial variations of N_2O emissions or N_2O production rates in soils and oceans (Avrahami and Bohanann, 2009; Santoro et al., 2011; Löscher et al., 2012). In addition, significant relationships between *nir*K or *nir*S abundances and N_2O emissions were observed in grasslands (Čuhel et al., 2010), arable soils (Clark et al., 2012; Jones et al., 2014), and the ocean (Arévalo-Martínez et al., 2015).

Estuaries are highly impacted by coastal nutrient pollution and eutrophication because of anthropogenic activity; they play a significant role in nitrogen cycling at the land–sea interface (Bricker et al., 2008; Damashek et al., 2016; Damashek and Francis 2018). Estuarine and coastal regimes have long been recognized as major zones of N_2O production in the marine system (Seitzinger and Kroeze, 1998; Mortazavi et al., 2000; Usui et al., 2001; Kroeze et al., 2010; Allen et al., 2011). In particular, eutrophic estuaries with extensive oxygen-deficient zones have been considered hotspot regions for N_2O production (Abril et al., 2000; De Wilde and De Bie, 2000; Garnier et al., 2006; Lin et al., 2016), with oversaturated N_2O and high N_2O concentrations and flux (De Wilde and De Bie 2000; De Bie et al. 2002; Garnier et al., 2006; Rajkumar et al., 2008; Barnes and Upstill-Goddard 2011; Lin et al., 2016). The dynamics of N_2O emissions in these ecosystems are regulated by complex physical and biogeochemical processes; for example, mixing between freshwater and oceanic waters influences the biogeochemistry of estuarine waters as well as microbial activity (Huertas et al., 2018; Laperriere et al., 2019).

Nitrification is often credited as the dominant N_2O production pathway in estuaries (De Bie et al. 2002; Barnes and Upstill-Goddard 2011; Kim et al. 2013; Lin et al. 2016; Huertas et al., 2018; Laperriere et al., 2019). Although AOA frequently outnumber AOB and dominate microbial communities, their contribution to nitrification remains controversial in estuarine and coastal waters (Bernhard et al., 2010; Zhang et al., 2014; Hou et al., 2018). Furthermore, the relative contributions of AOB and AOA to N_2O production is inconclusive (Monteiro et al., 2014) and there is a potential niche overlap between nitrifiers and denitrifiers in low oxygen conditions (Frame and Casciotti, 2010; Zhang

Deleted: and

Deleted: (Clark et al., 2012; Jones et al., 2014)

Deleted: , being

Deleted: due to

Deleted: ,

Deleted: -

Deleted: the

Deleted: as

Deleted: the

Deleted: d

Deleted: in abundance

Deleted: ; additionally

Deleted: . Moreover,

et al., 2014; Penn et al., 2016). AOB are reported to thrive in hypoxic environments and denitrification in the oxic ocean is suggested to occur within anoxic particle interiors (Frame and Casciotti, 2010; Ni et al., 2014). It is therefore of great importance to elucidate the biological sources of N_2O production in estuarine ecosystems to better understanding global N_2O emission patterns.

The Pearl River Estuary (PRE) is one of the world's most complex estuarine systems with a total discharge of 285.2×10^9 m^3 yr^{-1} (Dai et al., 2014). The PRE is surrounded by complex regions with a rich nitrogen supply that produces eutrophic waters (Dai et al., 2008). Moreover, increased oxygen consumption by organic matter degradation leads to the formation of hypoxic zones in the upper reaches of the PRE (Dai et al., 2006; He et al., 2014), which may support strong nitrification, denitrification, and N_2O production (Lin et al., 2016). In this study, N_2O-related biogeochemical parameters were measured, and distributions of AOB and AOA *amo*A and denitrifier *nir*S genes were quantified by quantitative polymerase chain reaction (qPCR) to investigate the relationship between N_2O production and spatial distribution of nitrifiers and denitrifiers along a salinity gradient in the PRE (Fig. 1). Moreover, in situ incubation experiments were performed in the hypoxic upper estuary to estimate (1) nitrification and N_2O production rates, (2) whether denitrification occurred during nitrification, and (3) N_2O yield (mol N_2O-N produced per mol ammonia oxidized). By combining the genetic datasets and incubation estimates, this study thus identified the relative contributions of AOB and AOA in producing N_2O in the PRE.

2 Materials and methods

2.1 Study area and sampling

A total of 22 sites along the salinity gradient of the PRE were sampled during a research cruise in July 2015, including 11 sites in the upper reaches (upstream of the Humen outlet) and 11 sites in the lower reaches (Lingdingyang) (Fig. 1). Water samples were taken from the surface (2 m) and bottom (4–15 m) of each site by using a conductivity, temperature, and depth (CTD) rosette sampling system (SBE 25; Sea-Bird Scientific, USA) fitted with 12 L Niskin bottles (General Oceanics). A total of 16 samples (from two depths at eight sites) were subjected to gene analysis (Fig. 1). A total of 1 L of water for gene

Deleted: ,
Deleted: anaerobic
Deleted: the
Deleted: ,
Deleted: the
Deleted: , runoff ranked 17th of the world rivers
Deleted: that supply
Deleted: inputs and
Deleted: that support active nitrification
Deleted: (de)
Deleted: or
Deleted: ¶
Deleted: and transcript levels
Deleted: AOA and AOB and *nir*S
Deleted: rates
Deleted: μ
Deleted: Inc
Deleted: One liter

analysis was serially filtered through 0.8 μm and then 0.22 μm pore size polycarbonate membrane filters (47 mm diameter, Millipore) within 30 min at a pressure <0.03 MPa to retain the particle-associated (PA) communities (>0.8 μm) and free-living (FL) communities (0.22–0.8 μm). For the upper estuary samples, more membrane filters were used to avoid the filters clogging. RNAlater solution (Ambion, Austin, Texas, USA) was quickly added to the samples to prevent RNA degradation. All of the filters were immediately flash frozen in liquid nitrogen and then stored at −80 ℃ until further analysis. Water samples for nutrient determination were filtered through 0.45 μm pore size cellulose acetate membranes and then immediately frozen at −20 ℃ until further analysis. Water samples for dissolved N_2O were collected into 125 mL headspace glass bottles to which 100 μL of saturated $HgCl_2$ was added; the bottles were immediately closed with rubber stoppers and aluminum crimp-caps and stored in the dark at 4 ℃ until analysis in the laboratory. All N_2O samples were collected during the July 2015 cruise except for samples from sites P03, P05, A01, A06, and A10 intended for N_2O isotopic composition analyses, which were sampled during a cruise in March 2010. Total suspended material (TSM) was collected by filtering 1–4 L of water onto pre-combusted and pre-weighed glass fiber filters (GF/Fs) (Whatman), and then stored at −20 ℃ until weighing in the laboratory.

2.2 Biogeochemical parameters, N_2O emissions and isotopic analysis of environmental samples

Temperature and salinity were measured with the SBE 25 CTD system. Dissolved oxygen (DO) concentrations were measured using the Winkler method (Dai et al., 2006). Ammonia was measured using the indophenol blue spectrophotometric method (Pai et al., 2001) on board; nitrate, nitrite, and silicate were analyzed using routine spectrophotometric methods with a Technicon AA3 Auto-Analyzer (Bran-Lube, GmbH) (Han et al., 2012). N_2O concentrations were analyzed by gas chromatography (GC, Agilent 6890 μECD) coupled with a purge-trap system (Tekmar Velocity XPT) at 25 ℃ (Lin et al., 2016). N_2O standard gases of 1.02 and 2.94 ppmv N_2O/N_2 (National Center of Reference Material, China, Beijing) were used. The relative standard deviation of the slope of the standard working curve was 1.77% (n=8). The detection limit was calculated to be ~0.1 nmol L^{-1} and the precision was better than ±5%. When water samples were analyzed, every 5−10 samples were spiked with N_2O standards to calibrate the GC.

Deleted: in
Deleted: -
Deleted: -
Deleted: Ammonia/ammonium concentrations were analyzed onboard.
Deleted: were
Deleted: part
Deleted: (
Deleted:)
Deleted: membranes
Deleted: -
Deleted: ,
Deleted: continuously
Deleted: the
Deleted: with a SBE 43 Dissolved Oxygen DO probe Sensor (Sea-Bird Co.). All DO concentrations used in this study was measured
Deleted: and calibrated on board by
Deleted: with
Deleted: the
Deleted: to

The excess N_2O (ΔN_2O_{excess}) and N_2O saturation (S%) were calculated with Eq. (1) and (2):

$$\Delta N_2O_{excess} = N_2O_{observed} - N_2O_{equilibrium} \quad (1)$$

$$S\% = N_2O_{observed} / N_2O_{equilibrium} \times 100\% \quad (2)$$

where $N_2O_{observed}$ represents the measured concentrations of N_2O in the water, and the equilibrium values of N_2O ($N_2O_{equilibrium}$) were calculated by Eq. (3) and (4) (Weiss and Price, 1980):

$$N_2O_{equilibrium} = xF \quad (3)$$

$$\ln F = A_1 + A_2(100/T) + A_3 \ln(T/100) + A_4(T/100)^2 + S[B_1 + B_2(T/100) + B_3(T/100)^2] \quad (4)$$

where x is the mole fraction of N_2O in the atmosphere and T is the absolute temperature. In this study, we used the global mean atmospheric N_2O (327 ppb) from 2015 (http://www.esrl.noaa.gov/gmd). The fitted function F and constants A1, A2, A3, A4, B1, B2 and B3 were proposed by Weiss and Price (1980).

The N_2O flux (F_{N_2O}, μmol m^{-2} d^{-1}) through the air–sea interface was estimated based on Eq. (5):

$$F_{N_2O} = k_{N_2O} \times \rho \times K_H^{N_2O} \times \Delta pN_2O = k_{N_2O} \times 24 \times 10^{-2} \times (N_2O_{observed} - N_2O_{equilibrium}) \quad (5)$$

where k_{N_2O} (cm h^{-1}) is the N_2O gas transfer velocity depending on wind and water temperature, $K_H^{N_2O}$ is the solubility of N_2O, and ΔpN_2O is the average sea–gas N_2O partial pressure difference. k_{N_2O} was estimated using Eq. (6) according to Wanninkhof (1992):

$$k_{N_2O} = 0.31 \times u_{av}^2 \times (Sc_{N_2O}/600)^{-0.5} \quad (6)$$

where u_{av} is the average wind speed 10 m above the water surface. In this study, a CO_2 Schmidt number (Sc) of 600 at 20 ℃ in fresh water (Wanninkhof, 1992) was used for estuarine systems (Raymond and Cole, 2001). The Sc is defined as the kinematic viscosity of water divided by the diffusion coefficient of the gas and calculated from temperature (Wanninkhof, 1992). For N_2O in waters with salinities <35 and temperatures ranging from 0−30 ℃, Sc_{N_2O} was estimated using Eq. (7) according to Wanninkhof (1992):

$$Sc_{N_2O} = 2055.6 - 137.11\ t + 4.3173\ t^2 - 0.05435\ t^3 \quad (7)$$

where t is the in situ temperature of the sampling site.

To determine the isotopic composition of N_2O, the gas samples were introduced into a trace gas cryogenic pre-concentration device (PreCon, Thermo Finnigan), as described in Cao et al. (2008) and Zhu et al. (2008), and then $\delta^{15}N$-N_2O was analyzed using an isotope ratio mass spectrometer (IRMS,

Deleted: aquatic
Deleted: (
Deleted:)
Deleted: aquatic
Deleted: aquatic
Deleted: are
Deleted: as
Formatted: Superscript
Deleted: -
Deleted: -
Deleted: -
Deleted: aquatic
Deleted: -
Deleted: *calculated using Eq. (6) and (7) (Wanninkhof, 1992) and k600 is used for a freshwater system (Raymond and Cole, 2001):* ¶
Deleted: 2
Deleted: c
Deleted: -
Deleted:
Deleted: of
Deleted: y
Deleted: i
Deleted: the following
Deleted: c
Formatted: Not Superscript/ Subscript
Formatted: Not Superscript/ Subscript

Thermo Finngan MAT-253, Bremen, Germany). The molecular ions of N_2O (N_2O^+, m/z 44, 45 and 46) were quantified by IRMS to calculate isotope ratios for the entire molecule ($^{15}N/^{14}N$ and $^{18}O/^{16}O$). The $\delta^{15}N$ values of N_2O in samples were calculated using the $^{15}N/^{14}N$ of the pure N_2O reference gas and samples (Frame and Casciotti, 2010; Mohn et al., 2014). The reference gas was previously calibrated against N_2O isotopic standard gas ($\delta^{15}N$ (vs Air-N_2) = −0.320‰) produced by Shoko Co. Ltd. (Tokyo, Japan) and the $\delta^{15}N$ value (vs Air-N_2) of the N_2O reference gas is 6.579±0.030‰. The precision of the method for $\delta^{15}N$-N_2O was estimated as 0.3‰.

Deleted:

Deleted: to be

Deleted: uantitative

2.3 Nucleic acid extraction and qPCR

DNA was extracted using the FastDNA™ SPIN Kit for Soil (MP, USA) according to the manufacturers' protocol with minor modifications. RNA was extracted using TRIzol reagent (Ambion, Austin, Texas, USA), and then eluted with 50 μL of RNase-free water. The extracted RNA was treated with DNase I (Invitrogen, Carlsbad, CA) to remove any residual DNA. DNA contamination was checked by amplifying the bacterial 16S rRNA genes before reverse transcription. Total RNA without DNA contamination was reverse transcribed to synthesize single-strand complementary DNA (cDNA) using the First-Strand cDNA Synthesis Kit (Invitrogen, Austin, Texas, USA).

The transcript and copy abundances of bacterial and archaeal *amo*A genes and bacterial *nir*S genes were examined using qPCR and a CFX96 Real Time PCR system (BIO-RAD, Singapore). The *β*-proteobacterial and archaeal *amo*A were amplified using primer sets amoA-1F and amoA-2R (Kim et al., 2008) and Arch-amoAF and Arch-amoAR (Francis et al., 2005), respectively; *nir*S was amplified using primers nirS-1F and nirS-3R (Braker et al., 1998; Huang et al., 2011). Quantitative PCR amplification for the *β*-proteobacterial and archaeal *amo*A was carried out as described previously (Mincer et al., 2007; Hu et al., 2011). For the amplification of *nir*S, the qPCR reaction mixture was prepared in accordance with Zhang et al. (2014) and thermal cycling conditions were as described in Huang et al. (2011). Standards for the qPCR reactions consisted of serial 10-fold dilutions (10^7 to 10^0 copies per uL) of plasmid DNA containing amplified fragments of the targeted genes (accession numbers MH458281 for *β*-proteobacterial *amo*A, KY387998 for archaeal *amo*A, and KF363351 for *nir*S). The amplification efficiencies of qPCR were always between 85%–95% with R^2 >0.99. The

Deleted: ere

Deleted: applied

Deleted: by

Deleted: ,

specificity of the qPCR reactions was confirmed by melting curve analysis, agarose gel electrophoresis and sequencing analysis. Inhibition tests were performed by 2-fold and 5-fold dilutions of all samples and indicated that our samples were not inhibited.

2.4 Incubation experiments

Incubation experiments were performed in the surface and bottom waters at sites P01 (2 and 5 m water depth) and P05 (2 and 12 m) upstream of the Humen outlet (Fig. 1). Water samples were collected from Niskin bottles through a clean polytetrafluoroethylene (Teflon) silicone hose, and carefully filled into 125 mL clean headspace glass bottles without gas bubbles. The bottles were immediately closed with an air-tight butyl rubber stopper and aluminum crimp-cap. A total of 43 bottles were set up for surface and bottom at sites P01 and 34 bottles at P05. Samples from four parallel bottles were taken to determine the initial (t_0) dissolved N_2O concentration, and triplicate samples were taken to measure the initial dissolved inorganic nitrogen (DIN) concentration, which included ammonium, nitrite, and nitrate. The remaining 36 (P01) and 27 (P05) bottles were incubated in the dark at in situ temperatures (±1 ℃). At site P01, samples from six parallel bottles were taken at 3, 6, 18, and 24 h during the incubation experiment for N_2O determination after injecting saturated mercuric chloride ($HgCl_2$, 1:100 v:v) into the bottles; triplicate samples were also taken at the same time for DIN measurements by filtering through 0.7 μm pore size GF/Fs under pressure <0.03 MPa. Concentrations of N_2O, ammonium, nitrite, and nitrate were measured as described in Sect. 2.2. At site P05, samples were taken after 3, 6, and 12 h incubation and the other procedures were the same as described for site P01.

The effect of DIN assimilation is negligible during incubation in the dark (Ward, 2008). Therefore, the potential processes of nitrogen transformation and N_2O production can be determined according to "mass balance" in a closed incubation system. The main processes were analyzed based on the dynamic variations of DIN (ΔDIN), ammonia (ΔNH_3+NH_4^+), nitrite (ΔNO_2^-), nitrate (ΔNO_3^-), and N_2O (ΔN_2O) concentrations during incubation. The average rates of nitrification and N_2O production were estimated using the slopes of the linear regression between concentrations versus incubation time when DIN was in balance (i.e. no denitrification). All of the concentration-based rates described from the incubations represent net rates. The N_2O yield during nitrification was calculated with Eq. (8);

Deleted: ®
Deleted: were
Deleted: ed
Deleted: either depth
Deleted: for either depth
Deleted: volume ratio of
Deleted: -
Deleted: -
Deleted: ¶
During nitrification, NO_2^- is an intermediate product accumulated from ammonia oxidation that is then further oxidized to nitrate.
Deleted: hus, t
Deleted: or (9)

N_2O_{yield} (%) = $\Delta N_2O\text{-}N$ / $\Delta(NH_3 + NH_4^+)\text{-}N$ (8)

2.5 Statistical analyses

Since a normal distribution of the individual data sets was not always met, we used the non-parametric Wilcoxon rank-sum tests for comparing two variables. The bivariate correlations between environmental factors and functional genes were described by Spearman correlation coefficients (ρ value). False discovery rate (FDR)-based multiple comparison procedures were applied to evaluate the significance of multiple hypotheses and identify truly significant comparisons (FDR-adjusted P value) (Pike, 2011). The maximum gradient length of detrended correspondence analysis was shorter than 3.0, thus redundancy analysis (RDA) based on the qPCR data was used to analyze variations in the AOA and AOB distributions under environmental constraints in the software R (version 3.4.4) Vegan 2.5–3 package. The qPCR-based relative abundances and environmental factors were normalized via Z transformation (Magalhães et al., 2008). The null hypothesis, that the community was independent of environmental parameters, was tested using constrained ordination with a Monte Carlo permutation test (999 permutations). Significant environmental parameters ($P < 0.05$) without multicollinearity (variance inflation factor <20) (Ter Braak, 1986) were obtained. Standard and partial Mantel tests were run in R (version 3.4.4, Vegan 2.5–3 package) to determine the correlations between environmental factors and the AOA and AOB distributions. Dissimilarity matrices of communities and environmental factors were based on Bray-Curtis and Euclidean distances between samples, respectively. Based on Spearman correlation, the significance of the Mantel statistics was obtained after 999 permutations. Statistical tests were assumed to be significant at a P value of <0.05.

3 Results

3.1 Distribution of nutrients, DO, and N_2O along a salinity transect of the PRE

The studied transect was divided into a northern region upstream of the Humen outlet and southern area (Lingdingyang) (Fig. 1); these regions have distinct biogeochemical characteristics. Salinity exhibited low values (0.1 to 4.4) upstream of the Humen outlet, and sharply increased from 0.7 to 34.2 downstream in Lingdingyang (Fig. 2a). The ammonium/ammonia concentrations decreased from 167.2

Deleted: $_{N2O}$

Deleted: $_{NH3}$

Deleted: N_2O_{yield} (‰) = ΔN_{N2O} / $\Delta N_{(NO2^- + NO3^-)}$ (9) ¶

Deleted: *R*

Deleted: and two-tailed tests (*P* value)

Deleted: D

Deleted: R

Deleted: communities

Deleted: the

Deleted: P

Deleted:)

Deleted: ammonia oxidizer compositions

Deleted: Kendall's product-moment

μmol L^{-1} (site P01 surface water) to 20.9 μmol L^{-1} (site P07 bottom water) upstream of the Humen outlet and consistently decreased downstream in Lingdingyang (5.7 μmol L^{-1} to below detection limit) (Fig. 2b). Correspondingly, the sum of nitrate and nitrite concentrations increased from 93.6 μmol L^{-1} (site P01 bottom water) to 172.3 μmol L^{-1} (site P03 surface water) upstream, but it sharply decreased seaward to Lingdingyang (Fig. 2c). The DO concentrations were distinctly lower upstream of the Humen outlet with nearly one-half of the samples below the hypoxic threshold (63.0 μmol L^{-1}; Rabalais et al., 2010). Generally, the DO concentrations increased seaward from 155.7 to 238.0 μmol L^{-1} in the surface waters of the Lingdingyang area, whereas they varied from 74.0 to 183.3 μmol L^{-1} in the bottom waters (Fig. 2d).

In contrast to the DO concentrations, the N_2O concentrations were distinctly higher upstream of the Humen outlet (48.9–148.2 nmol L^{-1}) than in Lingdingyang, where they decreased seaward from 24.6 to 5.4 nmol L^{-1} (Fig. 2e). Similarly, higher ΔN_2O_{excess} (42.0–141.3 nmol L^{-1}) with saturations from 701.1% to 2175.1% was observed upstream; lower ΔN_2O_{excess} (-1.4–17.8 nmol L^{-1}) was present in the Lingdingyang area with the saturations ranging from 86% to 363% (Fig. 2f). The estimated water–air N_2O fluxes were 100.4 to 344.0 μmol m^{-2} d^{-1} upstream and decreased in Lingdingyang (42.4 to -2.6 μmol m^{-2} d^{-1}) (Fig. 2g). Together, the PRE acts as a N_2O source that releases to the atmosphere and notably, a significant negative relationship was observed between ΔN_2O_{excess} or N_2O flux and DO (P < 0.01 for each) in the upper estuary (Fig. 2i and j). The isotopic compositions of N_2O ($\delta^{15}N$-N_2O) showed an enrichment of $^{15}N_2O$ seaward, varying from -27.9 to 7.1‰ (Fig. 2h). Overall, upstream of the Humen outlet was characterized by hypoxic waters rich in nitrogen-based nutrients, where ammonium concentrations decreased and the sum of nitrite and nitrate concentrations increased seaward, corresponding to distinctly higher N_2O fluxes released to the atmosphere.

3.2 Distributions of *amo*A and *nir*S genes along the salinity transect

The total abundance of AOA *amo*A (sum of FL and PA communities) varied from 3.10×10^3 to 6.87×10^5 copies L^{-1} in the surface waters (Fig. 3a) and 6.40×10^4 to 4.21×10^7 copies L^{-1} in the bottom waters; an increase along the salinity transect was observed in the bottom (Fig. 3b). In contrast, the total abundance

Deleted:
Deleted:
Deleted:
Deleted:
Deleted:
Deleted:
Deleted:
Deleted:
Deleted:
Deleted:
Deleted:
Deleted:
Deleted:
Deleted:
Deleted:
Deleted: Therefore
Deleted: entire
Deleted: ,
Deleted: ,
Deleted: ,
Formatted: Not Superscript/ Subscript
Formatted: Not Superscript/ Subscript
Deleted: and transcript levels
Deleted:
Deleted:

of AOB *amo*A generally decreased seaward along the salinity transect for the surface (4.23×10^2 to 2.13×10^4 copies L^{-1}) and bottom waters (4.49×10^3 to 8.79×10^4 copies L^{-1}) (Fig. 3c and d). Overall, the abundance of AOA *amo*A was significantly higher than AOB ($P < 0.01$). The total abundance of *nir*S varied from 9.12×10^4 to 2.00×10^7 copies L^{-1} and was higher than both AOA ($P < 0.05$) and AOB *amo*A ($P < 0.01$) in the surface waters and AOB *amo*A in the bottom water ($P < 0.01$) (Fig. 3e and f). Notably, these three genes were predominantly distributed in the PA communities compared to the FL communities in the PRE transect (Fig. 3). The transcripts of the three genes were analyzed in the PA communities of the two incubation sites upstream of the Humen outlet. The transcript abundances of AOA *amo*A (7.44×10^3 to 4.62×10^5 transcripts L^{-1}) were one to three orders of magnitude higher than AOB *amo*A (3.62×10^2 to 5.00×10^2 transcripts L^{-1}) at P01 (Fig. 3a–d), whereas the transcript abundances of AOB *amo*A were relatively higher at P05 (AOB = 8.96×10^4 to 3.83×10^5 transcripts L^{-1}; AOA = 1.26×10^4 to 1.39×10^5 transcripts L^{-1}). The *nir*S gene showed a similar transcript level with AOA *amo*A at P01 (2.20×10^4 to 6.69×10^4 transcripts L^{-1}), but one order of magnitude lower transcript level than both AOA and AOB *amo*A at P05 (8.59×10^3 to 1.12×10^4 transcripts L^{-1}) (Fig. 3e and f).

3.3 Correlations between genes abundances and biogeochemical parameters

We analyzed the correlations between the genes abundances of AOA, AOB, or denitrifiers and biogeochemical parameters. The results indicate that AOA *amo*A abundance was significantly correlated ($P < 0.05-0.01$) to the hydrographic parameters temperature (negative) and salinity (positive), as well as silicate concentration (negative) (Table 1). However, AOB *amo*A abundance was significantly correlated ($P < 0.05-0.01$) to TSM concentration (positive), pH (negative), and DO (negative). Notably, there were positive correlations between AOB *amo*A abundances and all N_2O parameters as well as ammonia concentrations (Table 1; $P < 0.05-0.01$) except for the extremely low-abundance of FL AOB. No significant Spearman correlations were found between bacterial nitrite reductase *nir*S abundance and the measured biogeochemical parameters.

The RDA was used to further analyze variations in the AOA and AOB distributions under environmental constraints. The results confirmed that the relatively high AOB abundances in the upper estuary were constrained by low salinity water, high nitrite and TSM concentrations, low DO

Deleted: -
Deleted: -
Deleted: -
Deleted: -
Deleted: -
Deleted: -
Deleted: -
Deleted: -
Deleted: -
Deleted: To confirm the relationship between AOA, AOB, or denitrifier and N_2O production, we
Deleted: ir
Deleted: N_2O-related
Deleted: water mass
Deleted: ly
Deleted: ,
Deleted: ly
Deleted: and
Deleted: ly
Deleted: 2
Deleted: , suggesting that the water mixingmass may exert control on AOA distribution
Deleted: ly
Deleted: ly
Deleted: ly
Deleted: , which is consistent with our ...
Deleted: 2
Deleted: ,
Deleted: communities, suggesting a ...
Deleted: There n
Deleted: ammonia oxidizer communities
Deleted: the
Deleted: In the present study, the ...
Deleted: communities with
Deleted: high temperature and
Deleted: masses
Deleted: nutrient
Deleted: and

conditions, and high N_2O concentrations whereas high salinity water and opposite environmental conditions constrained the relatively high AOA abundances in the Lingdingyang area (Fig. 4). These constraints explained 89.3% of the variation in the ammonia oxidizer distribution along the PRE. Apparently, the communities with relatively high AOB abundances in the upper estuary positively influenced the concentration of N_2O in the water.

3.4 Nitrogen transformation and N_2O production in the incubation experiments

The in situ biogeochemical conditions of the incubation experiments are shown in Fig. 2 and listed in Table S1. Site P01 exhibited the lowest in situ DO concentrations (30.0 μmol L^{-1} in the bottom water and 30.9 μmol L^{-1} in the surface water). The concentration of DIN was generally unchanged in the early-to-middle (0–18 h) phase for the P01 surface water and early (0–6 h) phase for the P01 bottom water, but showed a distinct decrease in the end phase (Fig. 5a). The ammonia and nitrite concentrations consistently decreased and increased, respectively, during the incubation experiments; the nitrate concentrations decreased in the end phase after a slight increase (Fig. 5b). These results clearly indicate that nitrification occurred during the entire P01 incubations, and suggest that denitrification may be present in the end phase (Fig. 5g). The rates of ammonia oxidation during the entire incubations and nitrite oxidation during the early or early-to-middle phases were estimated by linear regressions of ammonia and nitrate concentrations, respectively (Fig. 5a and b; Table 2). Correspondingly, the estimated average N_2O production rate (24 h) was 0.62 nmol L^{-1} h^{-1} in P01 surface water and 0.70 nmol L^{-1} h^{-1} in P01 bottom water; the estimated N_2O production rates from nitrification were 0.60 nmol L^{-1} h^{-1} in the surface water (18 h) and 1.61 nmol L^{-1} h^{-1} in the bottom water (6 h; Fig. 5c). Thus, the estimated N_2O yield in the surface and bottom waters based on nitrification was 0.26% and 0.30% (Table 2).

In the incubation experiments at site P05, the DIN concentrations remained unchanged (Fig. 5d) and the ammonia concentrations consistently decreased and the nitrite and nitrate concentrations increased (Fig. 5e). The rates of ammonia and nitrite oxidation were also estimated by linear regressions of ammonia and nitrate concentrations, respectively (Fig. 5d and e; Table 2). The ammonia oxidation rates were approximately equal to the sum of the increased nitrite and nitrate concentration rates. Thus,

Deleted: and pH
Deleted: as well as
Deleted: ;
Deleted: the
Deleted: with high salinity
Deleted: water masses and
Deleted: communities with
Deleted: 5
Deleted: 87.3
Deleted: 3
Deleted: -
Deleted: -
Deleted: ing
Deleted: 4
Deleted: but
Deleted: ing
Deleted: 4
Deleted: ing
Deleted: 4
Deleted: 1
Deleted: -
Deleted: -
Deleted: -
Deleted: -
Deleted: -
Formatted: Not Superscript/ Subscript
Deleted: -
Deleted: -
Deleted: -
Deleted: 4
Deleted: 1.28
Deleted: 1.49
Deleted: μmol N_2O produced per mol ammonia oxidized
Deleted: 1
Deleted: 4
Deleted: 4
Deleted: 4
Deleted: 1

nitrification occurred during the incubation experiments without denitrification. The estimated N_2O production rates from nitrification were 1.15 nmol L^{-1} h^{-1} in the P05 surface water and 1.41 nmol L^{-1} h^{-1} in the P05 bottom water (Fig. 5f); the estimated N_2O yields based on nitrification were 0.21% (surface) and 0.32% (bottom) (Table 2).

The N_2O production rates and yields normalized to total AOA and AOB *amo*A gene copies (sum of PA and FL fractions or only PA fractions) or transcripts (only PA fraction) were calculated (Table S3). The highest average *amo*A gene copy-specific N_2O production rates and yields were in the surface water of site P05, where the highest nitrification rate was observed (Table 2). The highest average *amo*A gene transcript-specific N_2O production rates and yields were in the bottom water of site P01, where the highest N_2O production rate was observed (Table 2).

4 Discussion

4.1 Contribution of nitrification versus denitrification to N_2O production in the hypoxic upper estuary

The spatial variations of N_2O concentration, its saturation, and water–air N_2O flux along the PRE are consistent with our previous study (Lin et al., 2016), indicating that higher N_2O in the upper estuary ensures the PRE acts as a source of atmospheric N_2O. The in situ incubation experiments clearly indicated that nitrification predominantly occurred in the hypoxic waters of the upper estuary along with significant N_2O production, and suggested that denitrification could be concurrent at the lowest DO site (P01) where the maximum N_2O and ΔN_2O_{excess} concentrations were observed. These results confirm previous speculation that extreme enrichment of ammonia in the water column due to high loads of anthropogenic-sourced nutrients and organic matter in an upper estuary (Dai et al., 2008; He et al., 2014) could result in strong nitrification under low O_2 solubility conditions (Dai et al., 2008); thus, N_2O is produced as a byproduct through nitrification and is oversaturated in the PRE (Lin et al., 2016). The PRE sediments also act as a source of N_2O, which is released into the overlying waters through denitrification (Tan et al., 2019); however, in estuarine waters, nitrification apparently is the main source of N_2O production. Previous studies also proposed that nitrification may be the major source of N_2O production in the water column in estuarine systems, such as the Guadalquivir (Huertas et al.,

Deleted: -
Deleted: -
Deleted: -
Deleted: -
Deleted: 4
Deleted: 1.03
Deleted: µmol N_2O produced per mol ammonia oxidized
Deleted: 1.58
Deleted: µmol N_2O produced per mol ammonia oxidized
Deleted: 1
Deleted: ¶
We attempted to accurately assess the relative contributions of AOA and AOB to N_2O production in the PRE by plotting t
Deleted: (Fig. 7a)
Deleted: (Fig. 7b)
Deleted: (sum of
Deleted:)
Deleted: along X-Y axes that represent the relative contributions of AOA and AOB to the total *amo*A gene or transcript pools.
Deleted: also
Deleted: 1
Deleted: s
Deleted: were
Deleted: 1
Deleted: -
Deleted: makes
Deleted: ing
Deleted: the
Deleted: estuary

2018), Schelde (De Wilde and De Bie, 2000), and Chesapeake Bay (Laperriere et al., 2019). However, in the estuarine sediments, N_2O production was attributed to both nitrification and denitrification, such as in the Tama (Japan) (Usui et al., 2001) and Yangtze (China) estuaries (Liu et al., 2019; Wang et al., 2019), where denitrification is the major nitrogen removal pathway with N_2O production and consumption.

The isotopic composition of N_2O ($\delta^{15}N$-N_2O) was consistent with the above interpretation. According to previous studies (Table S2), the $\delta^{15}N$ of N_2O produced during ammonia oxidation by AOB strains ranged from −68‰ to −6.7‰ (Yoshida, 1988; Sutka et al., 2006; Mandernack et al., 2009; Frame and Casciotti, 2010; Jung et al., 2014; Toyoda et al., 2017) and 6.3−10.2‰ in a marine AOA strain (Santoro et al., 2011). The $\delta^{15}N$ of N_2O produced during denitrification ranged from −37.2‰ to −7.9‰ (Toyoda et al., 2005); during nitrifier-denitrification by AOB strains it ranged from −57.6 ± 4.1‰ to −21.5‰ (Sutka et al., 2003; Sutka et al., 2006; Frame and Casciotti, 2010). Therefore, the much lower $\delta^{15}N$-N_2O (−27.9‰ to −12.6‰) upstream of the Humen outlet is consistent with AOB nitrification or denitrification processes, whereas enriched ^{15}N-N_2O (5.2−7.1‰) in the lower reaches approaches AOA nitrification and air ^{15}N-N_2O (Santoro et al., 2011). Taken together, the isotopic compositions of N_2O (Fig. 2h) and N_2O concentration distribution (Fig. 2e−g) suggest that the high concentrations of N_2O (oversaturation) were produced from strong nitrification by AOB and probably concurrent minor denitrification in the upper estuary, however in the lower reaches, low concentrations of N_2O could be explained by AOA nitrification or water atmospheric exchange of N_2O.

4.2 Correlations of AOB versus AOA with N_2O-related biogeochemical parameters along the PRE

The more abundant AOA *amo*A genes, relative to AOB, and the more abundant genes in the PA communities than FL communities are consistent with our previous study in the PRE (Hou et al., 2018), which also reported significant positive correlations between the AOB *amo*A gene abundance and the oxidation rate of ammonia to nitrate. This suggests that AOB might be active in the ammonium and particle-enriched PRE, despite their low abundance (Füssel, 2014; Hou et al., 2018). Lower oxygen availability in particle micro-niches has been reported to be favorable for both nitrification and denitrification potential in oxygenated water (Kester et al., 1997). The Spearman correlations and RDA

Deleted: estuary
Deleted: estuary
Deleted: estuary of
Deleted: E
Deleted: y of China
Deleted: the
Deleted: N2O
Deleted: -
Deleted: -
Deleted: -
Deleted: -
Deleted: -
Deleted: -
Deleted: -
Deleted: nitrifiers and denitrifiers
Deleted: than
Deleted: as well as
Deleted: the
Deleted: in addition,
Deleted: evidence supports
Deleted: more
Deleted: than AOA
Deleted: -
Deleted: (Füssel, 2014; Hou et al., 2018)

analyses in this study indicate that high nutrient and TSM concentrations and low DO and pH conditions were favourable for relatively high abundance of AOB in the upper estuary, which is also consistent with our previous PRE study that found high TSM concentrations and low DO and pH influenced substrate availability and thus AOB distribution (Hou et al., 2018). Moreover, AOB *amo*A abundances positively correlated to all N_2O-related parameters as revealed by the Spearman correlations and RDA analyses, suggesting a significant influence of AOB (mainly the PA fraction) on N_2O production/emission in the upper estuary. However, compared to AOB, AOA *amo*A distribution along the PRE transect appears to be regulated more by water mixing since AOA was significantly correlated to the hydrographic parameters and silicate concentration.

To further eliminate the co-varying effects of water mixing, substrate availability, and N_2O-related parameters along the salinity transect, and to identify the intrinsic/direct relationship between ammonia oxidizers and N_2O production, we performed standard and partial Mantel tests. We defined four types of environmental constraints: water mixing parameters (temperature, salinity, and silicate), substrate parameters (ammonia/ammonium, nitrite, and nitrate), parameters influencing substrate availability (DO, TSM, and pH), and N_2O-related parameters (N_2O and ΔN_2O_{excess}). For the water mixing parameters, we analyzed the relationships between potential temperature (θ), salinity, and silicate concentration with a three-dimensional scatter plot (Fig. S1) that indicates low salinity and high silicate contents were the best indicators for river input in the ocean (Moore, 1986). Thus, we chose temperature, salinity, and silicate as proxies to trace estuarine water masses and mixing. Water mixing parameters (standard and partial Mantel tests, $P < 0.01$) and those influencing substrate availability (standard and partial Mantel tests, $P < 0.05$) significantly controlled variations in the distribution of AOA and AOB along the PRE transect (Fig. 6a and c), supporting the Spearmen and RDA conclusions. Notably, variations in the distribution of AOA and AOB were significantly correlated with N_2O production (standard and partial Mantel test, $P < 0.01$) after eliminating the co-varying effects of other parameters (Fig. 6d), demonstrating the significant contribution of ammonia oxidizers to N_2O production.

Deleted: To confirm the relationship between AOA, AOB, or denitrifier and N_2O production, we analyzed the correlations between their genes abundances and N_2O-related biogeochemical parameters. The results indicate that AOA *amo*A abundance was significantly correlated (P <0.05−0.01) to the water mass parameters temperature (negatively), salinity (positively), and silicate concentration (negatively) (Table 2), suggesting that the water mass may exert control on AOA distribution. However, AOB *amo*A abundance was significantly correlated (P <0.05−0.01) to TSM concentration (positively), pH (negatively), and DO (negatively), which is consistent with our previous PRE study that found high TSM concentrations and low DO and pH influenced substrate availability and thus AOB distribution (Hou et al., 2018). AOB *amo*A abundances positively correlated toand all N_2O-related parametersas well as ammonia concentration (Table 2; P <0.05−0.01), suggesting a significant influence of AOB on N_2O production/emission There no significant Spearman correlations were found between bacterial nitrite reductase *nir*S abundance and the measured biogeochemical parameters. The RDA was used to further analyze variations in the ammonia oxidizer communities under the environmental constraints. In the present study, the environmental constraints included four types: water mass parameters (temperature, salinity, and silicate), substrate parameters (ammonia/ammonium, nitrite, and nitrate), parameters influencing substrate availability (DO, TSM, and pH), and N_2O parameters. The results confirmed that the communities with relatively high AOB abundances in the upper estuary were constrained by high temperature and low salinity water masses, high nutrient and TSM concentrations and low DO and pH conditions, as well as high N_2O concentration; whereas the opposite water masses and environmental conditions constrained the communities with high AOA abundances in the Lingdingyang area (Fig. 5). These constraints explained 87.3% of the variation in the ammonia oxidizer distribution along the PRE. Apparently, the communities with relatively high AOB ...

Deleted: ¶
Partial Mantel tests were applied

Deleted: t

Deleted: mass

Deleted:

Deleted: mass

4.3 Contribution of AOB versus AOA to N_2O production

We attempted to accurately assess the relative contributions of AOA and AOB to N_2O production in the PRE by plotting the N_2O production rates (Fig. 7a) and yields (Fig. 7b) normalized to total (sum of AOA and AOB) *amo*A gene copies or transcripts at sites P01 and P05 along the x-y axes that represent the relative contributions of AOA and AOB to the total *amo*A gene or transcript pools. Notably, compared to AOA, higher AOB abundance in the *amo*A gene-based DNA or cDNA pool resulted in distinctly higher (disproportionately higher relative to enhanced abundance) average *amo*A gene copy or transcript-specific N_2O production rates (Fig. 7a) and yields (Fig. 7b), suggesting that AOB may have higher cell-specific activities in the upper estuary and thus be more active in producing N_2O than AOA. Previous studies based on pure cultures of AOB and AOA strains provided evidence that AOB have higher N_2O yields (0.09 to 26%) (Yoshida and Alexander, 1970; Goreau et al., 1980) than AOA (0.002 to 0.09%) during ammonia oxidation (Löscher et al., 2012; Stieglmeier et al., 2014). The higher N_2O yield from AOB has also been observed in soils despite a lower abundance of AOB (Hink et al., 2017; Hink et al., 2018). Based on results indicated by Fig. 7, we conclude that AOB may have higher relative contributions to the high N_2O production in the upper estuary where low DO, high concentrations of N_2O and ΔN_2O, and high N_2O flux were observed.

Ammonia oxidizers are sensitive to oxygen during N_2O production (Santoro et al., 2011; Löscher et al., 2012; Stieglmeier et al., 2014). Studies based on pure cultures of AOB strains *Nitrosomonas marina* NM22 and *Nitrosococcus oceani* NC10, and AOA strain *Nitrosopumilus maritimus* showed higher N_2O yields and production during nitrification by both AOA and AOB when O_2 concentrations varied from aerobic to hypoxic conditions (Löscher et al., 2012). However, when O_2 concentrations varied from hypoxic to anaerobic conditions (i.e. in a lower O_2 concentration range), the AOB strain *Nitrosospira multiformis* and AOA strains *Nitrososphaera viennensis* and *Nitrosopumilus maritimus* showed that AOB had distinctly higher N_2O yields at lower oxygen conditions and, in contrast, AOA had lower N_2O yields at lower oxygen concentrations (Stieglmeier et al., 2014). In addition, results from the cultured AOB strain *Nitrosomonas marina* C-113a indicated increasing N_2O yields with higher cell concentrations (Frame and Casciotti, 2010). This evidence supports our conclusions that the high

Deleted: X

Deleted: Y

Deleted: The highest average *amo*A gene copy-specific N_2O production rates and yields were in the surface water of site P05, where the highest nitrification rate was also observed (Table 1). The highest average *amo*A gene transcript-specific N_2O production rates and yields were in the bottom water of site P01, where the highest N_2O production rates were observed (Table 1).

Deleted: for both incubation sites

Deleted: the more

Deleted: abundant

Deleted: were

Deleted: , the

Deleted: the

Deleted: the

Deleted: strain *Nitrosospira multiforimis*

Deleted: *Nitrososphaera viennensis* and *Nitrosopumilus maritimus* have

Deleted: has

Deleted: 2.7

Deleted: ‰

Deleted: 3

Deleted: ‰

concentration of N_2O (oversaturated) may be mainly produced from strong nitrification by the high abundance of AOB in the low DO conditions in the upper estuary.

In addition, it is possible that comammox (COMplete AMMonia OXidiser) species, newly discovered in terrestrial systems (Daims et al., 2015; Santoro, 2016; Kits et al., 2017), are also involved in N_2O production (Hu and He, 2017) given the similar ammonia oxidation pathway to AOB. It has been further reported that the comammox *Nitrospira inopinata* has a lower N_2O yield than AOB due to a lack of NO reductases and the formation of N_2O from the abiotic conversion of hydroxylamine (Kits et al., 2019). However, comammox has not been widely observed in estuarine waters. Also, *nir*K-type denitrifiers may contribute to N_2O production despite being much less abundant than *nir*S-type denitrifiers (Huang et al., 2011; Maeda et al., 2017). Furthermore, *nir*S-type denitrifiers are more likely to be capable of complete denitrification because of a higher co-occurrence of the N_2O reductase gene (*nos*Z) with *nir*S than *nir*K (Graf et al., 2014). However, there is currently no direct evidence that denitrification or nitrifier-denitrification is responsible for N_2O production in the PRE water column. A release of N_2O into the overlying waters through denitrification was reported for PRE sediments (Tan et al., 2019). Further study is needed to clarify the potential of both *nir*K and *nir*S-type denitrifiers in N_2O production from the interface between sediment and water in the PRE.

5 Conclusions

This study explored the relative contributions of AOB and AOA in producing N_2O in the PRE by combining isotopic compositions and concentrations of N_2O, distributions and transcript levels of AOB and AOA *amo*A and denitrifier *nir*S genes, and incubation estimates of nitrification and N_2O production rates. Our findings indicate that the high concentrations of N_2O and ΔN_2O_{excess} and the much lower $\delta^{15}N\text{-}N_2O$ are primarily attributed to strong nitrification by AOB. There is also probably concurrent minor denitrification in the upper estuary where AOB abundances are higher before decreasing seaward along the salinity transect. Low concentrations of N_2O and ΔN_2O_{excess} and enriched $^{15}N_2O$ could be explained by AOA nitrification in the lower reaches of the estuary. Collectively, AOB contributed the major part of N_2O production in the upper estuary, which is the major source of N_2O emitted to the atmosphere in the PRE.

Deleted: Our work
Deleted: the
Deleted: rates
Deleted: and
Deleted: were
Deleted: and
Deleted: ed
Deleted: in

Deleted: Section Break (Next Page)

Data availability

All data can be accessed in the form of Excel spreadsheets via the corresponding author.

The Supplement related to this article is available online.

Author contribution

M.D. and Y.Z. conceived and designed the experiments. L.M., H.L., and X.X. performed the experiments. L.M., Y.Z., H.L., and X.X. analyzed the data. L.M. and Y.Z. wrote the paper. All authors contributed to the interpretation of results and critical revision.

Competing interests

The authors declare no conflicts of interest.

Acknowledgments

We thank Qing Li for measuring ammonia concentrations on board, Jian-Zhong Su and Liguo Guo for measuring dissolved oxygen concentrations on board, and Tao Huang and Lifang Wang for measuring nitrate and nitrite concentrations. We also thank Lei Hou for her assistance in qPCR measurements and data analysis, and Mingming Chen and Huade Zhao for their assistance with the software. This research was supported by the National Key Research and Development Programs (2016YFA0601400) and NSFC projects (41676125, 41721005, and 41706086). We thank Kara Bogus, PhD, from Liwen Bianji, Edanz Editing China (www.liwenbianji.cn/ac), for editing the English text of a draft of this manuscript.

References

Abell, G. C. J., Revill, A. T., Smith, C., Bissett, A. P., Volkman, J. K., and Robert, S. S.: Archaeal ammonia oxidizers and *nirS*-type denitrifiers dominate sediment nitrifying and denitrifying populations in a subtropical macrotidal estuary, ISME J., 4, 286–300, 2010.

Abril, G., Riou, S. A., Etcheber, H., Frankignoulle, M., de Wit, R., Middelburg, J. J.: Transient tidal time-scale, nitrogen transformations in an estuarine turbidity maximumfluid mud system (the Gironde, south-west France), Estuar. Coast. Shelf S. 50 , 703–715, 2000.

Allen, D., Dalal, R. C., Rennenberg, H., and Schmidt, S.: Seasonal variation in nitrous oxide and methane emissions from subtropical estuary and coastal mangrove sediments, Australia, Plant Biol., 13, 126–133, 2011.

Arévalo-Martínez, D. L., Kock, A., Löscher, C. R., Schmitz, R. A., and Bange, H. W.: Massive nitrous oxide emissions from the tropical South Pacific Ocean, Nat. Geosci., 8, 530–533, 2015.

Avrahami, S., and Bohanann, J. M.: N_2O emission rates in a California meadow soil are influenced by fertilizer level, soil moisture and the community structure of ammonia-oxidizing bacteria, Glob. Change Biol., 15, 643–655, 2009.

Babbin, A. R., Bianchi, D., Jayakumar, A., and Ward, B. B.: Rapid nitrous oxide cycling in the suboxic ocean, Science, 348, 1127–1129, 2015.

Barnes, J., and Upstill-Goddard, R. C.: N_2O seasonal distributions and air–sea exchange in UK estuaries: Implications for the tropospheric N_2O source from European coastal waters, J. Geophys. Res., 116, G01006, 2011. http://dx.doi.org/10.1029/2009JG001156.

Bartossek, R., Nicol, G.W., Lanzen, A., Klenk, H. P., and Schleper, C.: Homologues of nitrite reductases in ammonia-oxidizing archaea: diversity and genomic context, Environ. Microbiol., 12, 1075–1088, 2010.

Bernhard, A. E., Landry, Z. C., Blevins, A., de la Torre, J. R., Giblin, A. E., and Stahl, D. A.: Abundance of ammonia-oxidizing archaea and bacteria along an estuarine salinity gradient in relation to potential nitrification rates, Appl. Environ. Microbiol., 76, 1285–1289, 2010.

Braker, G., Fesefeldt, A., and Witzel, K. P.: Development of PCR primer systems for amplification of nitrite reductase genes (*nir*K and *nir*S) to detect denitrifying bacteria in environmental samples, Appl. Environ. Microbiol., 64, 3769–3775, 1998.

Bricker, S. B., Longstaff, B., Dennison, W., Jones, A., Boicourt, K.,Wicks, C., and Woerner, J.: Effects of nutrient enrichment in the nation's estuaries: a decade of change, Harmful Algae, 8, 21–32, 2008.

Butterbach-Bahl, K., Baggs, E. M., Dannenmann, M., Kiese, R., and Zechmeister-Boltenstern, S.: Nitrous oxide emissions from soils: how well do we understand the processes and their controls? Philos. Trans. R. Soc. B-Biol. Sci., 368, https://doi.org/10.1098/rstb.2013.0122, 2013.

Canfield, D. E., Glazer, A. N., and Falkowski, P. G.: The Evolution and Future of Earth's Nitrogen Cycle, Science, 330, 192–196, 2010.

Cao, Y., Sun, G., Han, Y., Sun, D., and Wang, X.: Determination of nitrogen, carbon and oxygen stable isotope ratios in N_2O, CH_4, and CO_2 at natural abundance levels by mass spectrometer, Acta. Pedologica. Sinica., 45, 249–258, 2008 (Chinese).

Clark, I. M., Buchkina, N., Jhureea, D., Goulding, K. W. T., and Hirsch, P. R.: Impacts of nitrogen application rates on the activity and diversity of denitrifying bacteria in the Broadbalk Wheat Experiment, Philos. Trans. R. Soc. B-Biol. Sci., 367, https://doi.org/10.1098/rstb.2011.0314, 2012.

Coyne, M. S., Arunakumari, A., Averill, B. A., and Tiedje, J. M.: Immunological identification and distribution of dissimilatory heme cd1 and non-heme copper nitrite reductases in denitrifying bacteria, Appl. Environ. Microbiol., 55, 2924–2931, 1989.

Čuhel, J., Šimek, M., Laughlin, R. J., Bru, D., Chèneby, D., Watson, C. J., and Philippot, L.: Insights into the Effect of Soil pH on N_2O and N_2 Emissions and Denitrifier Community Size and Activity, Appl. Environ. Microbiol., 76, 6, 1870–1878, 2010.

Dai, M., Guo, X., Zhai, W., Yuan, L., Wang, B., Wang, L., Cai, P., Tang, T., and Cai, W. J.: Oxygen depletion in the upper reach of the Pearl River estuary during a winter drought, Mar. Chem., 102, 159–169, 2006.

Dai, M., Wang, L., Guo, X., Zhai, W., Li, Q., He, B., and Kao, S. J.: Nitrification and inorganic nitrogen distribution in a large perturbed river/estuarine system: the Pearl River Estuary, China, Biogeosciences, 5, 1545–1585, 2008.

Dai, M., Gan, J., Han, A., Kung, H. S., and Yin, Z.: Physical dynamics and biogeochemistry of the Pearl River plume, In Biogeochemical dynamics at major river-coastal interfaces, Linkages with Global Change. Bianchi, T. S., Allison, M. A., and Cai, W. J. (eds). Cambridge University Press, pp. 321–351, 2014.

Daims, H., Lebedeva, E. V., Pjevac, P., Han, P., Herbold, C., Albertsen, M., Jehmlich, N., Palatinszky, M., Vierheilig, J., and Bulaev, A.: Complete nitrification by Nitrospira bacteria, Nature, 528, 504–509, 2015.

Damashek, J., Casciotti, K. L., and Francis, C. A.: Variable Nitrification Rates Across Environmental Gradients in Turbid, Nutrient-Rich Estuary Waters of San Francisco Bay, Estuaries and Coasts, 39, 1050–1071, 2016.

Damashek, J. and Francis, C. A.: Microbial Nitrogen Cycling in Estuaries: From Genes to Ecosystem Processes, Estuaries and Coasts, 41, 626–660, 2018.

De Wilde, H. P. J., and De Bie, M. J. M.: Nitrous oxide in the Schelde Estuary: production by nitrification and emission to the atmosphere, Mar. Chem., 69, 203–216, 2000.

De Bie, M. J. M., Middelburg, J J., Starink, M., and Laanbroek, H. J.: Factors controlling nitrous oxide at the microbial community and estuarine scale, Mar. Ecol- Prog. Ser., 240, 1–9, 2002.

Frame, C. H., and Casciotti, K. L.: Biogeochemical controls and isotopic signatures of nitrous oxide production by a marine ammonia-oxidizing bacterium, Biogeosciences, 7, 2695–2709, 2010.

Frame, C. H., Lau, E., Joseph Nolan IV, E., Goepfert, T. J., and Lehmann, M. F.: Acidification Enhances Hybrid N_2O Production Associated with Aquatic Ammonia-Oxidizing Microorganisms, Front. Microbiol., 7, 1–23, 2017.

Francis, C. A., Roberts, K. J., Beman, J. M., Santoro, A. E., and Oakley, B. B.: Ubiquity and diversity of ammonia-oxidizing archaea in water columns and sediments of the ocean, P. Natl. Acad. Sci. USA, 102, 14683–14688, 2005.

Freing, A., Wallace, D. W. R., and Bange, H. W.: Global oceanic production of nitrous oxide, Philos. Trans. R. Soc. B-Biol. Sci., 367, https://doi.org/10.1098/rstb. 2011. 0360, 2012.

Füssel, J.: Impacts and importance of ammonia and nitrite oxidation in the marine nitrogen cycle, PhD thesis, Max Planck Institute for Microbial Ecology, Bremen, Germany, 166 pp., 2014.

Garnier, J., Cébron, A., Tallec, G., Billen, G., Sebilo, M., and Martinez, A.: Nitrogen behaviour and nitrous oxide emission in the tidal Seine River estuary (France) as influenced by human activities in the upstream watershed. Biogeochemistry, 77, 305–326, 2006.

Goreau, T. J., Kaplan, W. A., Wofsy, S. C., McElroy, M. B., Valois, F. W., and Watson, S. W.: Production of NO_2^- and N_2O by Nitrifying Bacteria at Reduced Concentrations of Oxygen, Appl. Environ. Microbiol., 40, 526–532, 1980.

Graf, D. R. H., Jones, C. M., and Hallin,. S.: Intergenomic comparisons highlight modularity of the denitrification pathway and underpin the importance of community structure for N_2O emissions. PloS One 9: e114118. https://doi.org/10.1371/journal.pone.0114118. s008. 2014.

Han, A., Dai, M., Kao, S.-J., Gan, J., Li, Q., Wang, L., Zhai, W., and Wang, L.: Nutrient dynamics and biological consumption in a large continental shelf system under the influence of both a river plume and coastal upwelling, Limnol. Oceanogr., 57, 486–502, 2012.

Hatzenpichler, R.: Diversity, Physiology, and Niche Differentiation of Ammonia Oxidizing Archaea, Appl. Environ. Microbol., 78, 7501–7510, 2012.

He, B., Dai, M., Zhai, W., Guo, X., and Wang, L.: Hypoxia in the upper reaches of the Pearl River Estuary and its maintenance mechanisms: A synthesis based on multiple year observations during 2000-2008, Mar. Chem., 167, 13–24, 2014.

Hink, L., Nicol, G. W., and Prosser, J. I.: Archaea produce lower yields of N_2O than bacteria during aerobic ammonia oxidation in soil, Environ. Microbiol., 19, 4829–4837, 2017.

Hink, L., Gubry-Rangin, C., Nicol, G. W., and Prosser, J. I.: The consequences of niche and physiological differentiation of archaeal and bacterial ammonia oxidisers for nitrous oxide emissions, ISME J., 12,1084–1093, 2018.

Hou, L., Xie, X., Wan, X., Kao, S. J., Jiao, N., and Zhang, Y.: Niche differentiation of ammonia and nitrite oxidizers along a salinity gradientnfrom the Pearl River estuary to the South China Sea, Biogeosciences, 15, 5169–5187, 2018.

Huang, S., Chen, C., Yang, X., Wu, Q., and Zhang, R.: Distribution of typical denitrifying functional genes and diversity of the *nir*S-encoding bacterial community related to environmental characteristics of river sediments, Biogeosciences, 8, 3041–3051, 2011.

Hu, A., Jiao, N., and Zhang, C. L.: Community structure and function of planktonic *Crenarchaeota*: changes with depth in the South China Sea, Microb. Ecol., 62, 549–563, 2011.

Hu, H. W., and He, J. Z.: Comammox–a newly discovered nitrification process in the terrestrial nitrogen cycle, J. Soils Sediments, 17, 2709–2717, 2017.

Huertas, I. E., Flecha, S., Navarro, G., andPerez, F. F., de la Paz, M.: Spatio-temporal variability and controls on methane and nitrous oxide in the Guadalquivir Estuary, Southwestern Europe, Aquat Sci., 80, 29, 2018.

Ji, Q., Babbin, A. R., Jayakumar, A., Oleynik, S., and Ward, B. B.: Nitrous oxide production by nitrication and denitrication in the Eastern Tropical South Pacific oxygen minimum zone, Geophy. Res. Lett., 42, 10, 755–10, 764, 2015.

Ji, Q., Buitenhuis, E., Suntharalingam, P., Sarmiento, J. L., and Ward, B. B.: Global Nitrous Oxide Production Determined by Oxygen Sensitivity of Nitrification and Denitrification, Global Biogeochem. Cy., 32, 1790–1802, 2018.

Jones, C. M., Spor, A., Brennan, F. P., Breuil, M. C., Bru, D., Lemanceau, P., Griffiths, B., Hallin, S., and Philippot, L.: Recently identified microbial guild mediates soil N_2O sink capacity, Nat. Clim. Chang., 4, 801–805, 2014.

Jung, M. Y., Well, R., Min, D., Giesemann, A., Park, S. J., Kim, J. G., and Rhee, S. K.: Isotopic signatures of N_2O produced by ammonia-oxidizing archaea from soils, ISME J., 8, 1115–1125, 2014.

Kester, R. A., de Boer, W., and Laanbroek, H. J.: Production of NO and N2O by pure cultures of nitrifying and denitrifying bacteria during changes in aeration, Appl. Environ. Microbiol., 63, 3872–3877, 1997.

Kim, O. S., Junier, P., Imhoff, J. F., and Witzel, K. P.: Comparative analysis of ammonia monooxygenase (*amo*A) genes in the water column and sediment–water interface of two lakes and the Baltic Sea, FEMS Microbiol. Ecol., 66, 367–378, 2008.

Kim, I. N., Lee, K., Bange, H.W., Macdonald, A. M.: Interannual variation in summer N_2O concentration in the hypoxic region of the northern gulf of Mexico, 1985–2007, Biogeosciences, 10, 6783–6792, 2013.

Kits, K. D., Sedlacek, C. J., Lebedeva, E. V., Han, P., Bulaev, A., Pjevac, P., Daebeler, A., Romano, S., Albertsen, M., Stein, L. Y., Daims, H., and Wagner, M.: Kinetic analysis of a complete nitrifier reveals an oligotrophic lifestyle, Nature, 549, 269–272, 2017.

Kits, K. D., Jung, M.Y., Vierheilig, J., Pjevac, P., Sedlacek, C. J., Liu, S., Herbold, C., Stein, L. Y., Richter, A., Wisse, H., Brüggemann, N., Wagner, M., and Daims, H.: Low yield and abiotic origin of N_2O formed by the complete nitrifier Nitrospira inopinata, Nat. Commun., 2019. https://doi.org/10.1038/s41467-019-09790-x

Kroeze, C., Dumont, E., and Seitzinger, S.: Future trends in emissions of N_2O from rivers and estuaries, J. Integr. Environ. Sci., 7, 71–78, 2010.

Laperriere, S. M., Nidzieko, N. J., Fox, R. J., Fisher, A. W., Santoro, A. E.: Observations of variable ammonia oxidation and nitrous oxide flux in a eutrophic estuary, Estuar Coast, 42, 33–44, 2019.

Lin, H., Dai, M., Kao, S. J., Wang, L., Roberts, E., Yang, J., Huang, T., and He, B.: Spatiotemporal variability of nitrous oxide in a large eutrophic estuarine system: The Pearl River Estuary, China, Mar. Chem., 182, 14–24, 2016.

Liu, C., Hou, L., Liu, M., Zheng, Y., Yin, G., Han, P., Dong, H., Gao, J., Gao, D., Chang, Y., Zhang, Z.: Coupling of denitrification and anaerobic ammonium oxidation with nitrification in sediments of the Yangtze Estuary: Importance and controlling factors, Estura. Coast. Shelf. S., 220, 64–72, 2019.

Löscher, C. R., Kock, A., Könneke, M., LaRoche, J., Bange, H. W., and Schmitz, R. A.: Production of oceanic nitrous oxide by ammonia-oxidizing archaea, Biogeosciences, 9, 2419–2429, 2012.

Lund, M. B., Smith, J. M., and Francis, C. A.: Diversity, abundance and expression of nitrite reductase *(nirK)*-like genes in marine thaumarchaea, ISME J., 6, 1966–1977, 2012.

Maeda, K., Toyoda, S., Philippot, L., Hattori, S., Nakajima, K., Ito, Y., and Yoshida, N.: Relative Contribution of nirK- and nirS- Bacterial Denitrifiers as Well as Fungal Denitrifiers to Nitrous Oxide Production from Dairy Manure Compost, Environ. Sci. Technol., 51, 14083–14091, 2017.

Magalhães, C., Bano, N., Wiebe, W. J., Bordalo, A. A., and Hollibaugh, J. T.: Dynamics of nitrous oxide reductase genes (*nosZ*) in intertidal rocky biofilms and sediments of the Douro River Estuary (Portugal), and their relation to N-biogeochemistry, Microb. Ecol., 55, 259–269, 2008.

Mandernack, K. W., Mills, C. T., Johnson, C. A., Rahn, T., and Kinney, C.: The $\delta^{15}N$ and $\delta^{18}O$ values of N_2O produced during the co-oxidation of ammonia by methanotrophic bacteria, Chem. Geol., 267, 96–107, 2009.

Mincer, T. J., Church, M. J., Taylor, L. T., Preston, C., Karl, D. M., and DeLong, E. F.: Quantitative distribution of presumptive archaeal and bacterial nitrifiers in Monterey Bay and the North Pacific Subtropical Gyre, Environ. Microbiol., 9, 1162–1175, 2007.

Mohn, J., Wolf, B., Toyoda, S., Lin, C. T., Liang, M. C., Brüggemann, N., Wissel, H., Dyckmans, A. E. S, J., Szwec, L., Ostrom, N. E., Casciotti, K. L., Forbes, M., Giesemann, A., R., Doucett, R. R., Well, Yarnes, C. T., Ridley, A. R., Kaiser, J., and Yoshida, N.: Interlaboratory assessment of nitrous oxide isotopomer analysis by isotope ratio mass spectrometry and laser spectroscopy: current status and perspectives, Rapid Commun Mass Spectrom. 28, 1995–2007, 2014.

Monteiro, M., Séneca, J., and Magalhães, C.: The History of Aerobic Ammonia Oxidizers: from the First Discoveries to Today, J. Microbiol., 52, 537–547, 2014.

Moore, W. S., Sarmiento, J. L., and Key, R. M.: Tracing the Amazon component of surface Atlantic water using 228Ra, salinity and silica, J. Geophys. Res., 91, 2574–2580, 1986.

Mortazavi, B., Iverson, R. L., Huang, W., Graham Lewis, F., Caffrey, J. M.: Nitrogen budget of Apalachicola Bay, a bar-built estuary in the northeastern Gulf of Mexico, Mar. Ecol.-Prog. Ser., 195, 1–14, 2000.

Naqvi, S. W. A., Bange, H. W., Farías, L., Monteiro, P. M. S., Scranton, M. I., and Zhang, J.: Marine hypoxia/anoxia as a source of CH_4 and N_2O, Biogeosciences, 7, 2159–2190, 2010.

Nevison, C. D., Lueker, T. J., and Weiss, R. F.: Quantifying the nitrous oxide source from coastal upwelling, Glob. Biogeochem. Cycle, 18, 1–17, 2004.

Ni, B. J., Peng, L., Law, Y., Guo, J., and Yuan, Z.: Modeling of Nitrous Oxide Production by Autotrophic Ammonia-Oxidizing Bacteria with Multiple Production Pathways, Environ. Sci. Technol., 48, 3916–3924, 2014.

Pai, S. C., Tsau, Y. J., and Yang, T. I.: pH and buffering capacity problems involved in the determination of ammonia in saline water using the indophenol blue spectrophotometric method, Analytica Chimica Acta, 434, 209–216, 2001.

Penn, J., Weber, T., and Deutsch, C.: Microbial functional diversity alters the structure and sensitivity of oxygen deficient zones, J. Geophys. Res. Lett., 43, 9773–9780, 2016.

Pike, N.: Using false discovery rates for multiple comparisons in ecology and evolution, Methods in Ecology and Evolution, 2, 278–282, 2011.

Rabalais, N. N., D´ıaz, R. J., Levin, L. A., Turner, R. E., Gilbert, D., and Zhang, J.: Dynamics and distribution of natural and human-caused hypoxia, Biogeosciences, 7, 585–619, 2010.

Rajkumar, A. N., Barnes, J., Ramesh, R., Purvaja, R., and Upstill-Goddard, R. C.: Methane and nitrous oxide fluxes in the polluted Adyar River and estuary, SE India., Mar. Pollut. Bull., 56, 2043–2051, 2008.

Ravishankara, A. R., Daniel, J. S., and Portmann, R. W.: Nitrous Oxide (N_2O): The Dominant Ozone-Depleting Substance Emitted in the 21st Century, Science, 326, 123–125, 2009.

Raymond, P. A., and Cole, J. J.: Gas exchange in rivers and estuary: choosing a gas transfer velocity, Estuaries Coasts, 24, 312–317, 2001.

Santoro, A. E., Buchwald, C., McIlvin, M. R., and Casciotti K. L.: Isotopic Signature of N_2O Produced by Marine Ammonia-Oxidizing Archaea, Science, 333, 1282–1285, 2011.

Santoro, A. E: The do-it-all nitrifier, Science, 351, 342–343, 2016.

Seitzinger, S. P., and Kroeze, C.: Global distribution of nitrous oxide production and N inputs in freshwater and coastal marine ecosystems, Glob. Biogeochem. Cycle, 12, 93-113, 1998.

Shaw, L. J., Nicol, G. W., Smith, Z., Fear, J., Prosser, J. I., Baggs, E. M.: *Nitrosospira* spp. can produce nitrous oxide via a nitrifier denitrification pathway, Environ. Microbiol., 8, 214–222, 2006.

Stein, L. Y.: Surveying N_2O-Producing Pathways in Bacteria, Methods Enzymol., 486, 131–152, 2011.

Stieglmeier, M., Mooshammer, M., Kitzler, B., Wanek, W., Zechmeister-Boltenstern, S., Richter, A., and Schleper, C.: Aerobic nitrous oxide production through N-nitrosating hybrid formation in ammonia-oxidizing archaea, ISME J., 8, 1135–1146, 2014.

Sutka, R. L., Ostrom, N. E., Ostrom, P. H., Gandhi, H., and Breznak, J. A.: Nitrogen isotopomer site preference of N_2O produced by Nitrosomonas europaea and Methylococcus capsulatus Bath, Rapid Commun. Mass Spectrom., 17, 738–745, 2003.

Sutka, R. L., Ostrom, N. E., Ostrom, P. H., Breznak, J. A., Gandhi, H., Pitt, A. J., and Li, F.: Distinguishing Nitrous Oxide Production from Nitrification and Denitrification on the Basis of Isotopomer Abundances, Appl. Environ. Microbiol., 72, 638–644, 2006.

Syakila, A., and Kroeze, C.: The global nitrogen budget revisited, J. Greenhouse Gas Meas. Manag., 1, 17–26, 2011.

Tan, E., Zou, W., Jiang, X., Wan, X., Hsu, T. C., Zheng, Z., Chen, L., Xu, M., Dai, M., Kao, S.: Organic matter decomposition sustains sedimentary nitrogen loss in the Pearl River Estuary, China, Sci. Total. Environ., 648, 508–517, 2019

Ter Braak, C. J. F. Canonical correspondence analysis: a new eigenvector technique for multivariate direct gradient analysis, Ecology, 67, 1167–1179, 1986.

Toyoda, S., Mutobe, H., Yamagishi, H., Yoshida, N., Tanji, Y.: Fractionation of N_2O isotopomers during production by denitrifier, Soil. Biol. Biochem., 37, 1535–1545, 2005.

Toyoda, S., Yoshida, N., and Koba, K.: Isotopocule analysis of biologically produced nitrous oxide in various environments, Mass Spectrom. Rev., 36, 135–160, 2017.

Treusch, A. H., Leininger, S., Kletzin, A., Schuster, S. C., Klenk, H., and Schleper, C.: Novel genes for nitrite reductase and Amo-related proteins indicate a role of uncultivated mesophilic crenarchaeota in nitrogen cycling, Environ. Microbiol., 7, 1985–1995, 2005.

Usui, T., Koike, I., and Ogura, N.: N_2O production, nitrification and denitrification in an estuarine sediment, Estuar. Coast. Shelf Sci., 52, 769-781, 2001.

Voss, M., Bange, H. W., Dippner, J. W., Middelburg, J. J., Montoya, J. P., and Ward, B.: The marine nitrogen cycle: recent discoveries, uncertainties and the potential relevance of climate change, Philos. Trans. R. Soc. B-Biol. Sci., 368, 20130121, 2013.

Wang, J., Kan, J., Qian, G., Chen, J., Xia, Z., Zhang, X., Liu, H., and Sun, J.: Denitrification and anammox: Understanding nitrogen loss from Yangtze Estuary to the east China sea (ECS), Environ. Pollut., 2019. https://doi.org/10.1016/j.envpol.2019.06.025.

Wanninkhof, R. I. K.: Relationship between wind speed and gas exchange over the ocean, J. Geophys. Res.-Oceans, 97, 7373–7382, 1992.

Ward, B. B. Nitrification in marine systems, In. Capone, D. G., Bronk, D. A., Mulholl, M. R., and Carpenter, E. J. (ed), Nitrogen in the Marine Environment (2nd Edition) [M]. Burlington: Academic Press, 199–261, 2008.

Weiss, R. F., and Price, B. A.: Nitrous oxide solubility in water and seawater, Mar. Chem., 8, 347–359, 1980.

Yamagishi, H., Westley, M. B., Popp, B. N., Toyoda, S., Yoshida, N., Watanabe, S., Koba, K., and Yamanak, Y.: Role of nitrification and denitrification on the nitrous oxide cycle in the eastern tropical North Pacific and Gulf of California, J Geophy. Res., 112, G02015, doi:10.1029/2006JG000227, 2007.

Yoshida, N.: ^{15}N-depleted N_2O as a product of nitrification, Nature, 335, 528–529, 1988.

Yoshida, T., and Alexander, M.: Nitrous Oxide Formation by Nitrosomonas europaea and Heterotrophic Microorganisms, Soil Sci. Soc. Amer. Proc., 34, 880–882,1970.

Yu, R., Kampschreur, M. J., Mark van Loosdrecht, C. M., and Chandran, K.: Mechanisms and Specific Directionality of Autotrophic Nitrous Oxide and Nitric Oxide Generation during Transient Anoxia, Environ. Sci. Technol., 44, 1313–1319, 2010.

Zhang, Y., Xie, X., Jiao, N., Hsiao, S. S. Y., and Kao, S. J.: Diversity and distribution of *amoA*-type nitrifying and *nir*S-type denitrifying microbial communities in the Yangtze River estuary, Biogeosciences, 11, 2131–2145, 2014.

Zhu, R., Liu, Y., Li, X., Sun, J., Xu, H. and Sun, L.: Stable isotope natural abundance of nitrous oxide emitted from Antarctic tundra soils: effects of sea animal excrement depositions, Rapid Commun. Mass Spectrom., 22, 3570–3578, 2008.

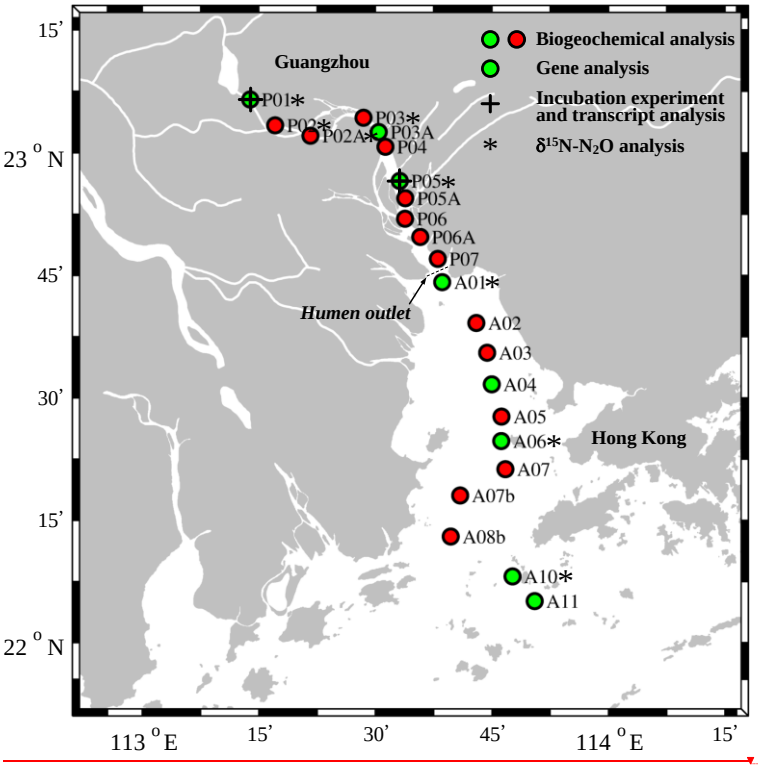

Figure 1: Map of the PRE showing the sampling sites. Biogeochemical analyses were performed on samples from all sites (green and red circles). The green circles indicate sites where genes were analyzed. The black crosses indicate in situ incubation experiment sites (P01 and P05). The black asterisks indicate sites where the isotopic composition of N_2O was analyzed.

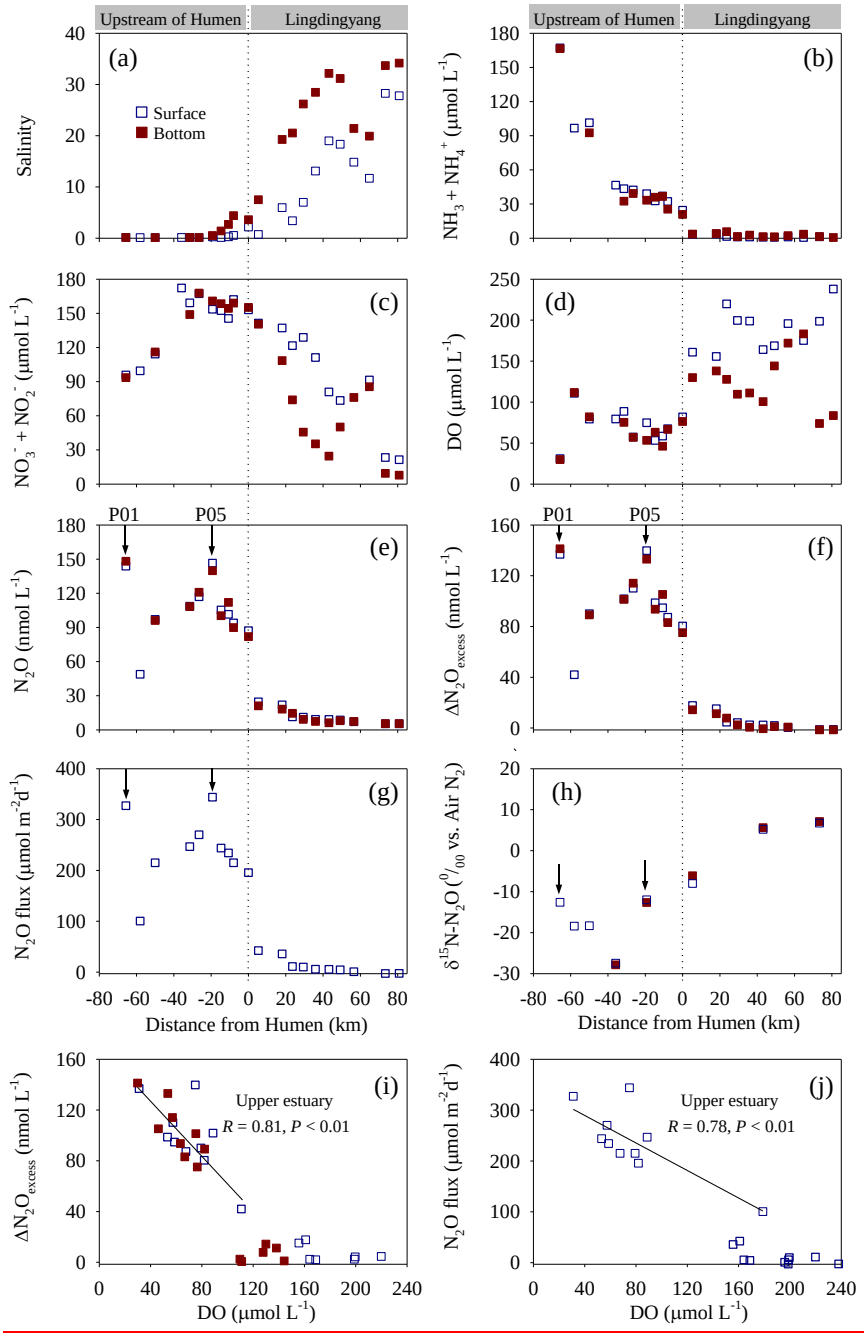
Upstream of Humen
Lingdingyang
(a)
Surface
Bottom
Salinity
(b)
$NH_3 + NH_4^+$ (μmol L^{-1})
(c)
$NO_3^- + NO_2^-$ (μmol L^{-1})
(d)
DO (μmol L^{-1})
P01
P05
(e)
N_2O (nmol L^{-1})
(f)
ΔN_2O_{excess} (nmol L^{-1})
(g)
N_2O flux (μmol $m^{-2}d^{-1}$)
(h)
$\delta^{15}N\text{-}N_2O$ ($^0/_{00}$ vs. Air N_2)
Distance from Humen (km)
(i)
Upper estuary
R = 0.81, P < 0.01
DO (μmol L^{-1})
(j)
R = 0.78, P < 0.01

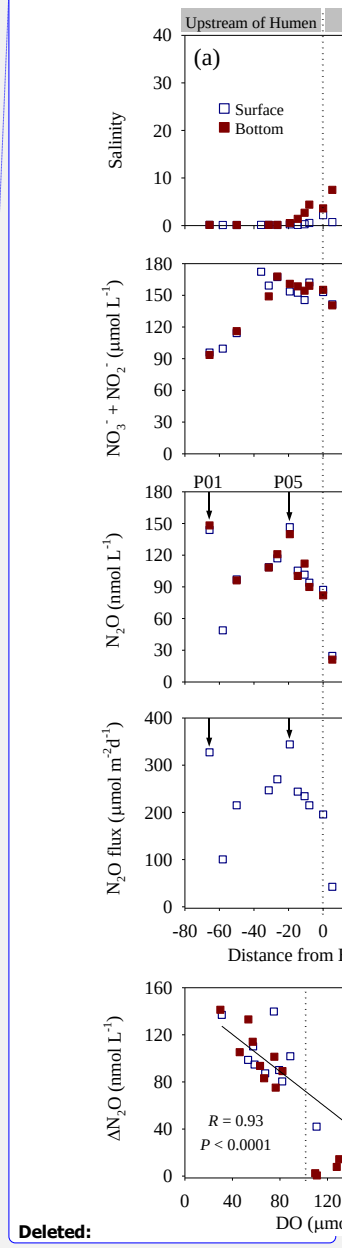
Upstream of Humen
(a)
Surface
Bottom
Salinity
$NO_3^- + NO_2^-$ (μmol L^{-1})
P01
P05
N_2O (nmol L^{-1})
N_2O flux (μmol $m^{-2}d^{-1}$)
Distance from
ΔN_2O (nmol L^{-1})
R = 0.93
P < 0.0001
DO (μmo

Deleted:

1

Figure 2: Distribution of biogeochemical factors along the PRE transect. (a) Salinity, (b) NH_3+NH_4^+, (c) NO_2^-+NO_3^-, (d) DO, (e) N_2O, and (f) ΔN_2O_{excess} concentrations, (g) N_2O flux, (h) $\delta^{15}N$-N_2O, (i) ΔN_2O_{excess} vs. DO, and (j) N_2O flux vs. DO. The dashed lines show the division of the transect into the northern (upstream of the Humen outlet) and southern (Lingdingyang) areas. The arrows indicate the sites where in situ incubation experiments were performed.

Deleted: /

Deleted: -

Deleted: -

Deleted: N2O

Deleted: the

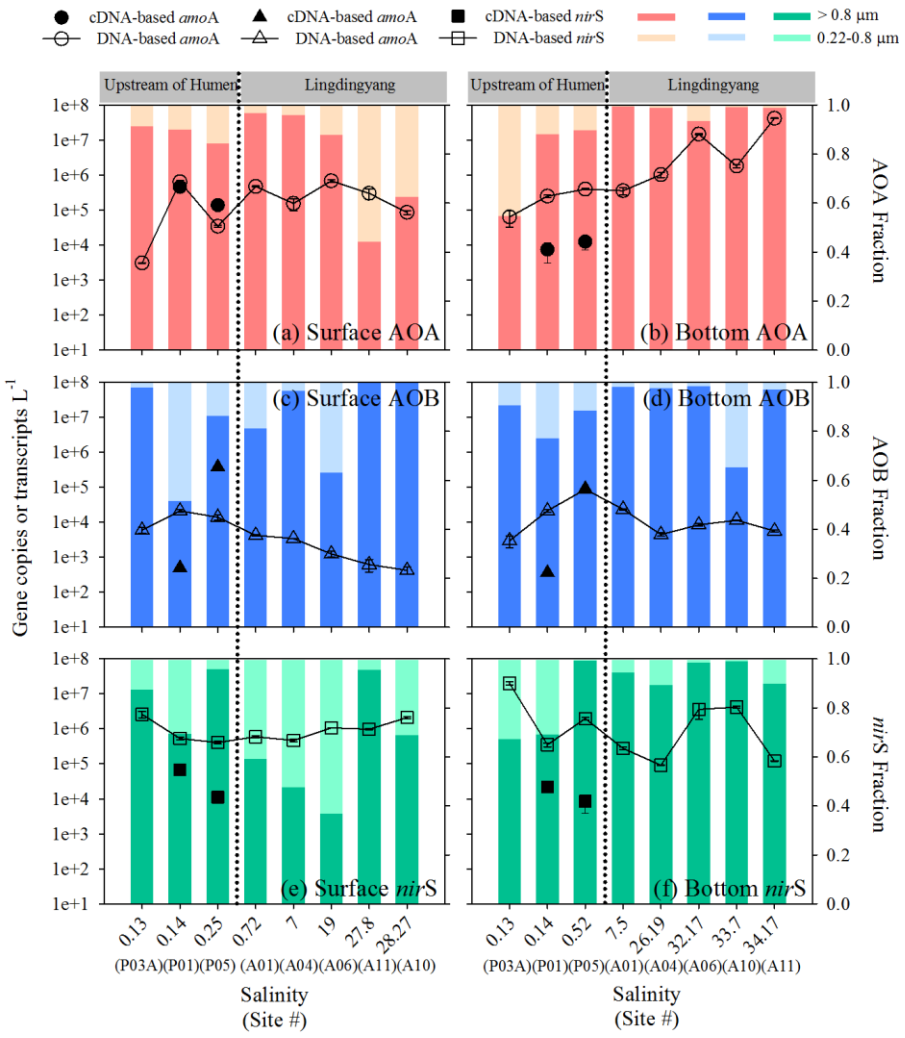

Figure 3: Abundance distribution of AOA and AOB *amo*A and bacterial *nir*S along the salinity gradient in the PRE. Abundances of AOA *amo*A genes (open circles) and PA transcripts (closed circles) and the relative abundances of PA and FL AOA *amo*A genes in (a) surface and (b) bottom waters. Abundances of AOB *amo*A genes (open triangles) and PA transcripts (closed triangles) and the relative abundances of PA and FL AOB *amo*A genes in (c) surface and (d) bottom waters. Abundances of

Deleted: water

Deleted: water

bacterial *nir*S genes (open squares) and PA transcripts (closed squares) and the relative abundances of PA and FL *nir*S genes in (e) surface and (f) bottom waters. The dashed lines indicate the division into the northern (upstream of the Humen outlet) and southern (Lingdingyang) areas.

Deleted: water

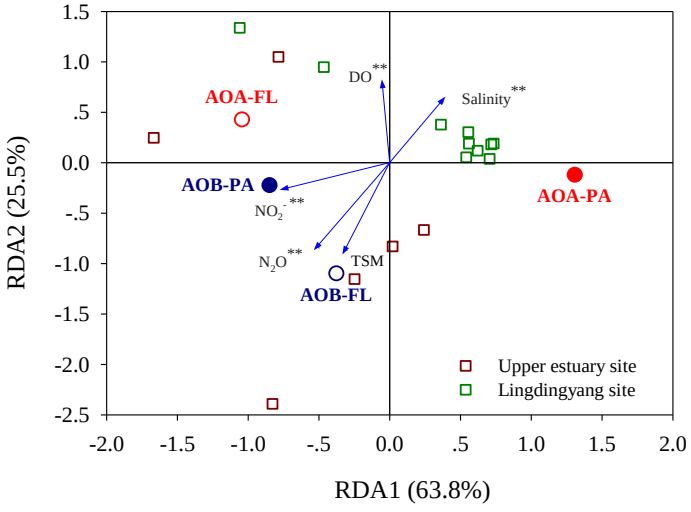

Figure 4: RDA of the relative abundance of AOA *amo*A and AOB *amo*A under biogeochemical constraints. Each square represents an individual sample. Vectors represent environmental variables. $^{*}P < 0.05$, $^{**}P < 0.01$ (Monte Carlo permutation test).

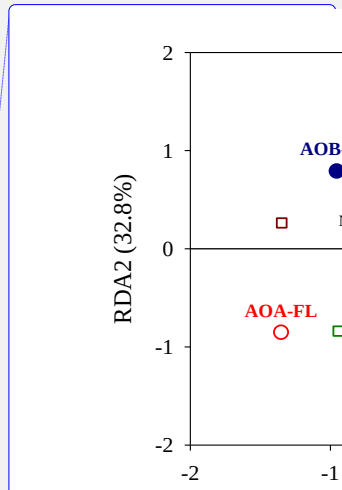

Deleted:

Deleted: 5

Deleted: Redundancy analysis

Deleted: -

Deleted: -

Deleted: ammonia-oxidizing communities

Deleted: community

Deleted: Temp, temperature.

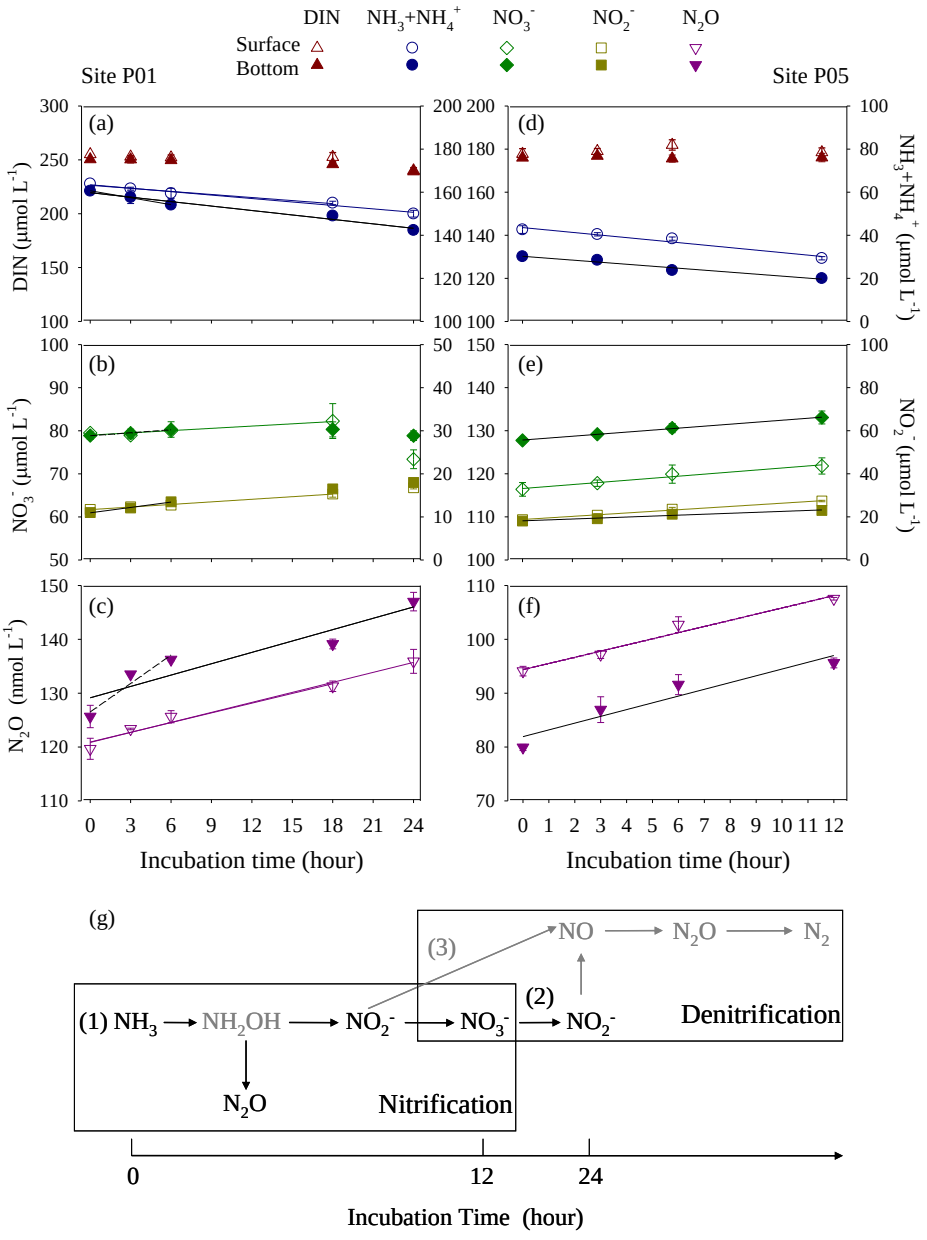
DIN
NH3+NH4+
NO3-
NO2-
N2O
Surface
Bottom
Site P01
Site P05
(a)
(b)
(c)
(d)
(e)
(f)
DIN (μmol L-1)
NO3- (μmol L-1)
N2O (nmol L-1)
NH3+NH4+ (μmol L-1)
NO2- (μmol L-1)
Incubation time (hour)
Incubation time (hour)
(g)
(1) NH3
NH2OH
NO2-
NO3-
(2)
NO2-
(3)
NO
N2O
N2
N2O
Nitrification
Denitrification
0
12
24
Incubation Time (hour)

Deleted:

Figure 5: Variations in nitrogen compounds and N_2O concentrations at sites P01 and P05 during the incubation experiments in surface (open symbols) and bottom (closed symbols) waters. (a, d) Total DIN (brown triangles) and NH_3+NH_4^+ (blue circles), (b, e) NO_3^- (green diamonds) and NO_2^- (dark yellow squares), (c, f) N_2O (purple inverted triangles). Linear regressions depend on whether variations in DIN concentration against time retain "mass balance" in a closed incubation system. The linear regressions of ammonia were used to estimate ammonia oxidation rates in (a) P01 over 18 and 24 h (surface water, blue lines) and 6 and 24 h (bottom water, black lines), and (d) P05 over 12 h (surface, blue line; bottom, black line). The linear regressions of nitrate estimated nitrite oxidation rates in (b) P01 over 18 h (surface water, green line) and 6 h (bottom water, black line), and (e) P05 after 12 h (surface, green line; bottom, black line). The nitrite linear regressions after 18 h (surface water, dark yellow line) and 6 h (bottom water, black line) in P01 and 12 h (surface, dark yellow line; bottom, black line) in P05 are also shown, but do not indicate oxidation rates. The N_2O linear regressions were used to estimate N_2O production rates in (c) P01 after 18 and 24 h (surface water, purple lines) and 6 and 24 h (bottom water, black lines; dashed line, no statistical significance test), and (f) P05 after 12 h (surface, purple line; bottom, black line). All regression equations, R^2, and P values are shown in Table 2. (g) A diagram showing transformations of nitrogen compounds and N_2O production during incubation experiments. Nitrification (1) occurred during the entire P01 and P05 incubations and denitrification (2 and/or 3) may be present in the end phase of the P01 incubation. The gray arrows indicate the pathways of nitrogen loss unanalyzed here, and the gray compounds indicate the unmeasured nitrogen compound.

Deleted: 4

Deleted: /

Deleted: ;

Deleted: -

Deleted: -

Deleted: ;

Deleted: formulas

Formatted: Font: Italic

Formatted: Superscript

Deleted: 1

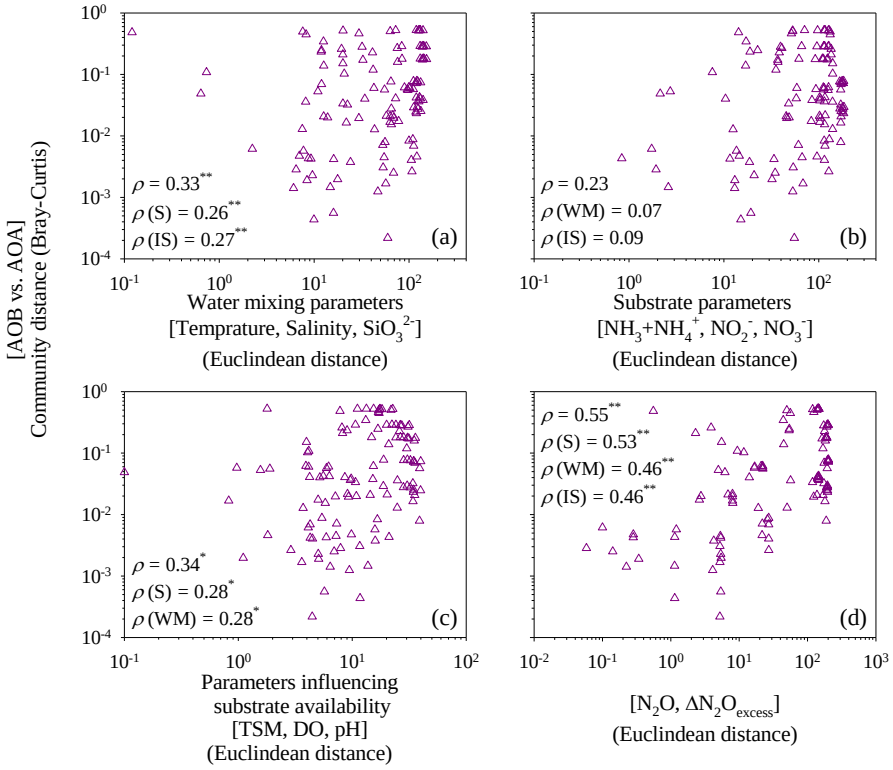

Figure 6: Correlations between the relative abundance of AOB versus AOA and (a) water mixing parameters (temperature, salinity, and silicate), (b) substrate parameters (ammonia/ammonium, nitrite, and nitrate), (c) parameters influencing substrate availability (TSM, DO, and pH), or (d) N_2O parameters (N_2O and ΔN_2O). The ammonia oxidizers matrix was calculated according to the relative AOA and AOB abundances. Dissimilarity matrices of the relative abundance of AOB *amo*A and AOA *amo*A were based on Bray-Curtis distances and environmental factors were based on Euclidean distances between samples. Standard and partial Mantel tests were run to measure the correlation between two matrices. Spearman correlation coefficient (ρ) values are shown for standard (first value)

Deleted: ...

Deleted: ammonia oxidizer community composition

Deleted: mass

Deleted: community

Deleted: communities

Deleted: -

Deleted: -

Deleted: or Kendall's

Deleted: R

and partial Mantel (second, third, and fourth) tests. The *P* values were calculated using the distribution of the Mantel test statistics estimated from 999 permutations. $^{*}P < 0.05$; $^{**}P < 0.01$.

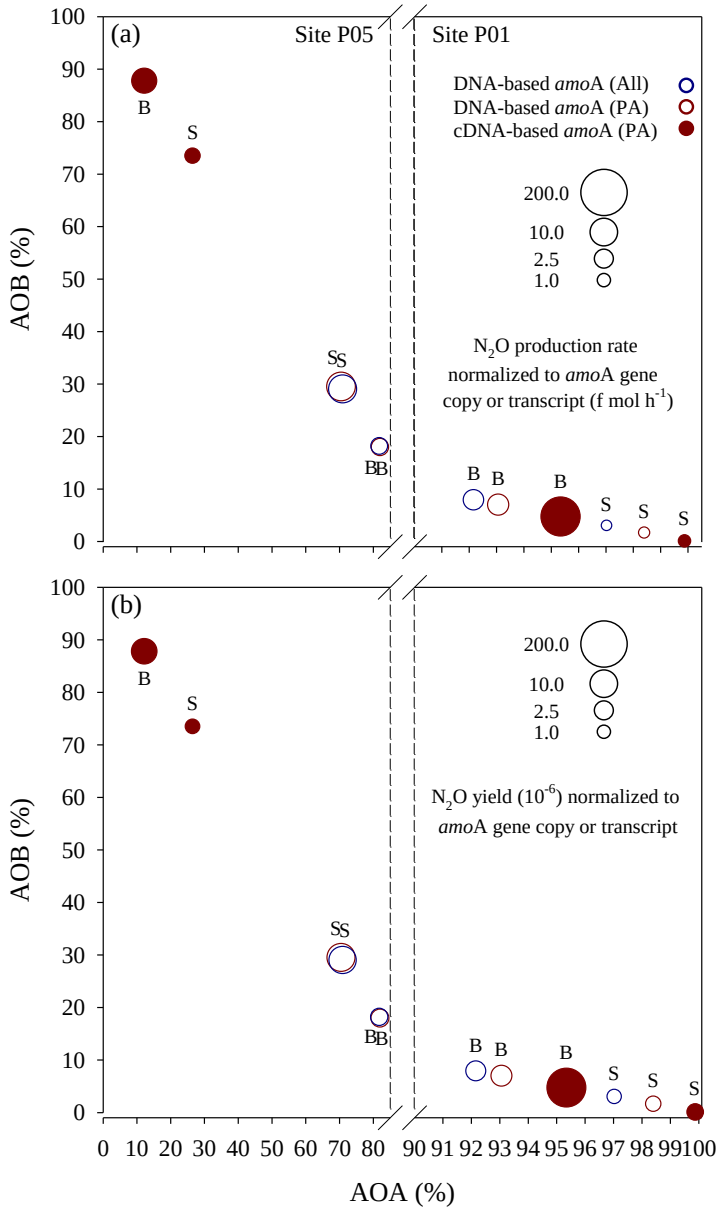
(a)
Site P05
Site P01
DNA-based amoA (All)
DNA-based amoA (PA)
cDNA-based amoA (PA)
200.0
10.0
2.5
1.0
N2O production rate normalized to amoA gene copy or transcript (f mol h-1)
(b)
N2O yield (10-6) normalized to amoA gene copy or transcript
AOB (%)
AOA (%)
0 10 20 30 40 50 60 70 80 90 91 92 93 94 95 96 97 98 99 100
0 10 20 30 40 50 60 70 80 90 100
B
S

1

Figure 7: N_2O (a) production rates and (b) yields normalized to total *amo*A gene copy or transcript numbers of AOA and AOB in a given sample. They are presented along the x-y axes that represent the relative contributions of AOA and AOB to the total *amo*A gene or transcript pools. S, surface; B, bottom.

Table 1 Rho (ρ) values for the relationships between nitrifier and denitrifier gene abundances and biogeochemical parameters in the PRE.

Biogeochemical parameters	PA + FL			PA (> 0.8 μm)			FL (0.22–0.8 μm)		
	AOA-*amo*A (n =16)	AOB-*amo*A (n =16)	*nir*S (n =16)	AOA-*amo*A (n =16)	AOB-*amo*A (n =14)	*nir*S (n =16)	AOA-*amo*A (n =16)	AOB-*amo*A (n =16)	*nir*S (n =16)
Temperature	−0.694*	0.359	0.085	−0.676*	0.303	0.165	−0.438	0.358	0.229
Salinity	0.644*	−0.339	−0.018	0.604*	−0.270	−0.047	0.403	−0.351	−0.356
SiO_3^-	−0.541*	0.559*	0.206	−0.497	0.503*	0.282	−0.350	0.481	0.238
TSM	−0.109	0.668*	0.047	−0.097	0.612*	0.194	0.191	0.565*	−0.071
pH	0.381	−0.656*	0.157	0.316	−0.615*	0.088	0.377	−0.605*	−0.059
DO	−0.074	−0.771**	−0.026	−0.121	−0.729**	−0.144	0.009	−0.697*	0.218
NH_3/NH_4^+	−0.482	0.646*	0.068	−0.482	0.571*	0.196	−0.325	0.587*	0.000
NO_3^-	−0.485	0.359	−0.138	−0.444	0.353	−0.112	−0.588*	0.213	0.115
NO_2^-	−0.588*	0.447	0.126	−0.556*	0.356	0.212	−0.421	0.288	0.265
N_2O	−0.421	0.641*	−0.194	−0.356	0.606*	−0.121	−0.385	0.490	0.047
ΔN_2O_{excess}	−0.527*	0.559*	−0.160	−0.480	0.517*	−0.081	−0.369	0.504	0.096
N_2O flux[a]	−0.190 (n = 8)	1.000** (n = 8)	−0.524 (n = 8)	−0.143 (n = 8)	1.000** (n = 8)	−0.310 (n = 8)	−0.571 (n = 8)	0.657 (n = 6)	−0.524 (n = 8)

[a]Surface data; *False discovery rate (FDR)-adjusted $P < 0.05$; **FDR-adjusted $P < 0.01$.

Deleted: 2
Deleted: -
Deleted: *
Deleted: -
Deleted: *
Deleted: -
Deleted: *
Deleted: -
Deleted: -
Deleted: -
Deleted: -
Deleted: -
Deleted: -
Deleted: -
Deleted: -
Deleted: -
Deleted: *
Deleted: -
Deleted: -
Deleted: -
Deleted: -
Deleted: *
Deleted: -
Deleted: -
Deleted: -
Deleted: -
Deleted: -

Table 2 Linear regressions of ammonia, nitrite, nitrate, and N_2O concentrations against time and N_2O yields during incubation experiments.

Site_Layer	Time (hour)	$\Delta(NH_3+NH_4^+)$ ($\mu mol\ L^{-1}\ h^{-1}$)			ΔNO_2^- ($\mu mol\ L^{-1}\ h^{-1}$)			ΔNO_3^- ($\mu mol\ L^{-1}\ h^{-1}$)			ΔN_2O ($nmol\ L^{-1}\ h^{-1}$)			N_2O yield (%)
		Equation	R^2	Rate[a]	Equation	R^2	Rate[a]	Equation	R^2	Rate[a]	Equation	R^2	Rate[a]	
P01_S	18	$y = -0.47x+163.20$	0.96*	0.47	$y = 0.20x+11.69$	1.00**	0.20	$y = 0.18x+78.98$	0.90*	0.18	$y = 0.60x+120.93$	0.96*	0.60[b]	0.26[b]
	24	$y = -0.53x+163.44$	0.98**	0.53	–	–	–	–	–	–	$y = 0.62x+120.85$	0.98**	0.62	–[c]
P01_B	6	$y = -1.08x+160.65$	1.00*	1.08	$y = 0.42x+10.95$	1.00*	0.42	$y = 0.23x+78.84$	0.98	0.23	$y = 1.61x+127.04$	0.98	1.61[b]	0.30[b]
	24	$y = -0.69x+159.76$	0.96**	0.69	–	–	–	–	–	–	$y = 0.70x+129.14$	0.86*	0.70	–[c]
P05_S	12	$y = -1.12x+43.58$	0.96*	1.12	$y = 0.73x+18.78$	1.00**	0.73	$y = 0.46x+116.58$	0.98**	0.46	$y = 1.15x+79.79$	0.98**	1.15[b]	0.21[b]
P05_B	12	$y = -0.89x+30.25$	0.96*	0.89	$y = 0.42x+18.17$	0.96*	0.42	$y = 0.44x+127.83$	1.00**	0.44	$y = 1.41x+81.57$	0.96*	1.41[b]	0.32[b]

[a]These rates are net rates since $\Delta(NH_3+NH_4^+)$ is the net consumption and ΔNO_2^-, ΔNO_3^-, and ΔN_2O is the net production during incubation.

[b]These rates and yields (when only nitrification occurred) were used to calculate the average *amo*A gene copy-specific N_2O production rates and N_2O yields in Figure 7.

[c]No estimation of N_2O yield was made due to nitrification and denitrification may occur concurrently and DIN was not in balance.

*$P < 0.05$; **$P < 0.01$.

–No regression analysis or no estimation made due to DIN was not in balance.

Deleted: 1
Deleted: /
Deleted: -
Deleted: -
Deleted: -
Formatted ...
Deleted: -
Formatted ...
Deleted: -…-
Deleted: -h-
Formatted ...
Deleted: a
Deleted: Liner Regression
Deleted: Liner
Deleted: Liner Regression
Deleted: Liner Regression
Deleted: 98
Deleted: 95
Deleted: 98
Deleted: 1.28
Formatted ...
Deleted: -
Deleted: 99
Deleted: 99
Deleted: -
Deleted: 99
Deleted: 99
Deleted: 1.49
Deleted: -
Deleted: 98
Deleted: 93
Deleted: -
Deleted: 98
Deleted: 99
Deleted: 99
Deleted: 1.03
Deleted: -
Deleted: 98
Deleted: 98

Supplement of

Major role of ammonia-oxidizing bacteria in N_2O production in the Pearl River Estuary

Li Ma[1,2], Hua Lin[1,2,3], Xiabing Xie[1], Minhan Dai[1,2], Yao Zhang[1,2]

[1]State Key Laboratory of Marine Environmental Science, Xiamen University, Xiamen 361101, China

[2]College of Ocean and Earth Sciences, Xiamen University, Xiamen 361101, China

[3]Key Laboratory of Marine Ecosystem and Biogeochemistry, State Oceanic Administration, Second Institute of Oceanography, Ministry of Natural Resources, Hangzhou 310012, China

Correspondence to: Yao Zhang (yaozhang@xmu.edu.cn)

Table S1 In situ biogeochemical parameters at the incubation experiment sites.

Site_Layer	Temperature (^{o}C)	DO (μmol L^{-1})	NH_4^+ (μmol L^{-1})	NO_3^- (μmol L^{-1})	NO_2^- (μmol L^{-1})
P05_S	30	61.3	40.1	126.1	20.5
P05_B	30	54.7	33.3	123.5	24.5
P01_S	29	30.9	167.2	84.0	11.9
P01_B	29	30.0	166.5	82.0	11.6

S, surface; B, bottom.

Table S2 Isotopic composition of N_2O during bacterial and archaeal ammonia oxidation, bacterial nitrifier-denitrification, and bacterial denitrification.

Pathway	Microorganisms	Species	Substrate	$\delta^{15}N\text{-}N_2O$	References
Ammonia oxidation	*β*-proteobacteria	*Nitrosomonas europaea*	NH_4^+	−68–−60‰	Yoshida, 1988; Toyoda et al., 2017
			NH_4^+	−46.9–−46.1‰	Sutka et al., 2006
			NH_4^+	−19.88 ±0.39‰	Jung et al., 2014
		Nitrosomonas marina C-113a	NH_4^+	−54.9–−15.2‰ (0.5% O_2)[a]	Frame and Casciotti, 2010
			NH_4^+	−13.6–−6.7‰ (20% O_2)[a]	
	γ-proteobacteria	*Methylomonas methanica*	NH_4^+	−39.4‰	Mandernack et al., 2009
	Archaea	CN25 (marine)	NH_4^+	6.3–10.2‰	Santoro et al., 2011
		MY1 (soil)	NH_4^+	−13.53 ±2.12‰	Jung et al., 2014
		MY2 (soil)	NH_4^+	−16.96 ±1.81‰	Jung et al., 2014
		MY3 (soil)	NH_4^+	−16.49 ±2.18‰	Jung et al., 2014
		JG1 (soil)	NH_4^+	−15.32 ±0.16‰	Jung et al., 2014
		AR (marine sediment)	NH_4^+	−12.91 ±1.50‰	Jung et al., 2014

Deleted: fractionation

Deleted: ^{15}N-

Deleted: -□8 □ …-

Deleted: -□6.9 □ …-

Deleted: -

Deleted: -…4.9 □ …-

Deleted: -…3.6 □ …-

Deleted: -

Deleted: □

Deleted: -

Deleted: -

Deleted: -

Deleted: -

Deleted: -

		CS (acid mine)	NH_4^+	−35.54 ±0.89‰	Jung et al., 2014
Hydroxylamine oxidation[b]	*β*-proteobacteria	*Nitrosomonas europaea*	NH_2OH	−38.1–−20.4‰	Sutka et al., 2003
			NH_2OH	−5.5–5.1‰	Sutka et al., 2006
			NH_2OH	−34.0–−13.8‰	Yamazaki et al., 2014
		Nitrosospira multiformis	NH_2OH	−3.9–1.7‰ (Average −0.3 ±2.9‰)	Sutka et al., 2006
		Nitrosomonas marina C-113a	NH_2OH	−6.7‰	Frame and Casciotti, 2010
	γ-proteobacteria	*Nitrosococcus oceani*	NH_2OH	−17.9–−5.8‰	Yamazaki et al., 2014
		Methylococcus capsulatus	NH_2OH	−0.3–1.7‰ (Average 0.0±1.2‰)	Sutka et al., 2003
			NH_2OH	1.3–5.2‰ (Average 3.4±1.9‰)	Sutka et al., 2006
Nitrifier-denitrification	*β*-proteobacteria	*Nitrosomonas* marina C-113a	NO_2^-	−57.6±4.1‰	Frame and Casciotti, 2010
		Nitrosomonas europaea	NO_2^-	−39.1–−31.0‰ (Average −34.8 ±2.7‰)	Sutka et al., 2003
		Nitrosospira multiformis	NO_2^-	−24.2–−21.5‰ (Average −22.9 ±0.6‰)	Sutka et al., 2006
Denitrification	*γ*-proteobacteria	*Pseudomonas fluorescens*	NO_3^-	−37.2–−14.9‰	Toyoda et al., 2005
	α-proteobacteria	*Paracoccus denitrificans*	NO_3^-	−20.0–−7.9‰	Toyoda et al., 2005

[a]O_2 conditions of the incubation experiments.

[b]Although the $\delta^{15}N$-N_2O when using NH_2OH as a substrate are listed here, the isotopic composition of N_2O only when using NH_4^+ as a substrate was discussed in natural environments.

Deleted: I

Deleted: fractionation for ^{15}N

Deleted: , although the values when using NH_2OH as a substrate are listed here

References

Frame, C. H., and Casciotti, K. L.: Biogeochemical controls and isotopic signatures of nitrous oxide production by a marine ammonia-oxidizing bacterium, Biogeosciences, 7, 2695–2709, 2010.

Jung, M. Y., Well, R., Min, D., Giesemann, A., Park, S. J., Kim, J. G., and Rhee, S. K.: Isotopic signatures of N_2O produced by ammonia-oxidizing archaea from soils, ISME J., 8, 1115–1125, 2014.

Mandernack, K. W., Mills, C. T., Johnson, C. A., Rahn, T., and Kinney, C.: The $\delta^{15}N$ and $\delta^{18}O$ values of N_2O produced during the co-oxidation of ammonia by methanotrophic bacteria, Chem. Geol., 267, 96–107, 2009.

Santoro, A. E., Buchwald, C., McIlvin, M. R., and Casciotti K. L.: Isotopic Signature of N_2O Produced by Marine Ammonia-Oxidizing Archaea, Science, 333, 1282–1285, 2011.

Sutka, R. L., Ostrom, N. E., Ostrom, P. H., Gandhi, H., and Breznak, J. A.: Nitrogen isotopomer site preference of N_2O produced by Nitrosomonas europaea and Methylococcus capsulatus Bath, Rapid Commun. Mass Spectrom., 17, 738–745, 2003.

Sutka, R. L., Ostrom, N. E., Ostrom, P. H., Breznak, J. A., Gandhi, H., Pitt, A. J., and Li, F.: Distinguishing Nitrous Oxide Production from Nitrification and Denitrification on the Basis of Isotopomer Abundances, Appl. Environ. Microbiol., 72, 638–644, 2006.

Toyoda, S., Mutobe, H., Yamagishi, H., Yoshida, N., Tanji, Y.: Fractionation of N_2O isotopomers during production by denitrifier, Soil. Biol. Biochem., 37, 1535–1545, 2005.

Toyoda, S., Yoshida, N., and Koba, K.: Isotopocule analysis of biologically produced nitrous oxide in various environments, Mass Spectrom. Rev., 36, 135–160, 2017.

Yamazaki, T., Hozuki, T., Arai, K., Toyoda, S., Koba, K., Fujiwara, T., and Yoshida,

N.: Isotopomeric characterization of nitrous oxide produced by reaction of enzymes extracted from nitrifying and denitrifying bacteria, Biogeosciences, 11, 2679–2689, 2014.

Yoshida, N.: ^{15}N-depleted N_2O as a product of nitrification, Nature, 335, 528–529, 1988.

Table S3 The abundances of DNA- and cDNA-based *amo*A gene and the N_2O production net rates and yields normalized to total *amo*A gene copy or transcript numbers of AOA and AOB in a given sample at the incubation experiment sites.

Site Layer	DNA-based AOB (All) (copies L^{-1})	DNA-based AOA (All) (copies L^{-1})	N_2O production rates (All) (fmol $cell^{-1}$ h^{-1})	N_2O yields (All) (10^{-6})	DNA-based AOB (PA) (copies L^{-1})	DNA-based AOA (PA) (copies L^{-1})	N_2O production rates (PA) (fmol $cell^{-1}$ h^{-1})	N_2O yields (PA) (10^{-6})	cDNA-based AOB (PA) (copies L^{-1})	cDNA-based AOA (PA) (copies L^{-1})	N_2O production rates (PA) (fmol $cell^{-1}$ h^{-1})	N_2O yields (PA) (10^{-6})
P05_S	14030	34427	23.70	21.30	12125	29082	27.90	25.00	382928	138646	2.20	1.97
P05_B	87915	397740	2.90	3.25	77820	357308	3.24	3.63	89559	12559	13.80	15.50
P01_S	19623	642905	0.91	1.93	9343	578974	1.02	2.18	500	461578	1.30	2.77
P01_B	21334	251163	5.91	5.47	16458	221184	6.77	6.27	362	7436	206.00	191.00

S, surface; B, bottom; All, sum of particle-attached and free-living fractions; PA, particle-attached fraction.

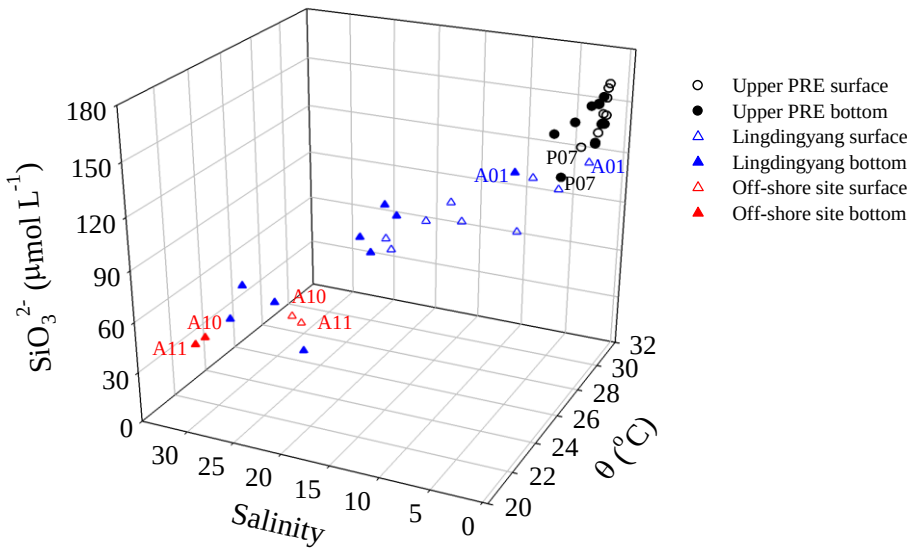

Figure S1: Three-dimensional scatter plot of potential temperature (θ) (°C), salinity, and silicate (SiO_3^{2-}) concentration.